

Protection of Electrical Power Systems in Maritime Applications

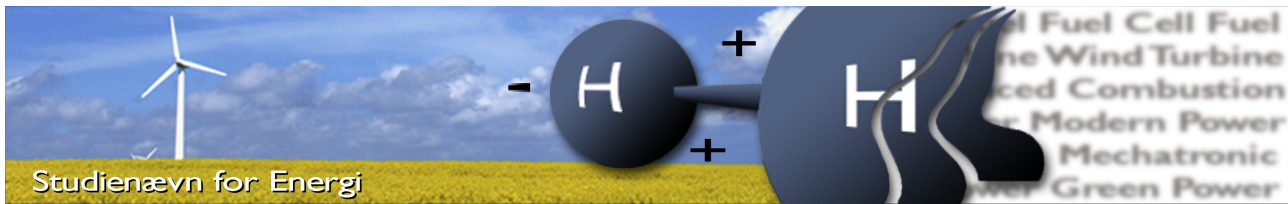
Analysis of Directional Overcurrent Protection Methods

Mikkel Hingbjerg Hansen

FACULTY OF ENGINEERING AND SCIENCE
MSc. in Electrical Power Systems and High Voltage

Masters Project





Studienævn for Energi

Title: Protection of Electrical Power Systems in Maritime Applications

Semester: 4th

Semester theme: Masters thesis

Project period: 1/9-2020 to 28/5-2021

ECTS: 50

Supervisors: Florin Iov & Cătălin Iosef Ciontea

Industry co-supervisors: Kjeld Madsen & Martin T. Arentsen

Project group: EPSH4-1037

Author: Mikkel Hingebjerg Hansen

Total: 105 pages

Appendix: 16 pages

Supplements: 0

Abstract

The main objective of this report is to analyse polarisation methods used in directional overcurrent protection and evaluate their use in power system relay protection schemes for maritime power systems. The purpose of this is to aid maritime industries in developing reliable, fast and selective protection schemes. This study is relevant because maritime power systems often have system configurations that make common protection schemes for land-based power systems unreliable or inapplicable. In addition, continuity of service for critical loads is paramount in maritime power systems, due to the potential consequences of failure. In this report, a general model of maritime power systems is developed along with relay models based on different directional overcurrent protection algorithms. A relay model is validated experimentally and the performance of relays in maritime power systems is investigated through simulation. The relay models are evaluated in the context of proposed protection schemes and key considerations in the development of protection schemes for maritime power systems, are identified.

By accepting the request from the fellow student who uploads the study group's project report in Digital Exam System, you confirm that all group members have participated in the project work, and thereby all members are collectively liable for the contents of the report. Furthermore, all group members confirm that the report does not include plagiarism.

Summary

I fremtidens maritime elektriske systemer kan det forventes, at systemers kompleksitet øges grundet højere krav til energieffektivitet og mindre forurening. Samtidig afhænger forsynings sikkerheden i maritime systemer af den korrekte udnyttelse af indbygget redundans ved brug af selektiv relæbeskyttelse. Hensigtsmæssig brug af relæbeskyttelse kan blive en udfordring i fremtidens maritime elektriske systemer på grund af variabel kortslutningseffekt og system konfigurationer i allerede komplekse system design.

Dette kandidat speciale er udarbejdet i samarbejde med DEIF A/S med formål at undersøge brugen af retningsbestemt overstrømsbeskyttelse i maritime applikationer. Rapportens fokus er polariserings metoder til retningsbestemmelse, for at hjælpe maritime industrier med at udarbejde hurtig, pålidelig og selektiv relæbeskyttelse.

Rapporten beskriver udviklingen af en generisk maritim system model til brug i dynamiske fejlstudier. Derudover er der udviklet beskyttelses algoritmer baseret på selvpolarisering, krydspolarisering og positiv sekvens polarisering. Disse algoritmer er implementeret i en relæ model, som er valideret eksperimentelt.

Baseret på simulations studier er en sensitivitets analyse af retningsbestemt overstrømsbeskyttelse gennemført med forbehold for pålidelighed, forsinkelse og selektivitet. Disse undersøgelser inkluderer påvirkningen af system belastning, fejl impedans, frekvensafvigelser og motorer i systemet. Et beskyttelses system til maritime applikationer udvikles baseret på retningsbestemt overstrømsbeskyttelse, og vurderes i forhold til potentielle fejltilfælde i systemet. Baseret på dette, er relevante overvejelser indenfor udviklingen af relæ beskyttelses systemer identificeret. Det konkluderes at krydspolarisering og positiv sekvens polarisering begge er anvendelige metoder til pålidelig retningsbestemt overstrømsbeskyttelse.

Acknowledgement

I would like to thank my supervisors, Associate Professor Florin Iov and Postdoc Cătălin Iosef Ciotea, for their dedicated guidance. I am thankful for their patient teaching and critical advice, without which this thesis would not have been possible.

My deepest gratitude I extend to Engineer Martin Trolle Arentsen, for his sincere curiosity and dedication to the quality of the work. He has helped elevate the work and I will always appreciate his crucial support.

I am also thankful for the collaboration of Senior Engineer Kjeld Madsen. His keen insight in the practical applications and considerations has helped grounding the work in real world problems. I would like to thank DEIF A/S for allowing this valuable collaboration and sharing their knowledge and equipment for the betterment of this project.

Finally, I want to thank my partner, Karen, for her unwavering support in life, as well as long hours spent improving the figures in this report.

Mikkel Hingebjerg Hansen

Aalborg, May 27th 2021.

Readers' Guide

References are specified with the Vancouver method as [number, page]. The bibliography is at the end of the report, where books are denoted "author, title, publisher, edition, year of publication and ISBN". Websites are denoted "author, title, URL, edition, year of publication and last visited in dd/mm/yy", when applicable. Technical reports are denoted "author, title, publisher and year". Additionally, the placement of the references determine which part of the text it refers to, as illustrated:

- | | | |
|-----------|----------------------|--------------------------|
| [1, p1]. | <i>Before period</i> | Refers to the sentence. |
| . [1, p1] | <i>After period</i> | Refers to the paragraph. |

When referring to figures and tables they are denoted with the number of the chapter and figure/table number. E.g. figure 3 in chapter 2 will be referred to as "Figure 2.3". The figure number is written below the given figure and the table number is written above the given table.

Nomenclature

Symbols

Symbol	Name	Unit
a,b,c	Phases	[-]
C	Capacitance	[F]
E	Voltage	[V]
f	Frequency	[Hz]
G	Synchronous Generator	-
H	Inertia Constant	[s]
I	Current	[A]
j	Complex Operator	-
L	Inductance	[H]
P	Active Power	[W]
Q	Reactive Power	[Var]
R	Resistance	[Ω]
S	Apparent Power	[VA]
t	time	[s]
T	Time period OR Torque	[s], [Nm]
V	Voltage	[V]
X	Reactance	[Ω]
X'	Transient Reactance	[Ω]
Z	Impedance	[Ω]
φ, δ	Phase angle	[$^\circ$]
θ	Characteristic angle	[$^\circ$]
ϕ	Polarising angle	[$^\circ$]
ω	Angular velocity	[$\frac{1}{s}$]

Subscripts

Symbol	Name
1,2,0	Positive, Negative and Zero Sequence
a,b,c,x,y,z	Phase specifier
AC	AC-side
B	base
C	Capacitance
Cu	copper loss
DC	DC-side
eq	equivalent
F	fault
G	Generator
g	Ground
ls	stator leakage
m	measured OR magnetising
prop	related to propulsion system
r	rotor
s	stator
th	threshold
tr	Transformer

Abbreviations

Abbreviation	Definition
3P	3-Phase-to-Phase
AC	Alternating Current
ANSI	American National Standards Institute
A/S	Aktie Selskab
CB	Circuit Breaker
CT	Current Transformer
DC	Direct Current
DEIF	Dansk Elektro Instrument Fabrik
DNV	Det Norske Veritas
DT	Definite Time

EI	Extremely Inverse
FLC	Full Load Current
HV	High Voltage
IDMT	Inverse Definite Minimum Time
IEC	International Electrotechnical Commission
IEEE	Institute of Electrical and Electronics Engineers
IPS	Integrated Power System
LR	Lloyd's Register
LTSI	Long Time Standard Inverse
LV	Low Voltage
MV	Medium Voltage
MSB	Main Switchboard Busbar
MTL	Maximum Torque Line
PI	Proportional Integral Control
PG	Phase-to-Ground
PP	Phase-to-Phase
PPG	Double-phase-to-Ground
PSS	Power System Stabiliser
pu	Per Unit
RB	Reverse Blocking
RCA	Relay Characteristic Angle
RMS	Root Mean Square
SI	Standard Inverse
SC	Short Circuit
VI	Very Inverse
VT	Voltage Transformer

Table of Contents

Chapter 1 Introduction	1
1.1 Background and Motivation	1
1.1.1 Electrification of ships	1
1.1.2 Overview of Maritime Power Systems	3
1.1.3 Challenges in Maritime Power Systems	3
1.1.4 Relay Protection of Maritime Power Systems	5
1.2 Scope of Thesis	7
1.2.1 Problem Statement	7
1.2.2 Objectives	7
1.2.3 Delimitation	7
1.3 Summary	8
Chapter 2 State of the Art	9
2.1 Overview of ANSI-67	9
2.2 Polarisation Methods	11
2.2.1 Positive Sequence Polarisation	11
2.2.2 Self-Polarisation	12
2.2.3 Cross-Polarisation	14
2.2.4 Polarisation Methods in Maritime Power Systems	15
2.3 Relay Coordination	16
2.3.1 Time Grading	16
2.3.2 ANSI-67 Protection Schemes	18
2.4 Summary	21
Chapter 3 Maritime Power System Modelling	22
3.1 System Overview	22
3.2 Component Models	23
3.2.1 Generators	23
3.2.2 Propulsion System	24

3.2.3	Motor Loads	25
3.2.4	Hotel Loads	26
3.2.5	Cables	26
3.2.6	Transformers	27
3.3	System Case Definitions	28
3.3.1	Fault Locations	28
3.3.2	Load Case Definitions	30
3.4	Model Verification	31
3.4.1	Generator Verification	31
3.4.2	Fault Dynamic Verification	33
3.5	Summary	39
Chapter 4	Relay modelling	40
4.1	Relay modelling	40
4.2	Relay Algorithm Verification	44
4.2.1	Verification of Self-polarisation, I_x/V_x variant	45
4.2.2	Verification of self-polarisation, I_x/V_{xy} variant	49
4.2.3	Verification of self-polarisation, I_{xy}/V_{xy} variant	50
4.2.4	Verification of Positive sequence polarisation, I_1/V_1	52
4.2.5	Verification of Cross-polarisation, I_x/V_{yz}	54
4.3	Summary	56
Chapter 5	Result validation	57
5.1	Experimental setup	57
5.2	Verification of experimental setup	59
5.3	Validation of Relay Operation	60
5.3.1	Reverse PP Fault	61
5.3.2	Reverse 3P Fault	61
5.3.3	Forward PP and 3P Fault	62
5.4	Summary	64
Chapter 6	Impact of polarisation methods on power system protection	65
6.1	Protection scheme	65
6.2	Impact of variable parameters on relay operation	68
6.2.1	Frequency deviation	69
6.2.2	Fault impedance	70

6.2.3	System loading	74
6.3	Considerations in relay protection of maritime power systems	77
6.3.1	Ground faults	77
6.3.2	Assumptions on RCA of polarisation methods	79
6.3.3	Variable Generation	80
6.3.4	Open main switchboard busbar loop	80
6.4	Summary	81
Chapter 7 Conclusion		82
7.1	Thesis Summary	82
7.2	Main Contributions	84
7.3	Future work	84
Bibliography		86
Appendix A Model Parameters		89
Appendix B Aggregation of Parallel Asynchronous Motors		91
Appendix C Additional Simulation Results		93

1 | Introduction

This report is a masters thesis in collaboration with DEIF A/S, who provide power management and protection solutions for a variety of systems including maritime applications. This chapter will detail the background and motivations for this project and outline the protection challenges faced by the maritime industry in regards to electrical power systems. The purpose of this is to clearly define the challenges considered in this report and state the objectives of this thesis.

1.1 Background and Motivation

Our society has for thousands of years been dependent on ships and boats, for trade, transport and warfare. In a global modern society, this is still true, but bark canoes have been replaced by tankers, cargo ships and ferries. These large modern vessels have become increasingly complex as demands are being made for efficiency, safety, environmental sustainability and reliability. These demands beget development in power generation technologies, propulsion systems, ancillary devices and electrical power systems.

1.1.1 Electrification of ships

Ships have been gradually electrified since the 1880s as motor, generation and converter technologies have evolved [2]. The first electrified ships used DC systems, like their land-based power system counterparts, but presently only a few application still rely on DC-systems, such as submarines and some military applications [2]. Due to modern trends in power systems such as larger penetration of DC-loads and integration of DC-sources e.g. PV, it is being considered whether maritime power systems could be exclusively DC in the future, however, this is not currently the case [1]. AC-applications were firstly installed as service loads and powered by steam turbines, while the propulsion systems remained steam-powered. However, to increase fuel efficiency electric motors were soon introduced, but was not the typical method of propulsion until the 1960s [3]. The invention of cycloconverters and variable frequency control, in the 1950s and 1970s respectively, allowed for the efficient use of induction motors in the ships propulsion systems [3]. As a result, ships have been almost fully electrified AC systems since the 1960s.

Conventionally, one set of generators were used for service loads and another set of generators for propulsion. This was a result of retrofitting existing ships with mechanical gearing between generation and propulsion with electrical drive systems, and such systems still exist today and is illustrated in

figure 1.1a [3]. In modern maritime power systems generation and loads are connected to one system to allow for more efficient load sharing and allow for increased flexibility in system configuration [3, 4]. This is called an Integrated Power System (IPS) and is outlined in figure 1.1b.

The flexibility provided by IPS is desirable in maritime applications for several reasons. The variable nature of loading of the systems entails that the propulsion system can make up to 90% of the total loading of the systems in some periods, which means that the load sharing capabilities of an IPS can increase both efficiency and rotor angle stability of the system [3]. Additionally, IPS allows for cheaper redundant interconnection between generation and the essential loads of the ship [3]. Redundancy in system design is a key design pillar in maritime power systems, due to the islanded nature of the systems and the potential for catastrophic consequences of a system failure. Loss of propulsion, steering or navigation, all of which rely on the electrical power system, can be dangerous for both the ships crew and its environment [2, 3]. Thus, power system reliability is paramount .

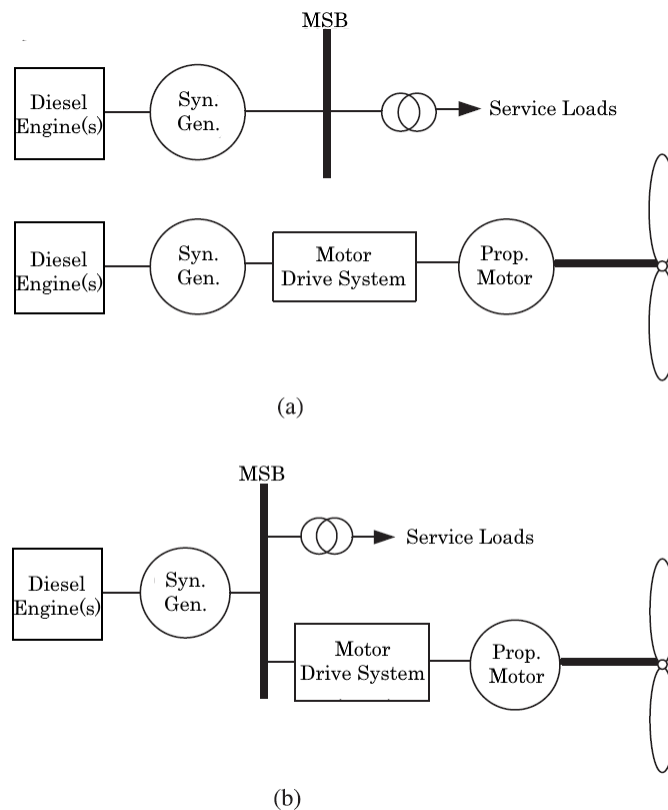


Figure 1.1: a) Conventional power system with segregated service load and propulsion system. b) IPS with the generation, service loads and propulsion interconnected through the main switchboard busbar(MSB). Inspired by [3]

1.1.2 Overview of Maritime Power Systems

Maritime power systems often follow the land-based conventions of the areas they are expected to operate in [5]. This means that they exist as either 50 Hz or 60 Hz systems, which allows for the use of industrial equipment from land-based applications, though some will need modification to the harsher conditions of maritime use. Modern maritime power systems are usually 3-phase, 3 wire AC systems with a consumer-level voltage of 230 V, 380 V or 440 V [5,6, pp5-7]. Some devices like generators, propulsion and auxiliary equipment are connected at higher voltage levels, which are commonly, but not exclusively, 6.6 kV, 6.9 kV or 11 kV [4,7, p23,5, p198]. These systems are either insulated or grounded to the hull of the ship through a high impedance, to avoid large ground currents as is required by classification societies [8].

Recommendations and regulations for the safe construction and operation of ships are defined by classification societies. These include organisations such as Nippon Kaiji Kyōkai (ClassNK), Det Norske Veritas - Germanischer Lloyd (DNV-GL) and Lloyd's Register (LR). Vessels must comply with these regulations to utilise most harbours and insurance services. The purpose of these classification societies is to ensure that ships comply with the design principles suitable to their function and size. Most classification societies base their regulations for electrical systems on IEC standards, but with added requirements for devices to withstand the vibrations, movement and weather conditions they are subjected to at sea [5].

To ensure the reliability of a maritime power system like the one presented in Figure 1.2, the power generation system is connected in a ring configuration to have redundant current paths in case of a fault. This is an example of closed-ring-multiple-infeed systems, which are common in modern maritime power systems [3]. However, redundancy in the systems' tie lines relies on the ability to detect and isolate faults in the system and reconfigure the component interconnections accordingly.

1.1.3 Challenges in Maritime Power Systems

The maritime industry has moved towards being fully electrified which has not happened without presenting new challenges. Increasing political and economical incentives to reduce emission and increase fuel efficiency has led to the incorporation of other technologies in the power generation system. These technologies include electronic injection of common rail diesel, waste-energy recovery, alternative fuel sources and PV. [3]

The continuous electrification of ships also leads to a large amount of power electronic converters, which can raise concern regarding harmonic pollution in maritime power systems, as well as power density challenges for particularly high power applications and military vessels [3]. However, a current

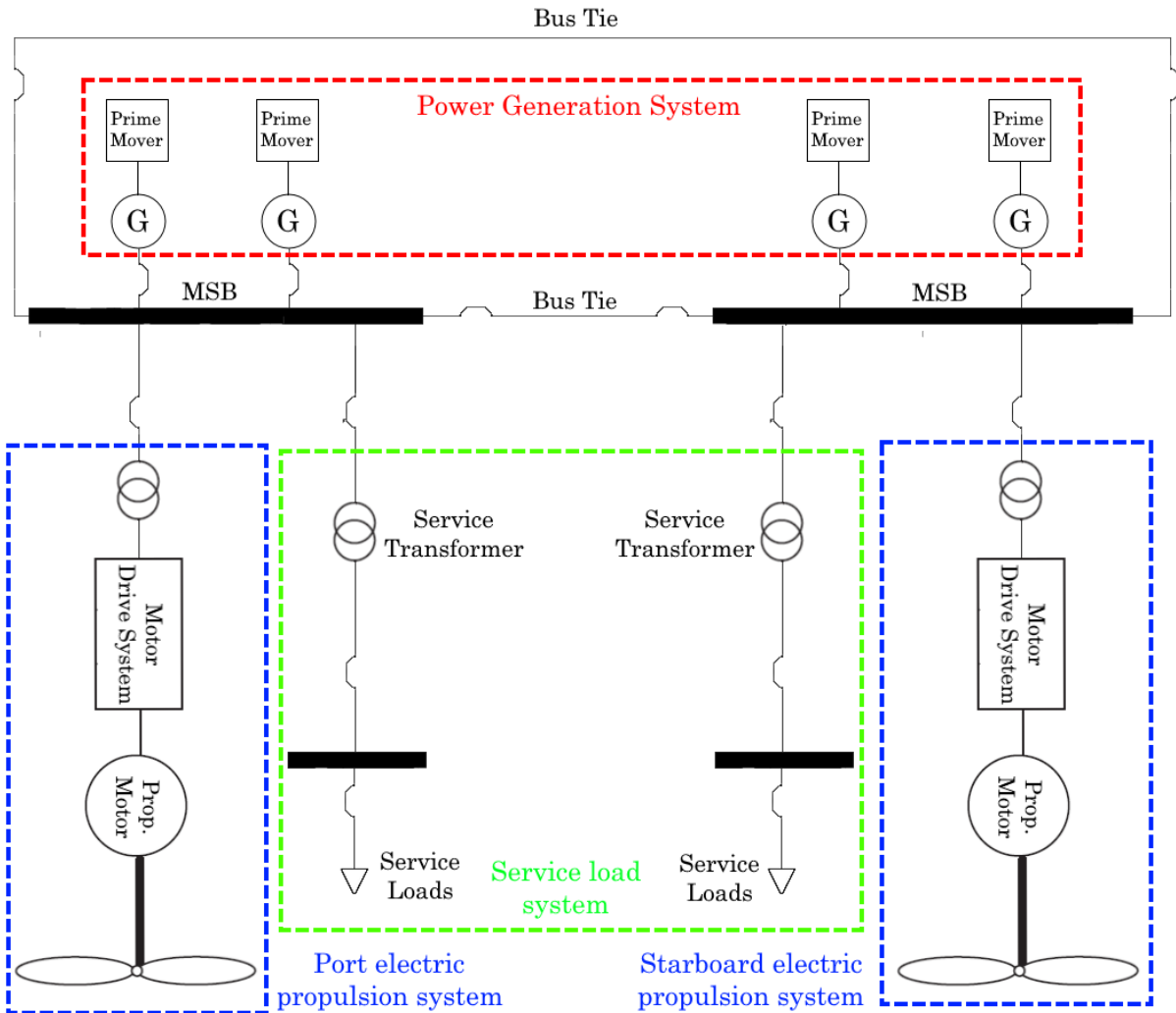


Figure 1.2: Example of IPS with redundant bus tie breakers for the (MSB). Inspired by [3].

and ever-present challenge in the maritime power systems is to ensure power system reliability and continuity of service. This is also true for land-based power systems but the challenges presented to maritime power systems can be different. Maritime power systems are essentially microgrids, due to their islanded nature and limited size. As such, some key differences in the assumptions in system analysis are listed in Table 1.1.

While experience from land-based power systems has been beneficial in maritime power system protection, the increasing complexity of maritime power systems, means that this may not continue to be the case [7, p16]. This complexity includes demands for power density and efficiency, new flexible power system designs with a high degree of redundancy, as well as variable generation, loads and system configurations [1, 3, 4]. To ensure continuity of service in future maritime power systems under these conditions, an examination of relay protection is required.

Table 1.1: Key differences in assumptions in land-based and maritime power systems [1,3,7, p16].

land-based power systems	Maritime power systems
In most cases, the system electrical frequency can be assumed to be constant at 50 or 60 Hz. Individual loads are small compared to the generation units and the inertia of land-based systems is generally large. Several generators with individual PSS and damping limits the extent of rotor oscillations	The electrical frequency of maritime power systems is most often rated at 50 or 60 Hz, but cannot be assumed to be constant, even during normal operation. The relative size of loads such as propulsion motors to the inertia of the systems, as well as a need for fast acting load sharing schemes, cause deviations from the rated frequency.
land-based distribution networks are often a mix of overhead lines and cables, with lengths ranging from a few 100 meters up to around 100 kilometres depending on the specific voltage level and the country.	In maritime power systems, electrical distances are short, often less than 100 meters, leading to strong coupling between individual gensets, as well as between generation and loads. The impedance of tie lines is often small to negligible.
In land-based power systems, system loading is forecast and the generation capacity is planned accordingly. Any deviations from the load profile are picked up by pre-planned reserves acting as slack generators.	The load profile of maritime power systems is highly variable, both in terms of load sizes but also load types. The same power system may have periods with systems loads that are almost exclusively induction motors, and other periods where the load is almost exclusively the propulsion system. With a highly variable load, planned power generation is impossible and maritime power systems rely on fast acting load sharing schemes using droop control to meet variable power demands.
Short-circuit(SC) power in a land-based power system may vary based on the geography of the system, however, it is usually constant for any given location.	SC power, and by extension SC currents, are highly variable in maritime power systems, due to the variability of generation and loads. For both economic reasons and to ensure continuity of service, maritime power systems are expected to operate with different amounts of gensets connected.

1.1.4 Relay Protection of Maritime Power Systems

To ensure power system reliability, protection relays must be able to correctly detect and isolate faults in the power system. This is to protect personnel and equipment and allow for the continued operation of the power system by utilisation of redundant tie-lines [5, p52]. The common types of relay protection utilised in maritime power systems are listed in Table 1.2.

Table 1.2: Common protection types for each system component in maritime power systems [7, p28,9,10, pp212-224]

Component	Protection types.	
Generator	Instantaneous OC (ANSI 50)	Inverse-time OC (ANSI 51)
	Undervoltage (ANSI 27)	Overvoltage (ANSI 59)
	Excitation Loss (ANSI 40)	Overfluxing (ANSI 24)
	Reverse-phase (ANSI 46)	Phase Balance (ANSI 60)
	Thermal (ANSI 49)	Frequency (ANSI 81)
	Directional power (ANSI 32)	Differential (ANSI 87)
Motor	Instantaneous OC (ANSI 50)	Inverse-time OC (ANSI 51)
	Undervoltage (ANSI 27)	Overvoltage (ANSI 59)
	Undercurrent (ANSI37)	Power Factor (ANSI 55)
	Rotor Stall (ANSI 51R)	Phase-Sequence (ANSI 47)
	Thermal (ANSI 49)	Frequency (ANSI 81)
	Loss of field (ANSI 40)	Differential (ANSI 87)
Transformer	Instantaneous OC (ANSI 50)	Inverse-time OC (ANSI 51)
Bus bar	Instantaneous OC (ANSI 50)	Inverse-time OC (ANSI 51)
	Differential (ANSI 87)	Ground Time Overcurrent (ANSI 51G)
Cable	Instantaneous OC (ANSI 50)	Inverse-time OC (ANSI 51)

Overcurrent (OC) relays are widespread in the maritime power system, since they are reliable in protecting equipment and personnel, but reliable relay coordination of OC relays is challenging in maritime power systems, due to variable generation and SC power, as well as system configurations containing loops and redundancy. In addition to OC relays, there are several methods of improving the protection selectivity of relays. These include distance protection (ANSI-21) for cables, differential protection (ANSI-87) for electrical machines, busbars and transformers and directional overcurrent protection (ANSI-67) [11]. Distance protection cannot be reliably utilised in maritime power systems due to short cable distances. Differential protection is used in maritime power systems for generator and motor protection, and sometimes it is utilised in busbar protection as well [7, p28]. To reliably use differential protection, the accuracy of current transformers(CT) is paramount and in maritime power systems, SC power is variable which makes CTs prone to saturation issues [11]. This can lead to over-sizing of CTs, increasing costs, weight and space requirements. Thus, differential protection is a valid option for select components such as generators and motors, but is not suitable throughout the power system. This leaves directional protection as an option for increasing selectivity of protection schemes in maritime power system protection. The main issue with directional protection is that in closed loop systems and systems with redundant connections, protection schemes can become complex [11].

1.2 Scope of Thesis

This thesis seeks to aid maritime industries in improving the selectivity of power system protection schemes during short-circuit faults, through the use of directional overcurrent (ANSI-67) protection in maritime power systems.

1.2.1 Problem Statement

Maritime power systems have a set of characteristics that are different from land-based power systems which may impact the performance and reliability of ANSI-67 protection algorithms. In addition, common power system configurations in maritime power systems provide challenges to the development of selective and reliable protection schemes for such systems. The main objective of this report is to evaluate ANSI-67 protection algorithms, in the context of closed-ring-multiple-infed maritime power systems and investigate protection schemes based on ANSI-67.

1.2.2 Objectives

Review a set of ANSI-67 algorithms and analyse the utilised polarisation methods for main switchboard busbar protection in a closed-ring-multiple-infed configurations.

Investigate the operation of relays utilising ANSI-67 in a benchmark maritime power system in a simulation environment, and validate relay models in an experimental setup.

Evaluate the performance of various polarisation methods for ANSI-67 protection, and analyse their impact on the development of protection schemes for closed-ring-multiple-infed maritime power systems.

1.2.3 Delimitation

To complete the objectives of this thesis within the constraints of this project and help focus the study, some limitations to the scope of the thesis are listed below.

Ungrounded systems. This thesis will not analyse the impacts of system grounding. In general maritime power systems exist with either high resistance grounding or ungrounded systems. In this report, high resistance grounding is used in models of a power system and as such any differences in power system protection in ungrounded systems compared to high resistance grounded systems, is not explored in depth. This limitation is made because, while it can be assumed that any results that are valid in a high resistance grounded system will also be valid in an ungrounded system, ungrounded systems would may study of additional phenomena such as overvoltages, restriking transient voltages and intermittent earth faults, which are not directly related to the core objectives of this thesis.

Phase angle measurement methods. When analysing polarisation methods for protection studies, a related study could be to investigate the effects of different phase angle measurement methods, on the accuracy of the polarisation methods during faults. While other phase angle measurement methods exists, the study of these will be outside of the scope of this thesis, and phase angle measurements are performed using fixed frequency Fourier Transform.

1.3 Summary

In this chapter a brief history of the electrification of ships is given. The main point of this is, that recent trends in maritime power systems will lead to more complex power systems in the future due to increased demands for efficiency, power density, reduced emissions and larger vessels. Continuity of service in maritime power systems is paramount, and it is ensured through redundant system design and reliable, selective relay protection. An overview is given, of the key differences in system analysis for maritime power systems compared to land-based power systems. Then, typical relay protection functions in maritime application is listed. One of the main challenges in the future of maritime power systems is to have sufficiently fast and selective protection schemes. Thus, the main objectives of this report are centred around investigating directional OC protection and evaluating its use in protection schemes for maritime applications.

2 | State of the Art

In this chapter, the concepts of developing a protection scheme based on ANSI-67 protection are outlined. This includes relay coordination and the basic concepts and functions in an ANSI-67 protection algorithm. Then possible polarisation methods are reviewed and compared based on literature studies.

2.1 Overview of ANSI-67

Directional OC protection (ANSI-67) is typically used in SC fault protection at locations with multiple fault current paths, as in figure 2.1. In maritime power systems the focus of Directional OC protection should be on 2-phase(PP) and 3-phase(3P). In systems with high SC currents, directional OC protection can be used for single-phase-to-ground(PG) fault protection, but this is not the case in maritime power systems. In maritime power systems, ground currents are low, due to the choice of grounding, and it can be challenging to distinguish between PP and 2-phase-to-ground(PPG) faults, in which case directional OC protection can be used to protect against PPG faults.

ANSI-67 functions by tripping when an overcurrent is detected in a specified direction, allowing for selective tripping depending on the location of the fault relative to the current transformer(CT). The overcurrent is simply a comparison between the measured current and a threshold, typically 1.1 or 1.2 of a nominal current[12, 83]. The nominal current can be determined by the current ratings of system components or the full load current(FLC), which is the largest current that can be expected in the system during normal operation.

The directional sensing of an ANSI-67 function requires a reference quantity to determine the direction of the fault. Detecting the current direction is typically done by comparing the angle of the measured

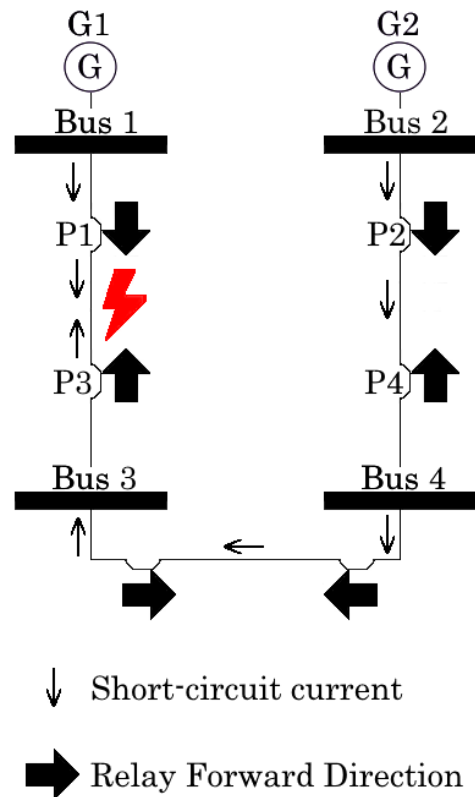


Figure 2.1: Example power system with fault fed from multiple sources.

current to a polarising quantity. The angle between the current and polarising quantity must be within a predefined margin to determine whether the current is in a forward or reverse direction.

There are several relevant choices of the polarising quantity which will be explained in detail later in this chapter, but a list of the most common ones are is presented here:

- The positive sequence voltage, called positive sequence polarisation[12, 13] .
- The phase voltage of the same phase as the measured current. This is called self-polarisation [14, p264].
- The phase to phase voltage of the remaining phases that are not the measured current. This is called cross-polarisation[14, p264,15, pp214-217].

In addition to the polarising quantity, the current can be chosen, though this is usually the measured phase current. This is detailed further for each polarisation method in the following section.

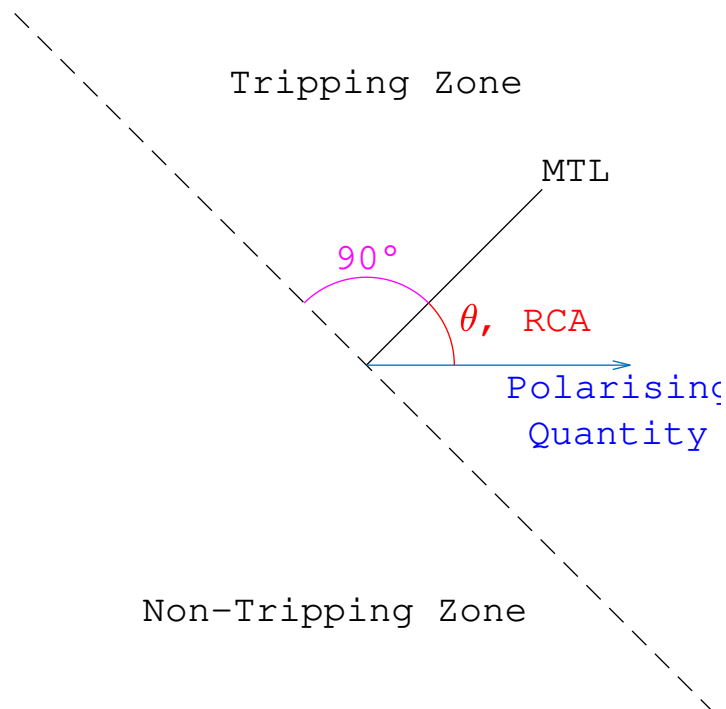


Figure 2.2: Polarising quantity and characteristic angle used to define the tripping zone.

To trip only when the current is in a specified direction, a tripping zone is defined using the polarising quantity. This tripping zone is usually a half-plane as shown in figure 2.2 and is defined by a line perpendicular to a characteristic quantity, conventionally called the Maximum Torque Line(MTL). The MTL is defined at a characteristic angle, θ , from the polarising quantity, sometimes called the Relay Characteristic Angle(RCA) in modern relay protection [12,15, p217]. This angle may vary depending on the specific system but in general, one RCA for each polarising quantity is enough to reliably detect the direction of the current in most systems.

If a current higher than the threshold is detected and it is in the forward direction of the relay, a fault is detected. This is called "pickup" and the time it takes from the fault inception to the pickup is referred to as pickup time or pickup delay [16].

Following pickup, the relay can trip, however, this may not be the correct action in the power system. An ANSI-67 algorithm will usually have an intentional delay to avoid false tripping and increase selectivity. False tripping is avoided by ensuring the pickup criteria are true for the duration of the delay. This is called coordination delay and in general ANSI-67 algorithms can be described by the flowchart in figure 2.3.

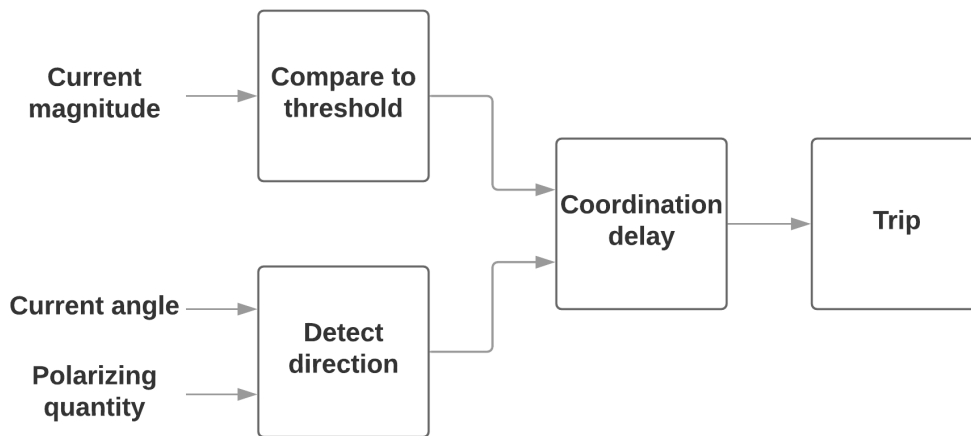


Figure 2.3: Basic outline of a directional OC protection algorithm.

2.2 Polarisation Methods

In this section, three polarisation methods are considered, and their advantages and challenges are described and will then be reviewed in the context of maritime power systems.

2.2.1 Positive Sequence Polarisation

A method that is commercially used for detecting the current direction, is using the positive sequence voltage, V_1 , as the polarising quantity and the positive sequence current, I_1 , as of the measured quantity [12, p. 83]. The advantage of doing so is that the angle between the V_1 and I_1 is unchanged by a forward fault. This is because the angle between the positive sequence components is exclusively dependent on the positive sequence impedance which, in the case of a balanced pre-fault system, is the equivalent system impedance. By assuming that the I_1 is lagging V_1 , the characteristic angle is chosen to be -45 degrees, resulting in a tripping zone as illustrated in figure 2.4 [13].

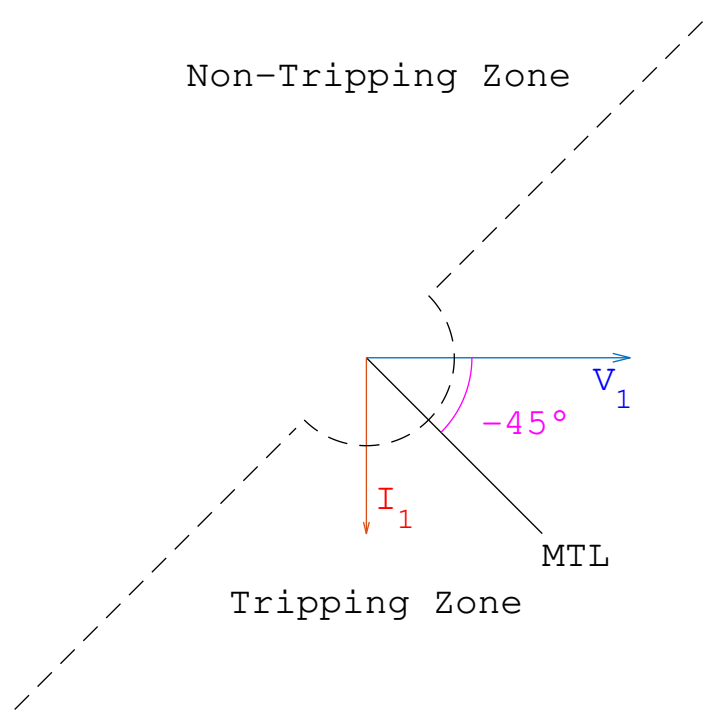


Figure 2.4: Positive sequence current compared to tripping zone.

Another advantage of positive sequence polarisation is that the positive sequence components are present for any fault. During a PP fault, negative and positive sequence components will be present, but during a 3P fault, only positive sequence components exist. However, at locations close to the fault, the phase voltages are nearly zero, which makes determination of the angle between V_1 and I_1 difficult. A method of handling this is to utilise a memory function when the voltage drops below a threshold, to remember the pre-fault angle of V_1 [12]. This memory should last for as long as needed and take the time grading of the relay into account. The pre-fault angle can be used when the polarising quantity is V_1 , as this angle is unchanged during a fault, however, the confidence of the stored angle will drop over time and should not be used indefinitely [13, p. 7].

2.2.2 Self-Polarisation

When the phase voltage of the same phase as the measured current is used for polarisation, this is called self-polarisation. Letting x and y indicate two different phases among phase a, b or c, three types of self polarisation exists and their polarising angles are calculated as listed below.

- $V_x/I_x, \phi = I_x\angle - V_x\angle$
- $V_{xy}/I_x, \phi = I_x\angle - (V_x - V_y)\angle$
- $V_{xy}/I_{xy}, \phi = (I_x - I_y)\angle - (V_x - V_y)\angle$

For V_x/I_x and V_{xy}/I_{xy} , the characteristic angle is commonly chosen as -45° as it is assumed that the

current lags the voltage, but the angle can be adjusted to -30° or -60° in systems with especially low or high X/R ratios [17, pp. 45-48]. In the case of V_{xy}/I_{xy} polarisation the characteristic angle is changed to either -30° or -90° depending on which phase-to-phase voltage is used as the polarising quantity as is illustrated in figure 2.5. In this example, the measured current is phase a.

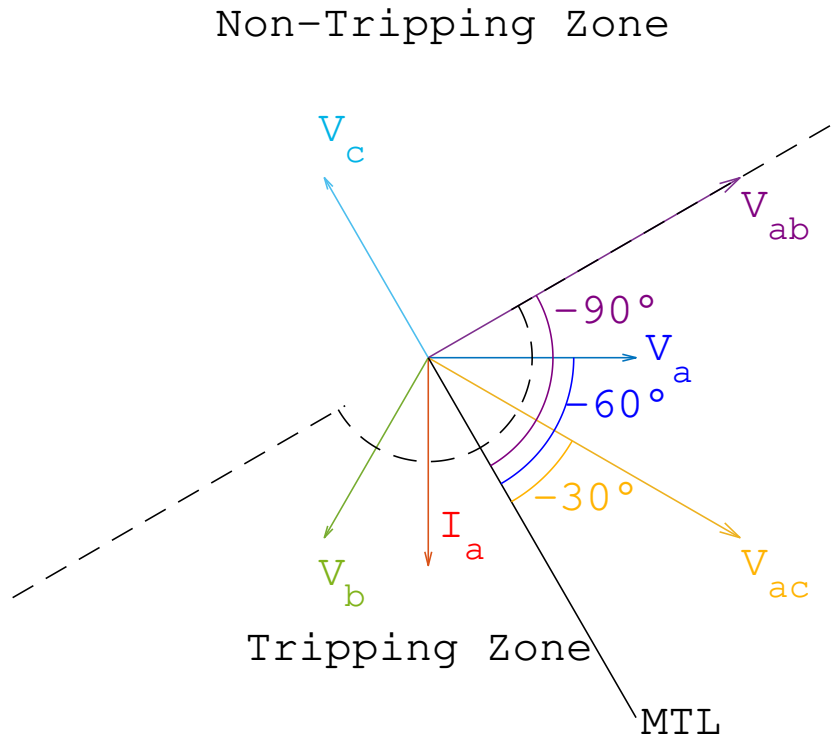


Figure 2.5: Phase a current compared to tripping zone defined by either phase a voltage or voltage difference from a to either remaining phase.

When using self-polarisation the sequence components need not be calculated as the measured quantities from the CTs and VTs can be used directly, depending on VT configuration. However, self-polarisation has similar challenges to those of positive sequence polarisation. During a 3P fault, both the phase and phase-to-phase voltages become close to zero at the fault location. Thus, the relay must remember the angle of the voltage pre-fault and use this as the polarising quantity for a short time following the fault. This is the case when using either V_x or V_{xy} as the polarising quantity.

During a PP fault while V_x is the polarising quantity, note that the voltage angle of the faulted phases will change and become equal. This is a disadvantage of V_x self polarisation as the phase angle estimation cannot be accurately performed during the transient of the polarising voltage. At best this will slow the operation of the relay and at worst this may cause the current to be determined in the wrong direction during the voltage transient.

During a PP fault if V_{xy} is the polarising quantity it is possible to choose y such that the polarising quantity is the phase-to-phase voltage of the faulted phases, which becomes close to zero. In this case,

the pre-fault voltage angle can be used as previously explained. Alternatively, it is possible to use the last phase-to-phase voltage, between the healthy phase and the phase of the current. In this case, the characteristic angle must also change from -30° to -90° or from -90° to -30° , as the polarising quantity is changed.

2.2.3 Cross-Polarisation

Cross polarisation is another method that is used for commercial relays with directional permissive tripping [16]. This method relies on the phase-to-phase voltage of the phases that are not the phase of the measured current. To simplify the determination of the characteristic angle, in this case, the polarity of the voltage measurement should be consistent, but can be chosen arbitrarily i.e. V_{cb} or V_{bc} . When assuming the current lags the phase voltage, two typical characteristic angles can be defined as in table 2.1. The resulting tripping zone is illustrated for the phase a current in figure 2.6.

Table 2.1: Characteristic angles based on [15, p. 214-217], for each combination of voltage and current in cross-polarisation.

Measured Current	Polarising Quantity	Characteristic angle
I_a	V_{bc}	45°
I_b	V_{ca}	45°
I_c	V_{ab}	45°
I_a	V_{cb}	-135°
I_b	V_{ac}	-135°
I_c	V_{ba}	-135°

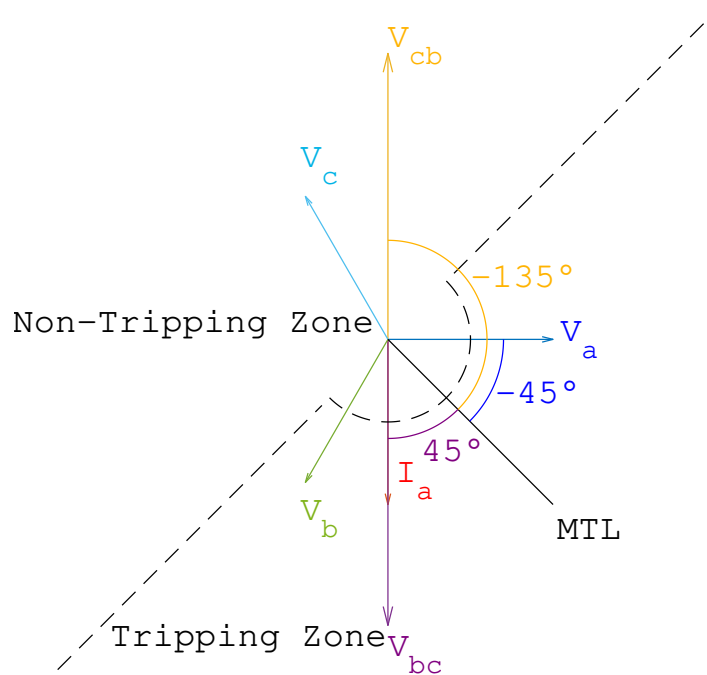


Figure 2.6: Phase a current compared to tripping zone defined by phase-to-phase voltage of remaining phases.

During a 3P fault, the voltages may be too low to accurately measure, which presents the same challenges as described for self- and positive sequence polarisation. This can be solved by storing the pre-fault voltage phasors and using those as the angle of the polarising voltage.

During a PP fault, one of the phase-to-phase voltages becomes close to zero, but an advantage of cross polarisation is that this voltage is used as the reference for the healthy phase. That means the polarising quantities of the faulted phases does not change drastically which may allow for faster determination of the polarising angle than for other polarisation methods.

2.2.4 Polarisation Methods in Maritime Power Systems

To consider how the described polarisation methods compare to each other in a maritime power system, some considerations that are in common for all the polarisation methods must be observed.

Pickup of other fault types. It is noted that while each polarisation method is described for PP and 3P faults, the polarisation methods are not dependent on these fault types to function. It follows that if a current higher than the threshold is observed as a result of a PG or PPG fault, the relay will still be able to detect the fault and trip accordingly. As long as the assumptions behind the choice of characteristic angle hold, the current direction detection will function as intended. However, in systems with insulated grounding, PG fault currents are mostly capacitive and in this case, the directional element may be misleading.

Low ground fault current magnitude. Due to the grounding topologies utilised in maritime power systems i.e. insulated grounding or high resistance grounding, it can be assumed that ground fault currents are low. This means that for PPG faults the zero-sequence current will be small compared to the positive- and negative-sequence and the relay will pickup PPG faults as though they were PP faults. It also follows that while the direction of PG faults may be estimated it is unlikely that the measured current will be above the current threshold. It can therefore be expected that, in addition to PP and 3P faults, each polarisation method will pickup PPG but not PG faults.

Short electrical distances. All the described polarisation methods share a challenge during 3P faults as the polarising quantities become zero close to the fault location. In land-based systems, when a 3P fault occurs close to the VT, sometimes the fault can be picked up by a neighbouring relay. This can be a reliable method of tripping the faulted component, though at the cost of some selectivity. In maritime power systems, electrical distances are short and it cannot be assumed that a neighbouring relay is far enough from the fault to be able to accurately measure the voltages. Therefore, neighbouring relays cannot be relied upon to trip in case the relay in question is unable to determine the current direction.

While these things are true for all the described polarisation methods in a maritime power system, the

considerations made for the individual methods are summarised in table 2.2.

Table 2.2: Characteristic angle and important considerations for each described polarisation method.

Polarisation method	Characteristic angle	Considerations
Positive sequence polarisation	-45	Positive sequence components are present during all fault types. Requires voltage memory during 3P-faults.
Self-polarisation(V_x)	-45	Requires voltage memory for 3P faults types. Requires recalculation of voltage angle following the voltage transient during a PP/PPG fault.
Self-polarisation(V_{xy})	-90, -30 45, -45	May require less fault impedance than other methods to have a detectable voltage during 3P fault. Will depend on VT configuration. May require voltage memory during 3P fault. Advantages/disadvantages to using I_x or I_{xy} to calculate polarising angle are not well documented.
Cross-polarisation	-135, 45	May require less fault impedance than other methods to have a detectable voltage during 3P fault. Will depend on VT configuration. May require voltage memory during 3P fault. May require settling and calculation time during PP/PPG fault.

2.3 Relay Coordination

Provided that the relays are able to reliably detect the direction fault current, they must also act in coordination with other relays to selectively trip the faulted component.

2.3.1 Time Grading

A typical method of relay coordination is time grading, which is used to trip selectively in cases where multiple relays pickup the same fault. Such a case is illustrated in figure 2.7 in which P2, P3 and P4 all detect the same fault. If P2 trips the fault would be cleared, but Bus 2 would also be tripped unnecessarily, and the relays would not be selective. Thus, time grading is used to delay the operation of P2 and P3 until P4 has had a chance to act.

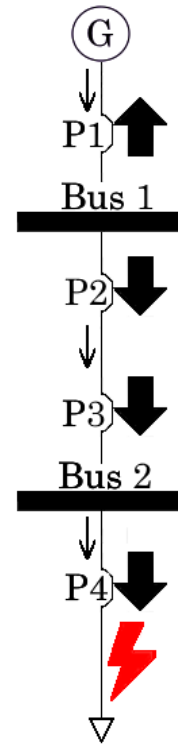


Figure 2.7: Single line diagram showing relays, P2, P3 and P4, in series such that all will detect the fault current.

There are two general types of time grading, definite and inverse time grading. Definite Time (DT) grading, as the name suggests is a constant time period that a fault must

persist to trip the relay. According to [16], the appropriate time delay can be estimated based on the operating time of circuit breakers(CB) and the pickup time of the relays but is typically around 150-300 ms pr. relay.

For inverse time grading, the delay is calculated based on the magnitude of the measured current, I_m , compared to the threshold, I_{th} . When k , α and β are parameters that can be adjusted to control the steepness of the time-current curve, the delay, t , can be determined by [16]:

$$t = \frac{k \cdot \beta}{\frac{I_m}{I_{th}}^\alpha - 1} \quad (2.1)$$

IEC categorises the commonly used time-current curves for a type of inverse time grading called Inverse Definite Minimum Time(IDMT), when $\beta = 1$, as:

- Standard Inverse (SI), $\alpha = 0.02$, $k = 0.14$
- Very Inverse (VI), $\alpha = 1$, $k = 13.5$
- Extremely Inverse (EI), $\alpha = 2$, $k = 80$
- Long Time Standard Inverse (LTSI), $\alpha = 1$, $k = 120$

The varied steepness of the time-current curves makes some of them act very slow at low current and very fast at high currents while others are less varied. Some of the time-current curves are illustrated in Figure 2.8.

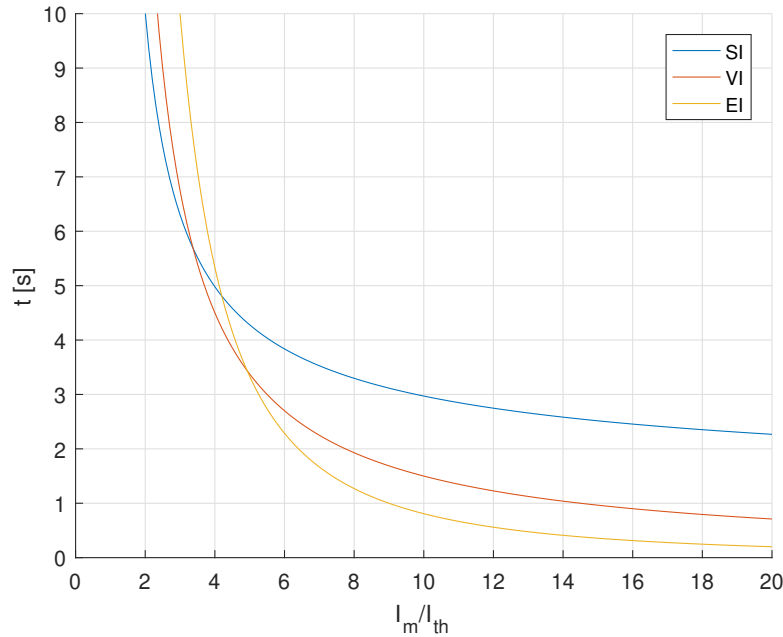


Figure 2.8: Time-current curve of SI, VI and EI IDMT.

Different tripping times at different OCs can be useful behaviour e.g. in asynchronous motor protection, to help the relay differentiate between transient OCs following a disturbance and persistent fault

currents. Another method of achieving this type of selectivity is by mixing time-current curves. An example of this is using SI for low magnitude currents and DT for high magnitude currents as in Figure 2.9. In this case, the I_m/I_{th} threshold is 10. This can be used in cases where IDMT increases the selectivity of relays, but is too slow to protect components at high current magnitudes.

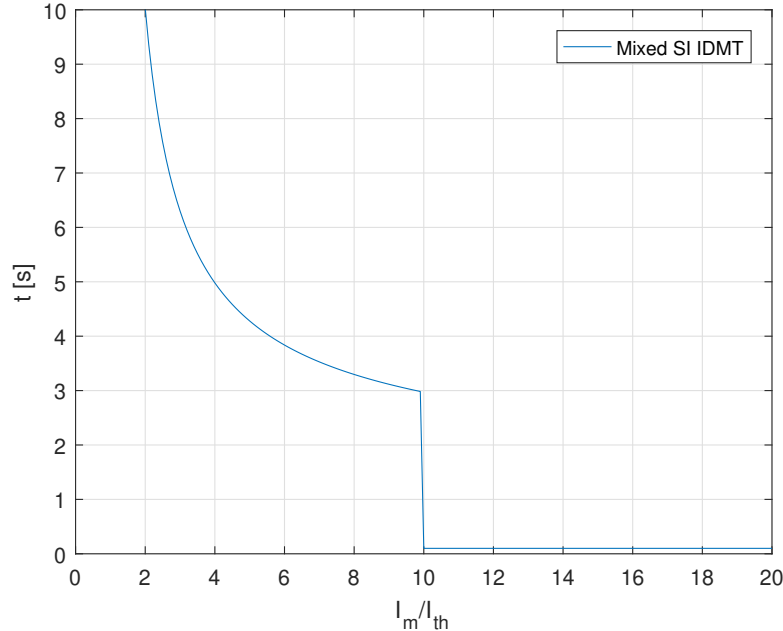


Figure 2.9: Time-current curve of mixed SI IDMT and DT.

2.3.2 ANSI-67 Protection Schemes

With an overview of the functions of an ANSI 67 algorithm described, it is prudent to consider how these functions can be used to selectively trip faulted components in a maritime power system. While time grading is a common method for selective tripping for feeder or cable fault, it is not sufficient in busbar protection or for cables in a closed loop configuration [18]. In maritime power systems electrical distances are short, which means that fault current may be too high to allow for the delay caused by time grading, as this may cause component damage or loss of synchronism in the generators. Additionally, SC power is variable and SC currents may be too low for a single set of IDMT settings to be selective. Therefore other methods can be utilised to allow for selective tripping when time grading is not sufficient.

Communication between the relays can be introduced to allow each relay to monitor which other relays in the system detect the fault. This can be utilised to block or permit relays and to trip the CBs, depending on the current system configuration and the states of multiple relays. Additionally, it is a simple task to add a signal to indicate when an overcurrent is detected in the reverse direction. This is called bi-directional overcurrent protection and is simply a second protection function with a 180° shift of the RCA [19]. With communication and bi-directional relays, the common use of ANSI 67 for

feeder protection can be expanded to cases relevant to maritime power systems, that would otherwise rely on differential or less selective protection OC protection schemes. These cases are:

- Busbar protection with 3 or more feeders [14, 16].
- Feeder and busbar protection in a multiple infed closed-loop [14, 16].
- Generator protection of parallel generators [5, pp96-97].

Busbar protection

In the example, in Figure 2.10 time grading of 200 ms is utilised and relays that are not time graded have been arbitrarily set at 50 ms coordination delay. The relays in this system will selectively trip for faults occurring in the generators, cables and remaining of the system. The directions chosen as the forward direction of the relay are a typical example of the settings used for generator and feeder protection because it can be assumed that the detected fault current will originate at the nearest genset.

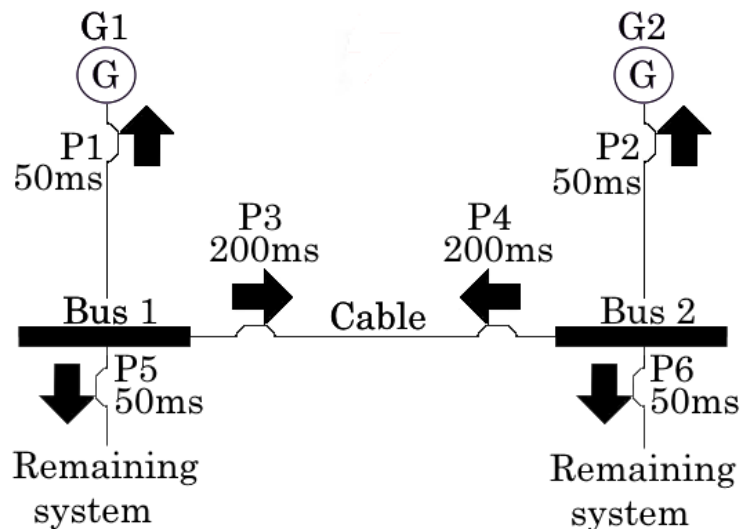


Figure 2.10: Partial outline of a directional OC protection scheme, using bidirectional relays and permissive tripping.

In case of a fault at Bus1, P1, P2 and P3 will all detect a reverse bias fault current while P4 will detect a forward bias fault current. In order to selectively trip Bus1, a Boolean check can be made as below when F and R denote the forward and reverse bias of the relay respectively.

Trip	P1(F)	P1(R)	P3(F)	P3(R)	P5(F)	P5(R)
Bus1	0	1	0	1	0	-

A similar logic can be constructed for Bus2 and is easily expanded for more feeders. This allows for selective tripping of busbars using only the states of directional overcurrent protection relays.

Closed loop configuration of gensets

In the example, in Figure 2.11 three busbars with one genset each are connected in a loop. No time grading is included as there is no meaningful way to define the first relay in the loop, however, time grading could still be used to increase selectivity for faults in the remainder of the system, which is not illustrated here. Note that for closed loop protection the forward direction of the relays is the same, defining a forward direction in the loop. Selective tripping of cables and busbars in the loop can be achieved by using Reverse Blocking (RB)[20]. RB functions by blocking the relay located in reverse current direction of a fault detection e.g. if P8 picks up a fault, P7 is blocked. Combining RB with interlocked pairs of CBs the resulting logic for the relay in the loop is shown in Table 2.3.

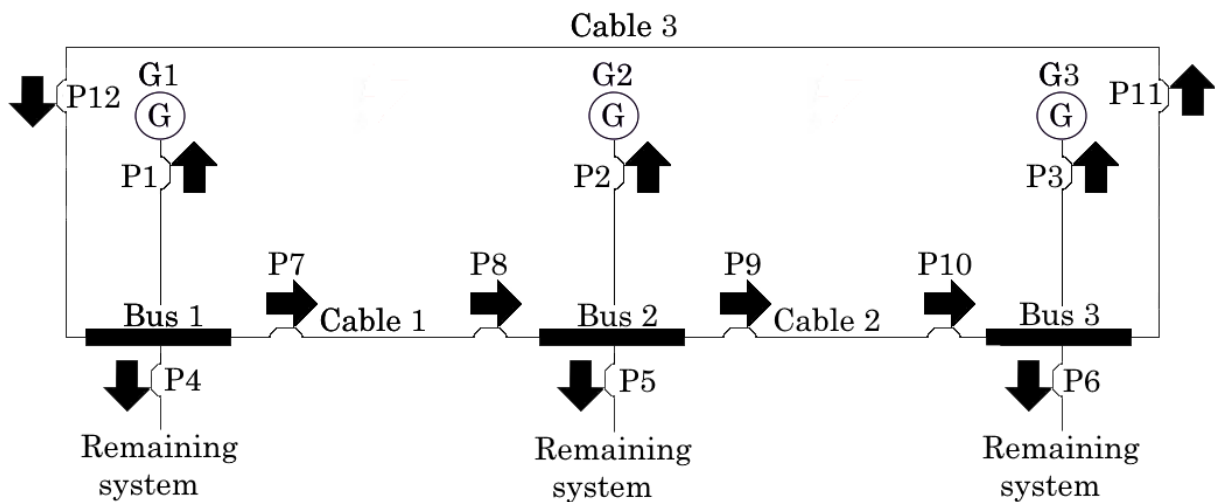


Figure 2.11: Partial outline of a directional OC protection scheme, using reverse relay blocking and interlocking CBs.

Table 2.3: Logic of RB and interlocked CBs in the loop.

Relay	Trigger	Action
P7	P8 High	Block
	P12 Tripped	Trip
P8	P9 High	Block
	P7 Tripped	Trip
P9	P10 High	Block
	P8 Tripped	Trip
P10	P11 High	Block
	P9 Tripped	Trip
P11	P12 High	Block
	P10 Tripped	Trip
P12	P7 High	Block
	P11 Tripped	Trip

When interlocking the CBs at the ends of each cable, this method provides complete selectivity for

busbar and cable faults in the ring. This method may be combined time grading for the selective protection of the remaining of the system, however, the RB operations including communication delays, must be faster than the smallest time grading in the system and take precedence.

2.4 Summary

In this chapter, an overview of the principle of directional OC protection is given. Three commercially available polarisation methods are reviewed and their advantages and challenges in the context of maritime power systems are identified. Relay coordination is then explained and several key concepts are explained, including time grading, bidirectional protection, CB interlocking and reverse relay blocking. Some initial directional OC based protection schemes are examined.

3 | Maritime Power System Modelling

This chapter presents an overview of a generalised maritime power system for fault protection studies. The models for each system component are described and several fault and load cases are defined. Finally, the model is verified through simulation.

3.1 System Overview

To model a maritime power system suitable for the general study of fault protection in such systems, the characteristics described in Section 1.1 are considered. The resulting system is outlined in Figure 3.1.

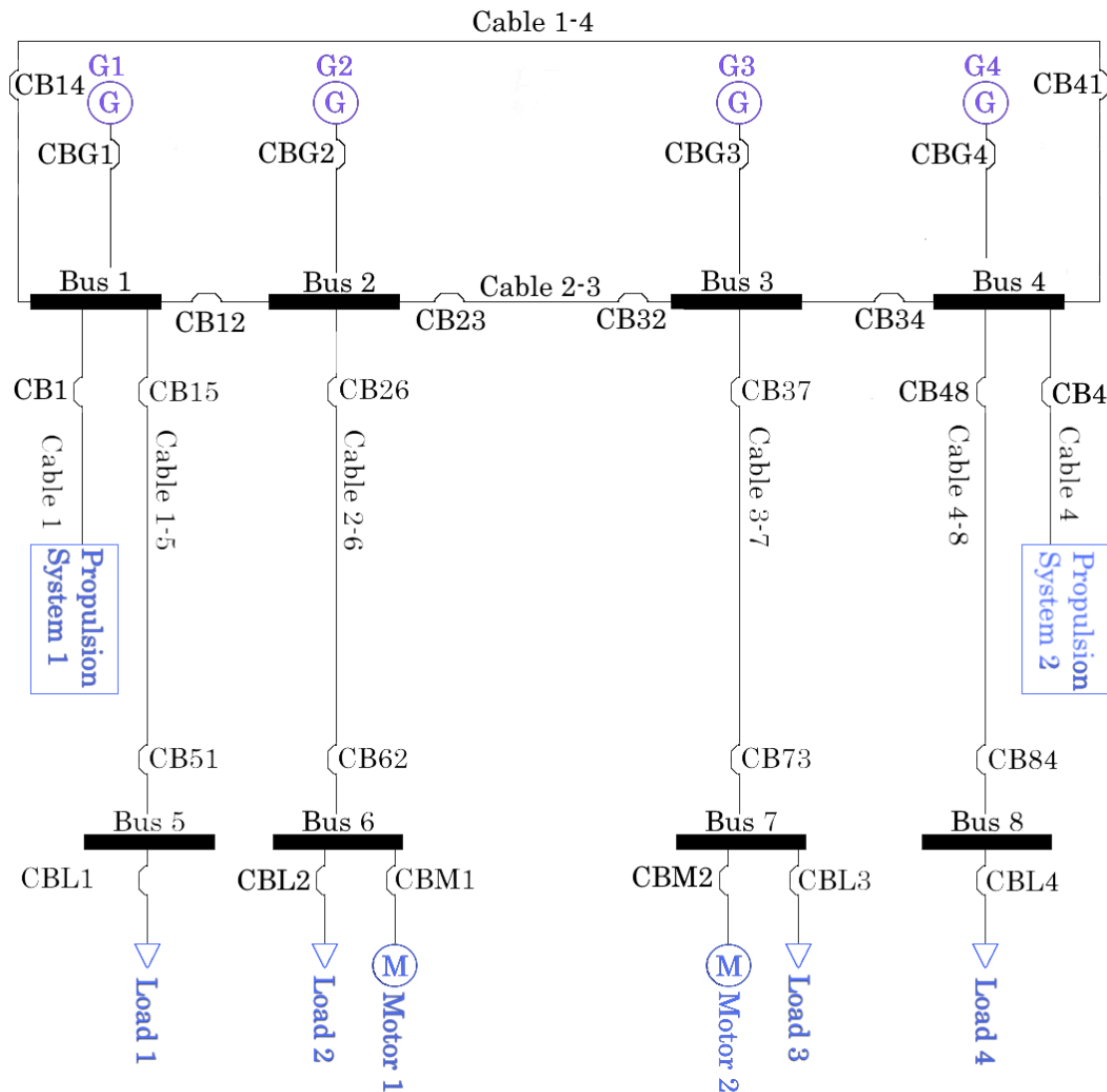


Figure 3.1: Diagram of maritime power system model.

The shown system has four diesel gensets connected in 2-by-2 MSBs and configured in a closed ring. The loop provides redundant connection of components such that for any fault location only the faulted component need be de-energised. In case of a bus or cable fault, that means that any loads dependant on the component is also disconnected. Thus, the loop only has sufficient redundancy in the system under the assumption that a single propulsion system is sufficient in bringing the vessel to a harbour in case of a fault, as one propulsion system could be disconnected in case of a fault at Bus 1 or 4. There are two propulsion systems, each connected at one of the pairs of MSB through a short cable. Additionally, hotel loads and motor loads representing bow thrusters or other auxiliary equipment are connected at the remaining busbars, namely Bus 5-8, connected to the main switchboard through cables. The power system model is implemented and tested using simulation software, Simulink®.

3.2 Component Models

In this section, the modelling of each component of the power system is described including generators, propulsion systems, passive and motor loads, as well as cables. The relevant component parameters are presented and the various transformers in a power system and their impact on fault protection studies are discussed as these are not explicitly modelled.

3.2.1 Generators

In maritime power systems, diesel generators are a common type of generation, though it is sometimes used in addition to gas turbines or other generation. For the modelled system the generation is simplified by letting all generation be diesel generators. There are four 4.5 MVA, 60 Hz, 6.6 Kv diesel generators, modelled based on the diesel generators in the Simscape Power System example "Marine Full Electric Propulsion Power System" [21]. As such they are salient pole generators with parameters given in table A.1 in Appendix A. Thus, the total rated generation in the power system is 18 MVA. The generators are grounded through a high resistance of 600Ω , chosen based on the system voltage and the maximum allowed earth fault current in maritime power systems [8]. The generator model includes speed governor and excitation systems and is structured in simulation software as in Figure 3.2.

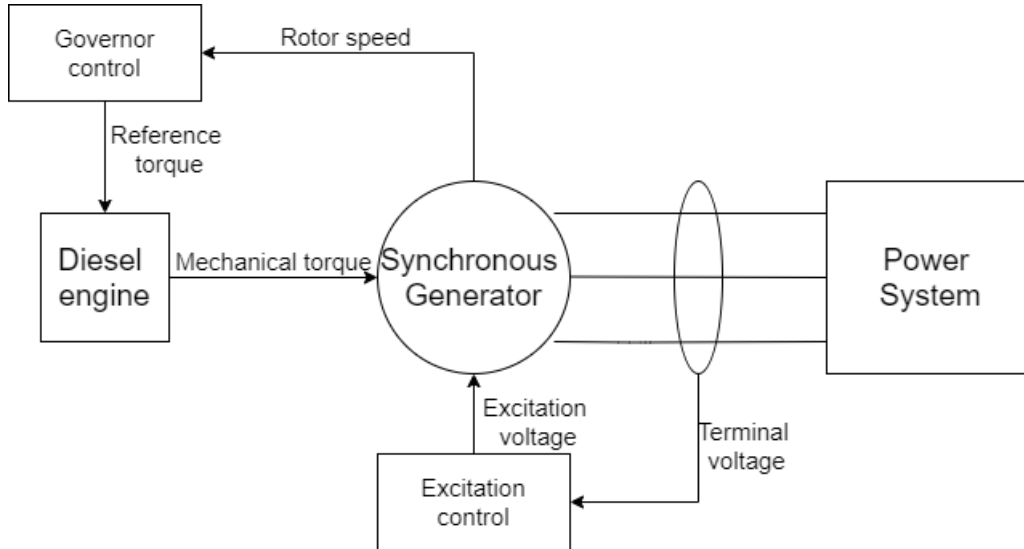


Figure 3.2: Structure of genset model.

Exciter: For the generators the AC1A excitation topology is used based on IEEE's recommendations in [22] using default Simscape values as in [21]. The AC1A topology is modified for this system by adding a lower limit to the output of the controller with the value of 10^{-6} rather than the default of 0. This limit prevents a division by zero when calculating the field voltage of the generator during the startup of the asynchronous motors and exclusively impacts the transient initialisation of the model. This changes nothing in the dynamic fault behaviour. More details can be found in Appendix A.

Governor: The governor is implemented with droop control acting on a PI control. The governor acts on a diesel generator modelled as a constant delay acting on an ideal torque source, with inertia and time constant specified in Table A.1 in Appendix A. The droop control is necessary when operating multiple generators in parallel as is the case for this system, as it facilitates load sharing as described in Section 1.1.

3.2.2 Propulsion System

The propulsion systems 1 and 2 can be a large portion of the system load and they are highly variable. Thus the model of them should have the ability to include variance in the propulsion loads when needed. In addition, modern propulsion systems are connected through drive systems as described in Section 1.1. The drive system performs voltage or speed control on the motor in the propulsion engine and as such isolates subtransient and fault behaviour of the motor from the power system. Thus, for fault, dynamic studies such as the one performed in this report the propulsion motor can be modelled as a variable resistance, as it supplies no SC power in this case. The drive system is then modelled as a rectifier, supplying the variable resistor with an average voltage. The output voltage of the rectifier,

V_{DC} can be calculated by:

$$V_{DC} = 3 \frac{\sqrt{2}}{\pi} V_{AC} \quad (3.1)$$

thus the resistance for a given loading of the propulsion system is calculated as:

$$R_{prop} = \frac{V_{DC}^2}{P_{prop}} \quad (3.2)$$

V_{AC} denotes the RMS phase-to-phase input voltage of the rectifier, R_{prop} is the resistance value of the load, P_{prop} is the power consumption of the propulsion system. In addition to the drive system, the propulsion system is connected to the power system through an isolating transformer, however, this component is neglected in the system overview in Figure 3.1. This is done because the impact of an isolating transformer in combination with the drive system becomes negligible to the fault dynamics in the system. Firstly, according to example isolating transformer in [23], the transformers will typically change the efficiency of the drive system by 1-2 %. Regardless of load condition, this change in power consumption of the propulsion systems will have no significant impact on the fault current magnitude during any SC fault. Secondly, the isolating transformer will have no impact on the phase angle of the fault current, which becomes apparent when examining the possible fault cases. For faults located on the primary side of an isolating transformer, i.e. the entirety of the system except for the drive system and propulsion thruster, no fault current will be supplied through the transformer because the drive system isolates the propulsion thruster and prevents the propulsion system from supplying any SC current. For fault locations on the secondary side of the transformer, the phase shift caused by the transformer will only be present in the current seen on the primary side of the transformer as the equivalent series impedance which is assumed to be negligible based on the low power loss in the isolating transformer.

3.2.3 Motor Loads

Motor loads 1 and 2 model the remaining motor loads in a maritime power system such as pumps, side or bow thrusters and auxiliary equipment. These are typically asynchronous motors and exist as both wound rotor and squirrel cage motors. The main difference in the dynamic behaviour of a wound rotor and a squirrel cage motor is that the wound rotor has a higher stator resistance and will typically supply lower SC currents and starting currents[24].

Squirrel cage motors are more common in maritime systems as these are usually used as bow thrusters [5]. The motors in this project will be modelled as squirrel cage motors based on the asynchronous motor load in the Simscape Power System example in [21]. The impedances of the motors are the default values in Simscape Power Systems and are given in per unit, which makes scaling the motor

to a given power and voltage level a simple task. However, the modelled motors represent multiple different motor loads lumped at the busbars 6 and 7, which means an aggregate of the various motor loads in the system must be found to properly model the dynamic behaviour of the motors during a fault.

Aggregation of induction machines

In case all of the motors have the same impedances per unit, these can be kept constant. The inertia and rated power of the aggregate machine then become the sum of the inertia and rated power of the parallel machines. This is the simplest possible case for the aggregation of parallel induction machines and the performance of this method is verified in Appendix B. For the purposes of this report, this method is sufficient as there is no need to use more specific induction machines than the default values of the Simscape Power System squirrel cage motors. The resulting motor parameters used in the power system model are given in A.2 in Appendix A.

For some combinations of induction machine, it is prudent to utilise more specific machines e.g. when lumping squirrel cage motors with rotor wound motors, or when aggregating machines of significantly different sizes. In this case, an alternative method of aggregating the induction machines is suggested based on [25] and this is presented in Appendix B.

3.2.4 Hotel Loads

Other than motor loads and propulsion loads, all additional loads such as heating, lighting, utilities etc. are modelled as lumped loads located at Busses 5 through 8. These are the hotel loads that are modelled as constant impedance loads, with a unity power factor. In reality, these would be a combination of load types, mostly connected through some topology of rectifier, with some being constant impedance and others being constant power or current loads. However, for fault dynamic studies the main characteristic of interest is whether they provide any SC current or otherwise affect the system behaviour during a fault. As none of the common load types in the hotel loads provides any SC power, these can be simplified as constant impedance loads. It is noted that these will be connected at a consumer level voltage rather than at 6.6 kV, however, the lumped loads are placed at 6.6 kV and the modelling of the transformers that allow for this simplification is discussed later in this section.

3.2.5 Cables

The cables in the system are modelled as π -models, as this is a sufficient model for cables of short lengths, which is the case in maritime power systems. The cables are three-core armoured copper cables and two cable cross-section sizes are chosen. 35mm^2 is chosen for the cables supplying Bus 4

and 8, as these are the smallest loads while $150mm^2$ is used for the remaining cables. The length of the cables is chosen by assuming generation and propulsion are located somewhat close to each other while the remaining loads are spread out and connected through long cables. As such two cable lengths are used which are arbitrarily chosen as 100m and 200m and the resulting cable parameters are shown in table A.3 in Appendix A.

3.2.6 Transformers

In a maritime power system, there are commonly two types of transformers. These are step-down transformers from distribution to consumer level and isolating transformers, for propulsion systems and other loads connected at the MV level. These are not included in the model overview in Figure 3.1 as the modelling of these is included in the modelling of the propulsion systems and cables. This can be done for the fault studies performed in this report, provided the transformers have negligible impact on the fault current dynamics. The impact of the isolating transformers is analysed in the context of the modelling of the propulsion system in Section 3.2.2.

Regarding the step-down transformers, these would be in series with the cables connecting the main switchboard to the load busses. To verify that the transformers can be lumped with the cables in this manner the equivalent series impedance is calculated for an example transformer, which can then be compared to the cables with which they are in series in order to quantify the impact of the transformers. The connections of the transformers are assumed to be delta-delta, as the power system is usually a three-wire system at medium voltage and this is common practice. Thus, there will be no transfer of zero sequence components and only the series impedance need to be evaluated. The series equivalent impedance of the transformers is calculated by Equation (3.3) derived from [26, pp. 101-105].

$$R_{tr} = \frac{P_{Cu} \cdot V_2^2}{S_{tr}^2}, \quad X_{tr} = \frac{v_{sh} \cdot V_2^2}{S_{tr}} \quad (3.3)$$

P_{Cu} is the copper loss, V_2 is the secondary voltage, v_{sh} is the SC voltage and S_{tr} is the transformer rated power. For an example step down transformer the parameters and results are given in Table 3.1. The transformer parameters are found for a given power rating using [27, p. 46]

Table 3.1: Example transformer parameters and equivalent series impedance.

Transformer type	V_1/V_2 [kV]	S_{tr} [kVA]	P_{Cu} [W]	v_{sh} [%]	Z_{tr} [m Ω]
Step-down transformer	6.6/0.4	2000	21000	6	0.84-j4.8

To quantify the impact of the transformer on the current angle, the change in X/R ratio caused by the transformer is calculated. The impedance of the Cables 1-5, 2-6, 3-7 and 4-8 in Table A.3 have an

X/R ratio at 60 Hz of

$$\frac{X}{R} = \frac{60 \cdot 2\pi \cdot 66.2 \cdot 10^{-6}}{53.6 \cdot 10^{-3}} = 0.4656 \quad (3.4)$$

While the X/R ratio of the transformer is,

$$\frac{X}{R} = \frac{4.8 \cdot 10^{-3} + 60 \cdot 2\pi \cdot 66.2 \cdot 10^{-6}}{(0.84 + 53.6) \cdot 10^{-3}} = 0.5466 \quad (3.5)$$

This change in X/R ratio corresponds to a change in angle of approximately 2.2° , which will have a negligible impact on the fault protection studies performed in this report and thus the transformers are not modelled.

Additionally, VTs and CTs are realised in simulations as ideal components, introducing no phase shift, power loss or saturation. Phasor measurements are performed using Fourier analysis assuming fundamental frequency at 60 Hz.

3.3 System Case Definitions

With the base power system model described and parameters defined, the variable parameters in simulations must be defined. These are the fault locations and the system loading, which are defined in a case structure.

3.3.1 Fault Locations

The illustrated power system is symmetrical, provided the component parameters are equal in each half of the system, which means that for fault protection studies it will not be necessary to analyse the operation of the relays for every possible fault location, because the operation will be predictable based on analysis of faults in a unique half of the system. As such the relevant fault locations are shown in figure 3.3.

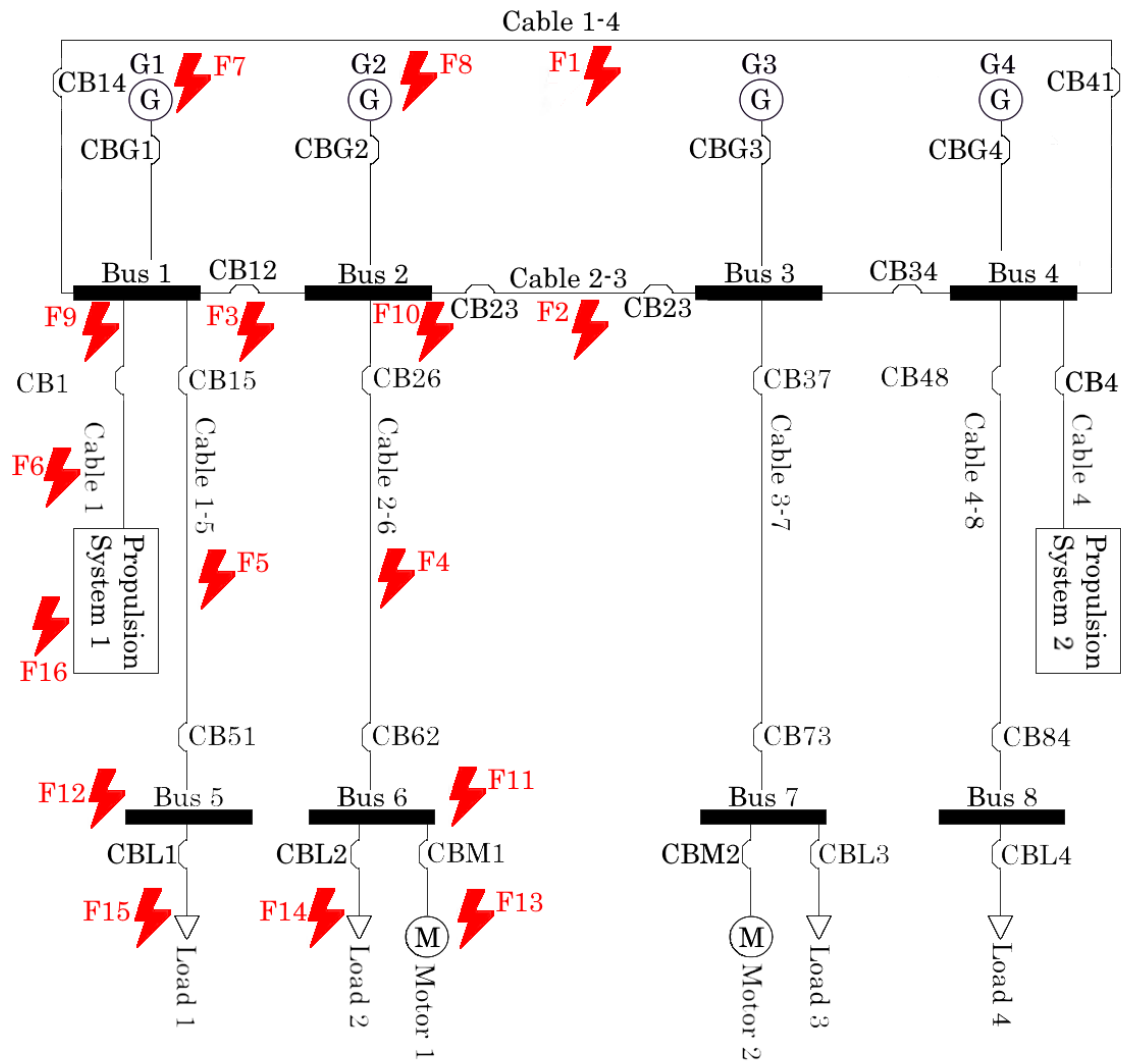


Figure 3.3: Fault locations of interest.

In this section, the fault locations are denoted F1-16 as defined in Table 3.2, as these are the names used internally in simulation software. In following sections the faults will be referred to by the component name where they are located.

Among the 16 initial fault locations, there are several redundant faults, for components in the series. F6 and F16 will be indistinguishable by relays in the remaining system. Only a relay between Cable 1 and Propulsion System 1 would be able to distinguish between these two fault locations and such a relay is not included in the model because there would be no reason to keep the cable energised if the propulsion system is faulted, while it would be impossible to energise the propulsion system without the cable. Thus, for fault protection studies F16 can be neglected.

A similar logic can be applied to F5, F12 and F15, however in this case all three fault location will still be analysed to mitigate the effect of simplifications made in the system. The simplification being that only one load is connected at the busbar because the loads can be lumped. In the case of multiple loads, the relays should be able to selectively trip the faulted component rather than the entire busbar. This is also evident at Bus 6 where multiple loads are connected, thus F11, F13 and F14 are all relevant fault locations to ensure selectivity.

3.3.2 Load Case Definitions

The loading of a maritime power system is variable, several load cases are defined for different operational modes and ship classes. As most of the loads are passive constant impedance loads, it is unlikely that these will have an impact on the protection studies performed in this report, provided the total loading of the generators is within reasonable limits. Therefore each load case is designed such that the generators operate at approximately 50% of rated power. However, the motor loads provide additional SC power and may introduce dynamic behaviour relevant

to the protection studies. Therefore, the load cases are chosen to have a varied ratio of motor loads and passive loads in the system. There are three load cases to be defined and the loads in each load case are shown in table 3.3.

Motor dominant load is a load case in which the asynchronous motors are 2/3rds of the system load. This load case can represent large vessels with large motors and pumps such as oil tankers, or smaller vessels where auxiliary propulsion engines can be as large as the main propulsion thrusters. The motor dominant load case is included to quantify the effects of a high ratio of asynchronous motor loads, as these may impact the operation of the ANSI-67 relay due to their SC power.

Thruster dominant load can commonly be assumed for large cargo vessels, where the main mission of the vessel is to travel long distances and the ships spend a high proportion of time in cruising mode. For such vessels, the propulsion systems can be as large as 50% of the rated power of the power system. It is unlikely that it will operate at 100% of capacity and for this load case 1/3rd of the rated power

Table 3.2: Fault locations

Fault name	Fault type and location
F1	Cable fault at Cable 1-4
F2	Cable fault at Cable 2-3
F3	Bus-tie fault between Busses 1 and 2
F4	Cable fault at Cable 2-6
F5	Cable fault at Cable 1-5
F6	Cable Fault at Cable 1
F7	Generator fault at G1
F8	Generator fault at G2
F9	Busbar fault at Bus 1
F10	Busbar fault at Bus 2
F11	Busbar fault at Bus 6
F12	Busbar fault at Bus 5
F13	Load fault at Motor 1
F14	Load fault at Load 2
F15	Load fault at Load 1
F16	Load fault at Propulsion system 1

of the system powers the propulsion thrusters, corresponding to 2/3rds of the total load.

Varied load is biased towards a larger part of the load being the propulsion system, as this is the common case for most vessels, however, the hotel loads and motor loads are still a large part of the system. As such the load types are somewhat balanced in this load case, and this case can be used as a reference for the two other more extreme cases.

For the defined load cases the system is assumed to be symmetrical and thus all loads of the same types are equal. However, to perform studies of asymmetrically loaded systems it is a simple matter to change the individual loads, but this can be done on a test-by-test basis rather than defined as individual load cases.

Table 3.3: Individual load sizes in system with 4 hotel loads, 2 propulsion systems and 2 motor loads, for a total load 9 MW in each case.

Load case	Hotel load 1 and 4 [MW]	Hotel load 2 and 3 [MW]	Propulsion thrusters[MW]	Motor loads [MW]
Motor dominant load	0.5	0.0	1.0	3.0
Thruster dominant load	0.5	0.5	3.0	0.5
Varied Load	1.0	1.0	1.5	1.0

3.4 Model Verification

The dynamic behaviour of the generators is verified as well as the fault dynamics of the system. This is done for the power system with a Varied load, as this model includes operational motor loads, which will have an impact on the observed fault currents.

3.4.1 Generator Verification

Before observing the entirety of the modelled system, a test of the performance of the generator governor and excitation system is performed. This is done in a simplified power system containing a single generator, G1, connected through Cable 1-5 to a delta-connected constant impedance load of 0.5 pu power at unity power factor.

For the first test, the dynamics of the excitation system is examined by subjecting the voltage reference of the exciter to a step input of 0.05 pu. The resulting generator performance is illustrated in Figure 3.4. Here it is observed that the fast voltage transient of the exciter settles at the new voltage reference of 1.05 pu within a few seconds. The terminal voltage does contain additional oscillations caused by the rotor oscillation that can be inferred from the oscillation in rotor speed. Keeping this oscillation in mind when examining the terminal voltage, the performance of the exciter is deemed acceptable and no additional tuning of the exciter is necessary for this system.

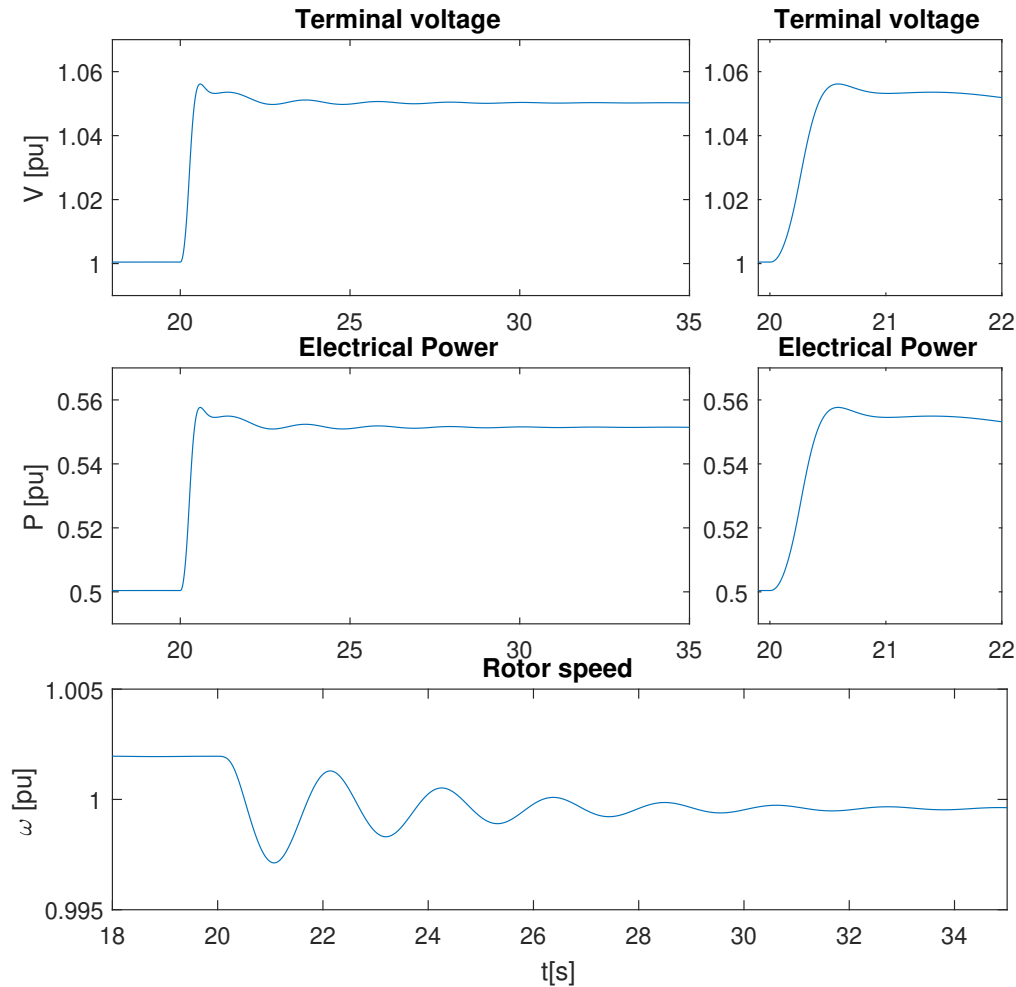


Figure 3.4: Genset terminal voltage, rotor speed and power in pu during step in exciter voltage reference.

A second test of the generator performance is simulated to observe the governor response. The system is subjected to a step in load of 0.1 pu and the resulting generator waveforms are observed in Figure 3.5. Following a step in load, a fast dynamic in the terminal voltage can be observed for the first second, as was the case when subjecting the excitation system to a step input. Following the exciter dynamic, the main component of the terminal voltage becomes the oscillation caused by the rotor oscillation, and when this dynamic settles the terminal voltage is back at 1 pu as expected. The rotor oscillation itself settles within 15 seconds as can be observed in the rotor speed. As the governor contains droop-control with a slope 5% it is expected that the rotor speed settles at a value of 0.005 pu less than the initial rotor speed following a load step of 0.1 pu. This can also be observed, thus the governor performs as expected and no additional tuning is necessary for this model. In addition, a voltage spike can be observed when the step occurs, but this is a numerical error and will not occur in future simulations, because the simulation time step will be smaller.

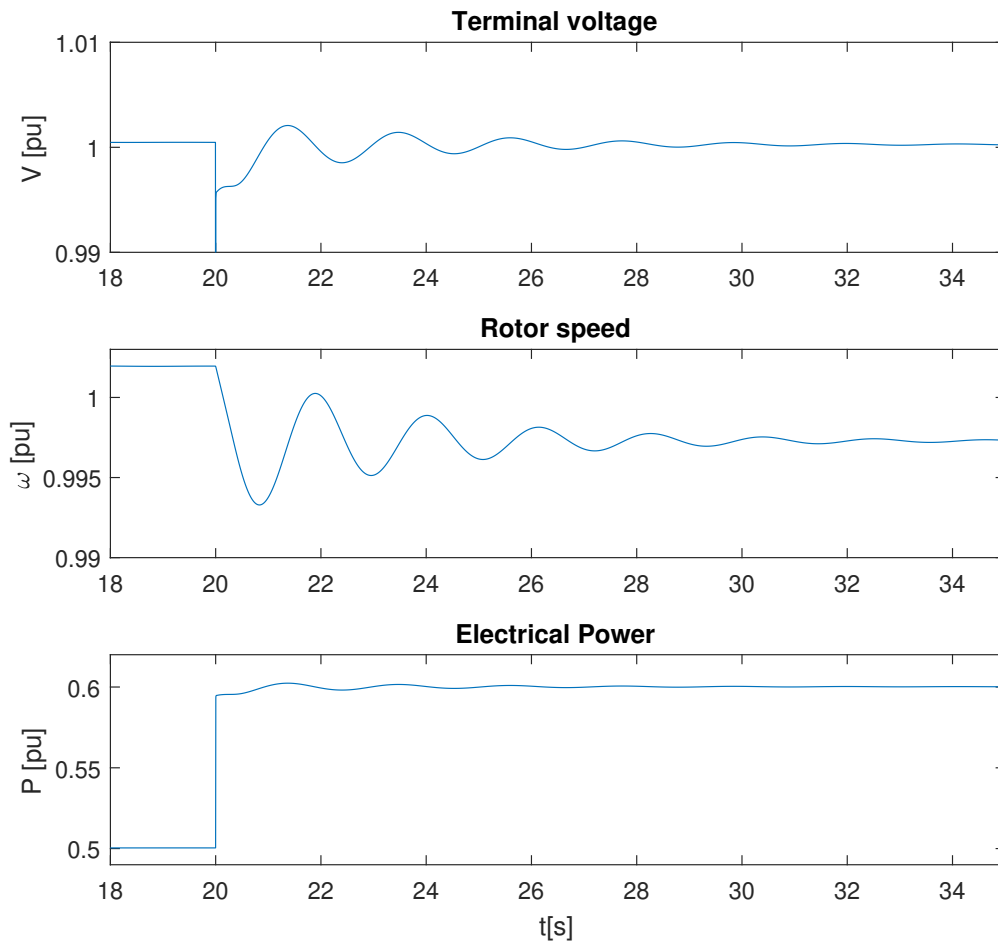


Figure 3.5: Genset terminal voltage, rotor speed and power in pu during load step.

3.4.2 Fault Dynamic Verification

With the performance of exciter and governor of the used genset model verified, the system model is examined. These simulation include the entire system as outlined in Sections 3.1 and 3.2. The current waveforms during a fault are examined in order to verify the fault behaviour of the model. These tests are performed for bolted PP and 3P faults at two different fault locations. One fault location is in the loop consisting of the MSBs which are where the largest fault currents will occur. The other location is at a cable connected to the asynchronous motor loads in order to observe the fault behaviour of this component in the system. As a result, four simulations are defined as in Table 3.4. In these simulations, the faults are applied at $t=20$ s and are cleared after 0.2 seconds.

Table 3.4: Overview of simulations performed in this section.

Test	System load	Fault location	Fault type	Polarisation
Verification 1	Varied load	Cable 2-3	Bolted 3P	NA
Verification 2	Varied load	Cable 2-3	Bolted PP	NA
Verification 3	Motor dominant load	Cable 2-6	Bolted 3P	NA
Verification 4	Motor dominant load	Cable 2-6	Bolted PP	NA

Verification 1: Bolted 3P fault at Cable 2-3

In Figure 3.6 the currents at each end of the faulted cable are observed. As the fault is symmetrical and has a low impedance, the observed currents are balanced with a high magnitude as expected. The fault is located at the Bus 2 terminal of the cable and the difference in current at each end of the cable is caused by the cable impedance between Bus 3 and the fault. During the fault, the terminal voltage and therefore the power output of the generators approach zero, as illustrated by Figure 3.7. As such the rotor speed starts to increase during the 3P faults as all loads are zero for a short time.

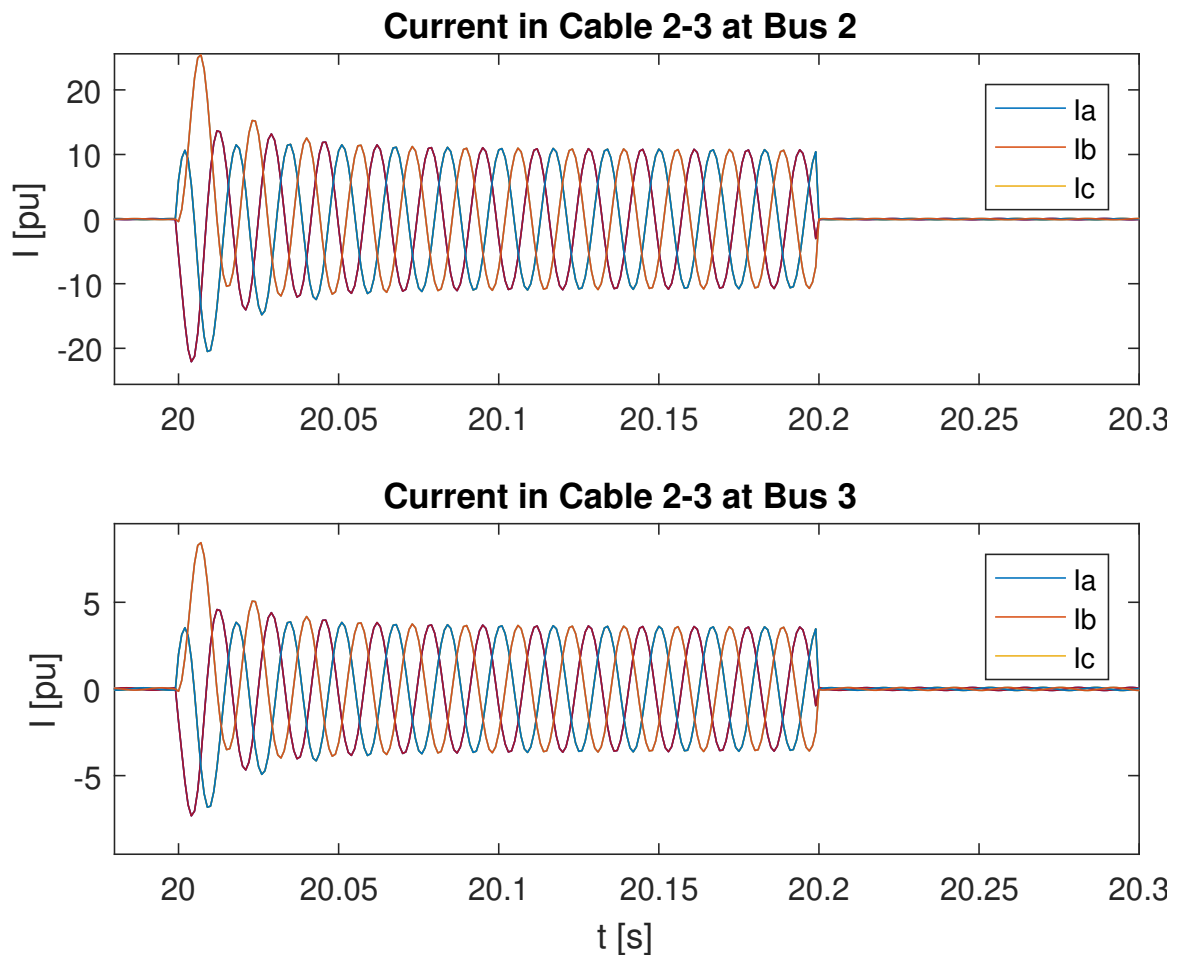


Figure 3.6: Currents at each end of Cable 2-3 during 3P fault.

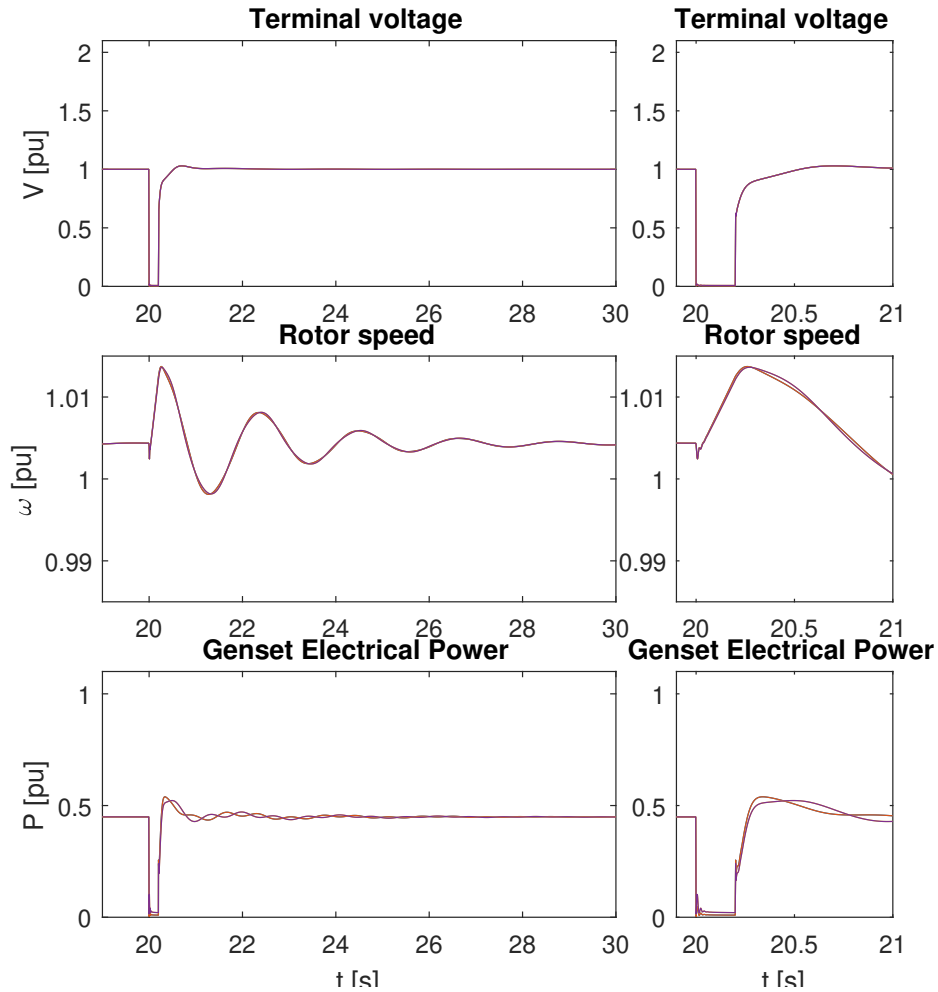


Figure 3.7: Genset parameters during 3P fault at Cable 2-3.

Verification 2: Bolted PP fault at Cable 2-3

During a PP fault, the observed currents in the faulted cable can be observed in Figure 3.8. The magnitude of the fault currents are comparable to those seen for a 3P fault in the previous test, but only in the faulted phases a and b. The current in the faulted phases is also in anti-phase, as expected. In this case, the loads are still supplied with some power while there is a fault in the system and with the addition of the fault current this enough to cause a drop in rotor speed as observed in Figure 3.9.

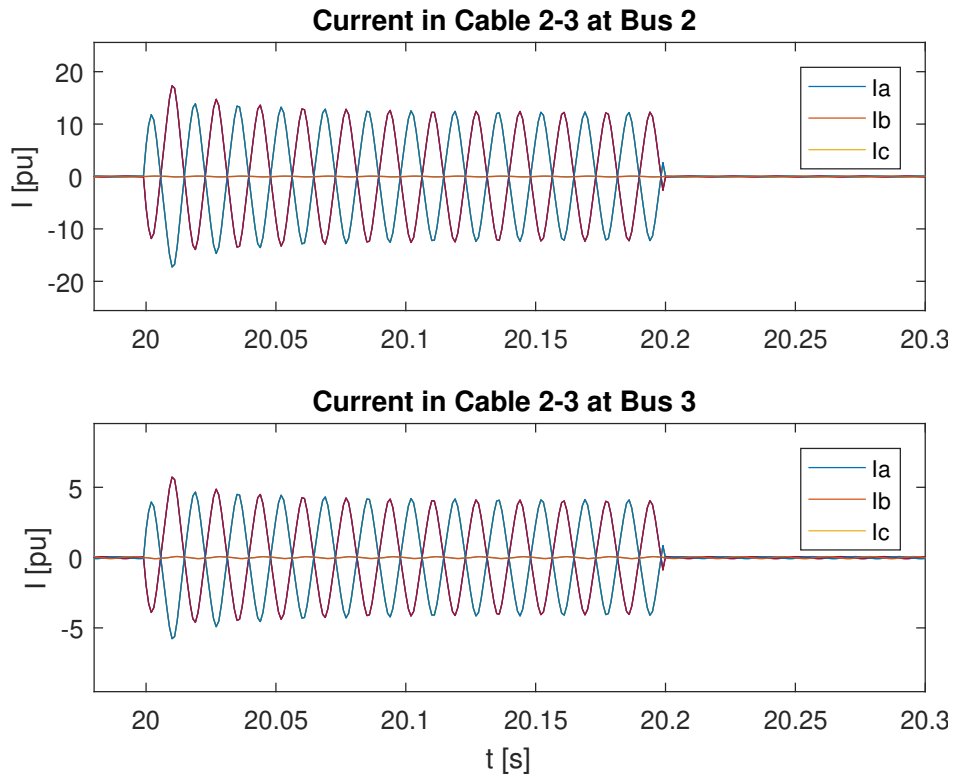


Figure 3.8: Currents at each end of Cable 2-3 during PP fault.

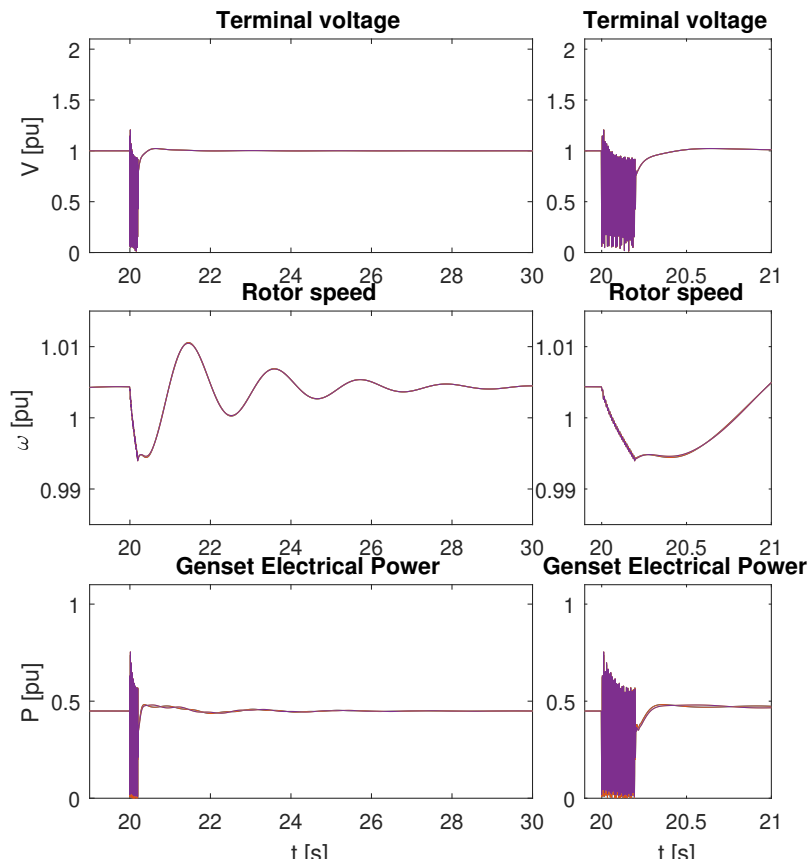


Figure 3.9: Genset parameters during PP fault at Cable 2-3.

Verification 3: Bolted 3P fault at Cable 2-6

The currents at each end of Cable 2-6 are shown in Figure 3.10 when a 3P fault occurs at that cable. A large symmetrical fault current is observed at the Bus 2 terminal of the cable. At Bus 6 only loads are connected including an induction motor which supplies some fault current during the first few periods of the fault. It is shown by the change in rotor speed in the figure that this does not de-energise the motor, but it is also not sufficient to keep the voltage at Bus 6 up and thus the current supplied by the motor quickly drops. It is noteworthy for relay coordination purposes, that the fault current supplied by the motor is higher than the steady state current in the cable but significantly lower than the fault current supplied by the generators. It is also noted that following the fault, the cable also carries an overcurrent as the motor is regaining speed, which must be accounted for in protection scheme to avoid false tripping.

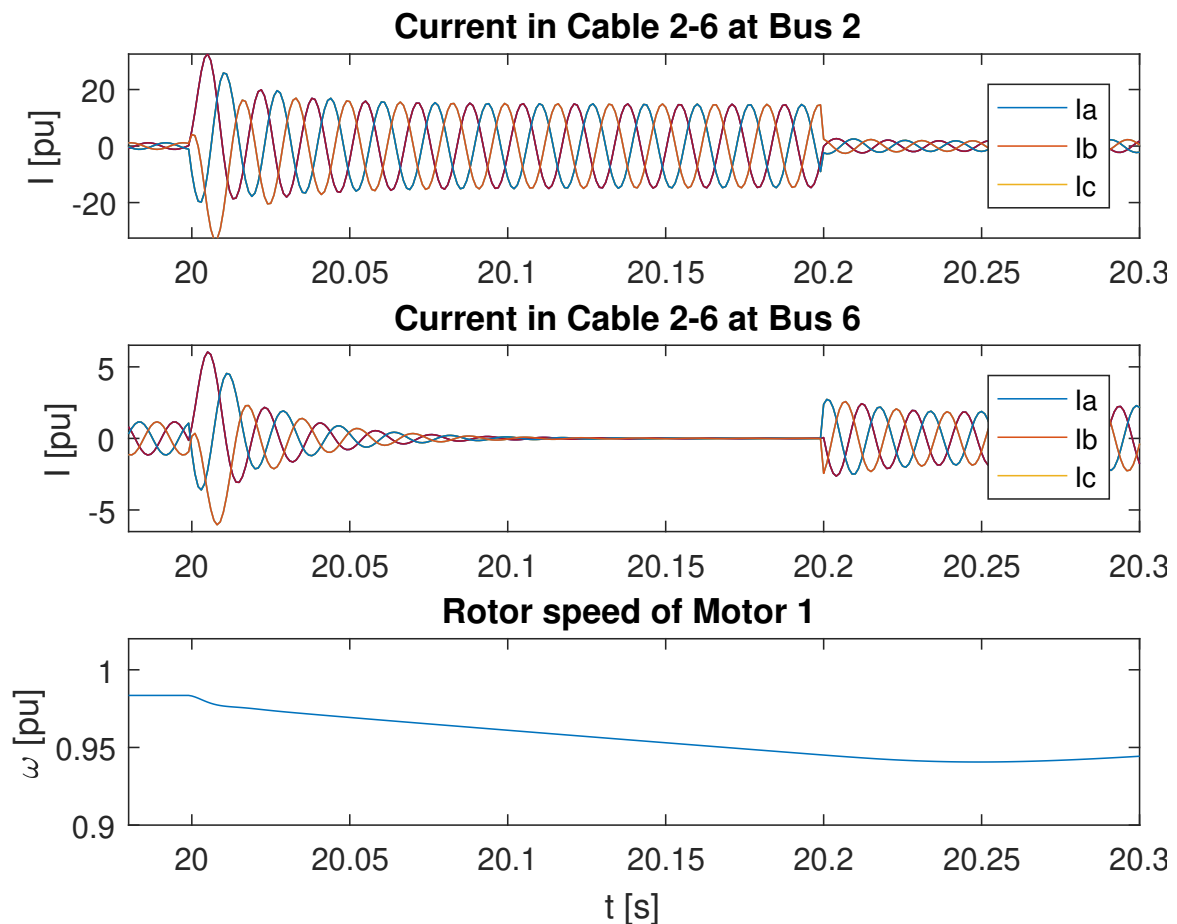


Figure 3.10: Currents at each end of Cable 2-6 during 3P fault.

Verification 4: Bolted PP fault at Cable 2-6

During a PP fault at Cable 2-6, the measured currents are observed in Figure 3.11, where the currents of the faulted phases a and b are large and in anti-phase at the Bus 2 terminal. This is the same result as observed in an earlier simulation of a PP fault in the system. At the Bus 6 terminal of the cable, currents can be observed in all three phases as the loads remain powered during the asymmetrical fault. The current waveforms are highly asymmetrical, which caused by both the fault impacting the voltages as well as the fault current injection from the motor load. Thus, some of the phases experience higher continuous currents than in the pre-fault steady state, however, the currents observed are still significantly lower than the fault currents supplied by the generators.

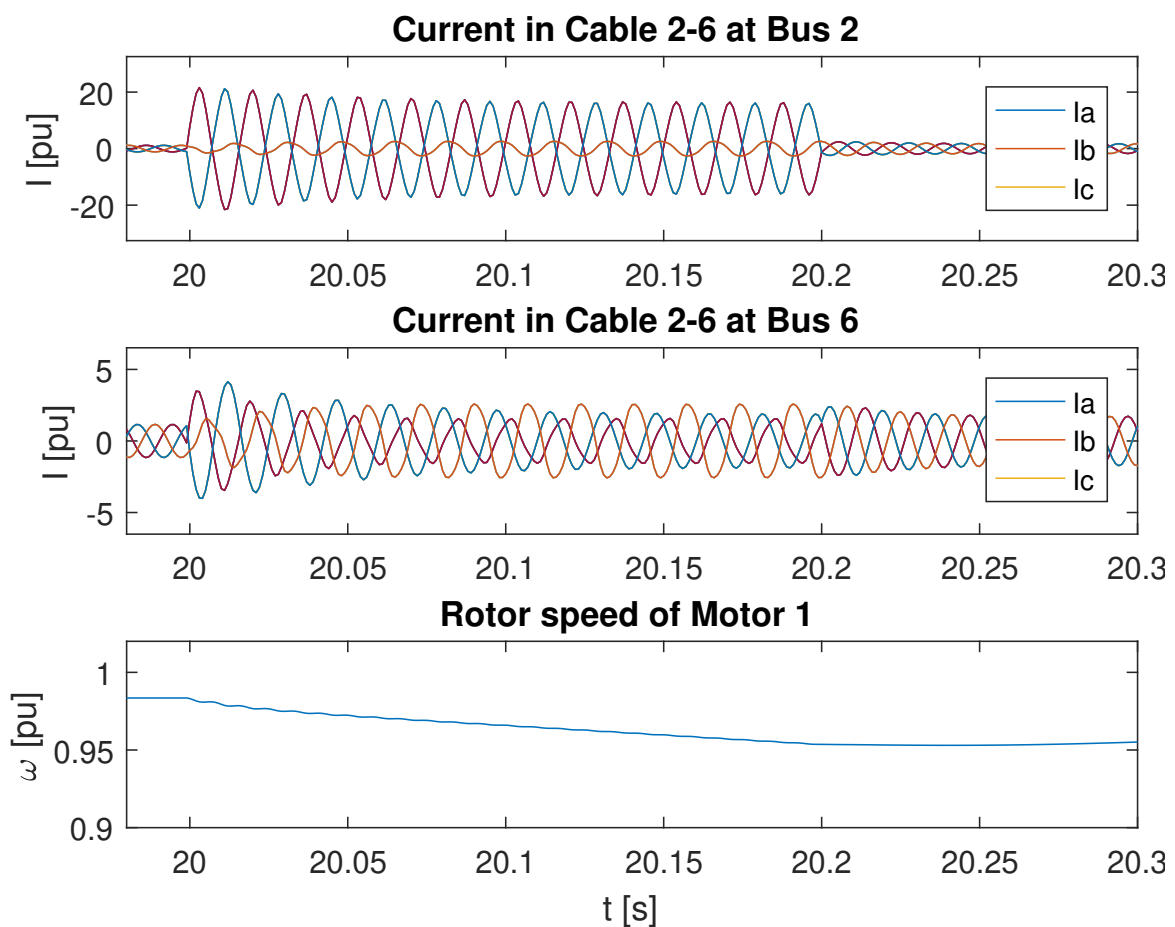


Figure 3.11: Currents at each end of Cable 2-6 during PP fault and rotor speed of the motor.

3.5 Summary

In this chapter, the system model is outlined, containing 4 gensets in a loop configuration supplying propulsion thrusters, auxillary motors and hotel loads through radial feeders. The component models along with the initial system parameters are explained and the various fault and load cases are defined. The operation of the gensets as well as the fault dynamics of the system is then verified through simulation. Notably, the initial simulations show that following a fault the motor loads can draw overcurrents, which is relevant to the choice of protection algorithm. Faults currents for bolted faults are observed to be of a magnitude of 15-20 pu. and voltage and rotor oscillations are stable and settle within a reasonable time frame.

4 | Relay modelling

In this chapter, the logic and modelling of ANSI-67 algorithms are discussed for each polarisation method. The implementation of these algorithms in simulation software is outlined and finally, each algorithm is verified in simulations.

4.1 Relay modelling

The functions of the relay are developed based on the functionalities and considerations made in Section 2.1. The logic is loosely inspired by the function block diagram in [12, p. 81] and implemented in Simulink®. The functions and logic of the resulting relay are outlined by the flowchart in Figure 4.1 and each function block is further explained below.

Current and Voltage sampling is done synchronously at 64 samples pr. cycle, based on [12]. With a system frequency of 60 Hz, this corresponds to a sampling frequency of 3840 Hz. This sampling is implemented in the model by running all relay functions with a constant time step of 0.26 *ms*. Thus the entire subsystem is updated at this time step making it a discrete system with the desired sampling frequency.

Current processing uses the sampled current as input and then outputs the current angle and phasor magnitude. In simulation these values are obtained using Discrete Fourier Transform (DFT), assuming a fundamental frequency of 60 Hz and thus obtaining the phase angle and magnitude of the first harmonic of the current waveform. Using this method the phase angle can be obtained one period after a significant change occurs corresponding to an ideal delay of 16.7 ms at 60 Hz. The current processing function assumes that all examined polarisation methods utilise the phase current angle to determine the direction of the fault current, but as discussed in section 2.1 this is not always the case. Thus, further variations to the current processing methods will be presented when applicable.

Overcurrent detection is performed by comparing the current magnitude obtained by the current processing function to the threshold setting, named the current magnitude setting. In case the measured magnitude is higher than the setting a high signal is forwarded to the tripping logic. Note that in any real system the current magnitude is scaled by a CT before being applied to the logic of the relay, but the CTs are not modelled in the system, thus the current magnitudes in the power system are applied directly to the modelled relay. There are several methods of setting the threshold to ensure pickup in case of a fault and avoid false tripping in highly loaded conditions. For example

relay in [12] the default setting is 1.2 times the nominal current, which is determined by the nominal current of the CT. Any method of setting the current threshold is highly subjective to the specific system, relay location and the judgement of the engineer determining the settings. The initial current threshold of the relay is chosen to be 1.2 pu with a base current being the rated current of the cable, however, the impacts of this setting will be quantified in Section 6.2.2.

Voltage processing is unique for each polarisation method and thus will be described in detail in the corresponding subsection to each variation of the relay. The logical function of the voltage processing block however is that the input is the sampled voltage waveform while the output is the voltage angle of whichever voltage is used as the polarising quantity. The voltage magnitude is not directly used in the logic and need not be forwarded as it is made irrelevant by the following functions.

Voltage memory receives the calculated voltage angle and delays the signal by a configurable number of samples. The delay in [12] is 100 ms, which at 50 Hz corresponds to 5 periods. Thus, the initial value of the delay is chosen as 5 periods corresponding to 320 samples. The delayed voltage angle can be used as the polarising quantity in case the voltage cannot be accurately measured. When a low voltage is detected the voltage memory function stops receiving the calculated voltage angle and stores the delayed voltage angle. This can be the case during low impedance 3P faults as all phase voltages approach zero at the fault location. The voltage memory is then utilised, but the stored voltage loses accuracy over time.

Low voltage detection is a function that will output a high signal when the voltage is too low to accurately estimate the phase angle. The threshold used should depend on the accuracy rating of the VT, however, VTs are not modelled. It can be assumed that for most applications VTs will have an IEC accuracy class of 0.5 or 1 [15, p. 202] and thus the setting used is as the low voltage limit is ± 0.01 pu. The function compares the voltage waveform to the setting and if the voltage is within the limits, the function outputs a high signal. To avoid triggering at the zero-crossings of the input voltage waveform, the voltage must be within the set limits for 32 samples. At 64 samples pr. cycle this corresponds to half period such that the comparison must include a peak of the waveform.

Choose voltage angle is a simple logic function that output either the stored voltage angle or the current voltage angle, depending on whether the signal from Low voltage detection is high or low, respectively.

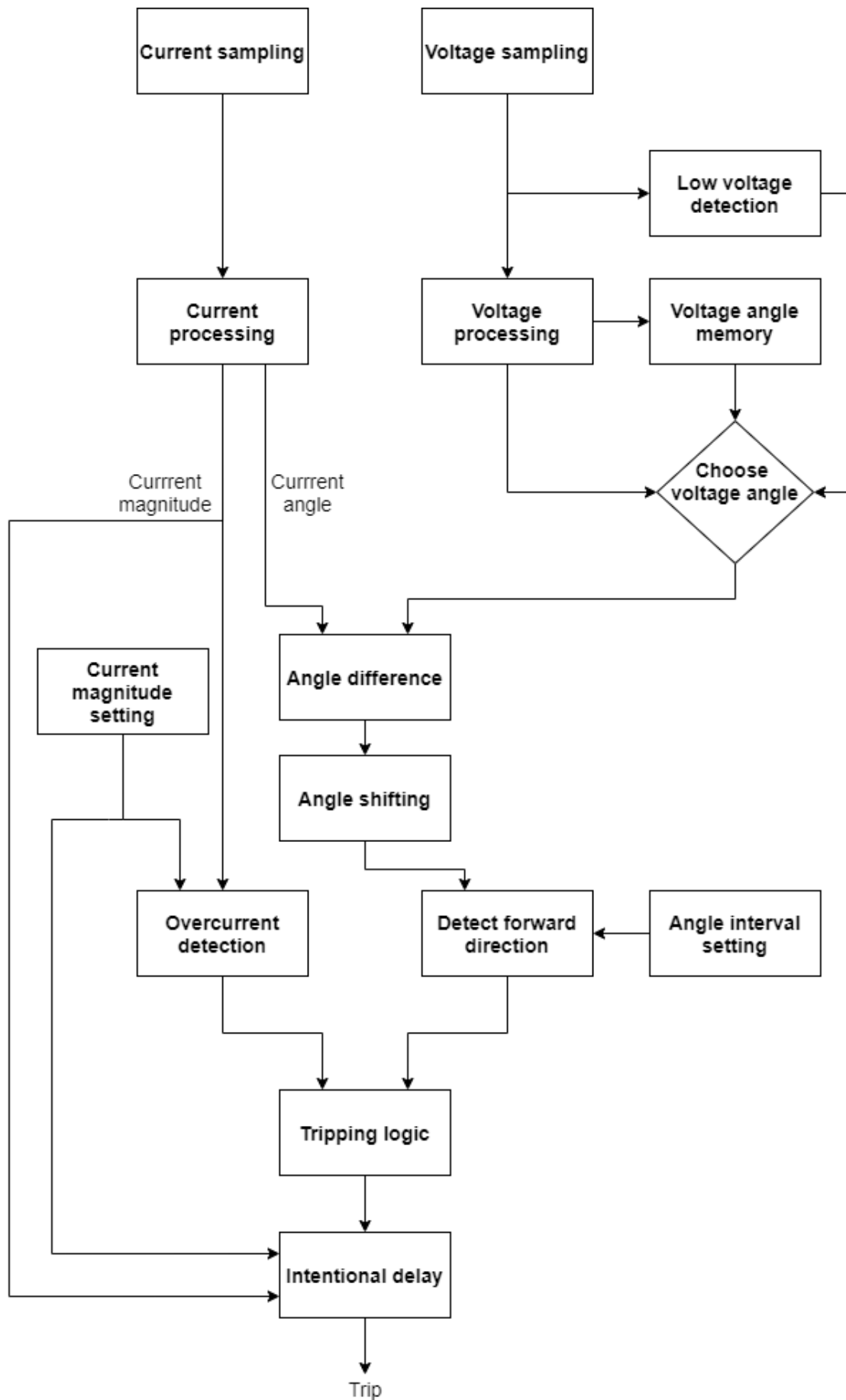


Figure 4.1: Flowchart of relay algorithm in developed relay model.

Angle difference is a mathematical function that computes the difference between the current angle and the voltage angle. The function receives the voltage and current angles in the range of ± 180 degrees as input. Thus, the output is the angle difference in the range of ± 360 degrees, which is an unnecessary double definition of the angle. Therefore the angle difference is then phase shifted by the subsequent function.

Angle shifting gets input in the range of ± 360 degrees and then shifts the angle to a more convenient range. It can be set to shift the angle to a range of ± 180 degrees by adding 360 degrees if the angle difference is below -180 and subtracting 360 degrees if the angle difference is above 180 degrees. The angle shifting function can also be set to shift the angle difference to the range of 0-360 degrees, by adding 360 degrees in case the angle difference is negative. The setting of the angle shifting function is chosen based on which range is more convenient when defining the tripping zone.

Detect forward direction is simply a check of whether the phase-shifted angle is within the tripping zone as defined by the angle setting. The angle setting contains a lower limit and an upper limit which is unique for each polarisation method but generally defined as ± 90 degrees of the Relay Characteristic Angle (RCA) as described in Section 2.2. Thus, the Angle interval setting only requires the RCA as input.

Tripping logic is a function that contains any logic related to when tripping of the relay is allowed. The simplest version of this logic and the one initially implemented in the relay is an AND statement such that if both inputs are high, the output is also high. Thus, if the current is higher than the pickup current and a forward direction of the current is detected, a tripping signal is forwarded to the final function.

Intentional delay is a resettable delay of the tripping signal. If the tripping signal is high for a period longer than the delay it is forwarded to a latch that will keep the signal high until the relay is manually reset. The delay prevents the relay from tripping due to transient behaviour or numerical errors, as fault detection must be persistent to trip the relay. The delay can also be used for time grading. The length of the delay is determined by a delay type setting and a minimum time delay. The delay type setting can be set to DT, IDMT SI and IDMT VI as described in section 2.3.1. When using IDMT SI or IDMT VI the delay is calculated based on the Current magnitude and Current magnitude setting, if the current is lower than 10 pu. For currents higher than this the delay becomes DT, using the minimum timer delay setting. If the relay is set to DT, the minimum time delay is always used. The minimum time delay is given as a number of samples and for the initial setting of the relay, the setting is 128 samples, corresponding to 2 periods of the fundamental frequency.

This section has been an overview of the general relay logic, however, each polarisation method introduces some variation to the functions which will be further explained before the operation of the relay is verified for a fault case.

4.2 Relay Algorithm Verification

To verify the operation of the algorithm for each polarisation method a fault case in the power system is chosen such that the various functions in the algorithm can be tested. Therefore, the fault location is at Cable 1-5, while observing the operation of the relays controlling CB14, CB15 and CB26 with forwarding direction defined as illustrated in Figure 4.2.

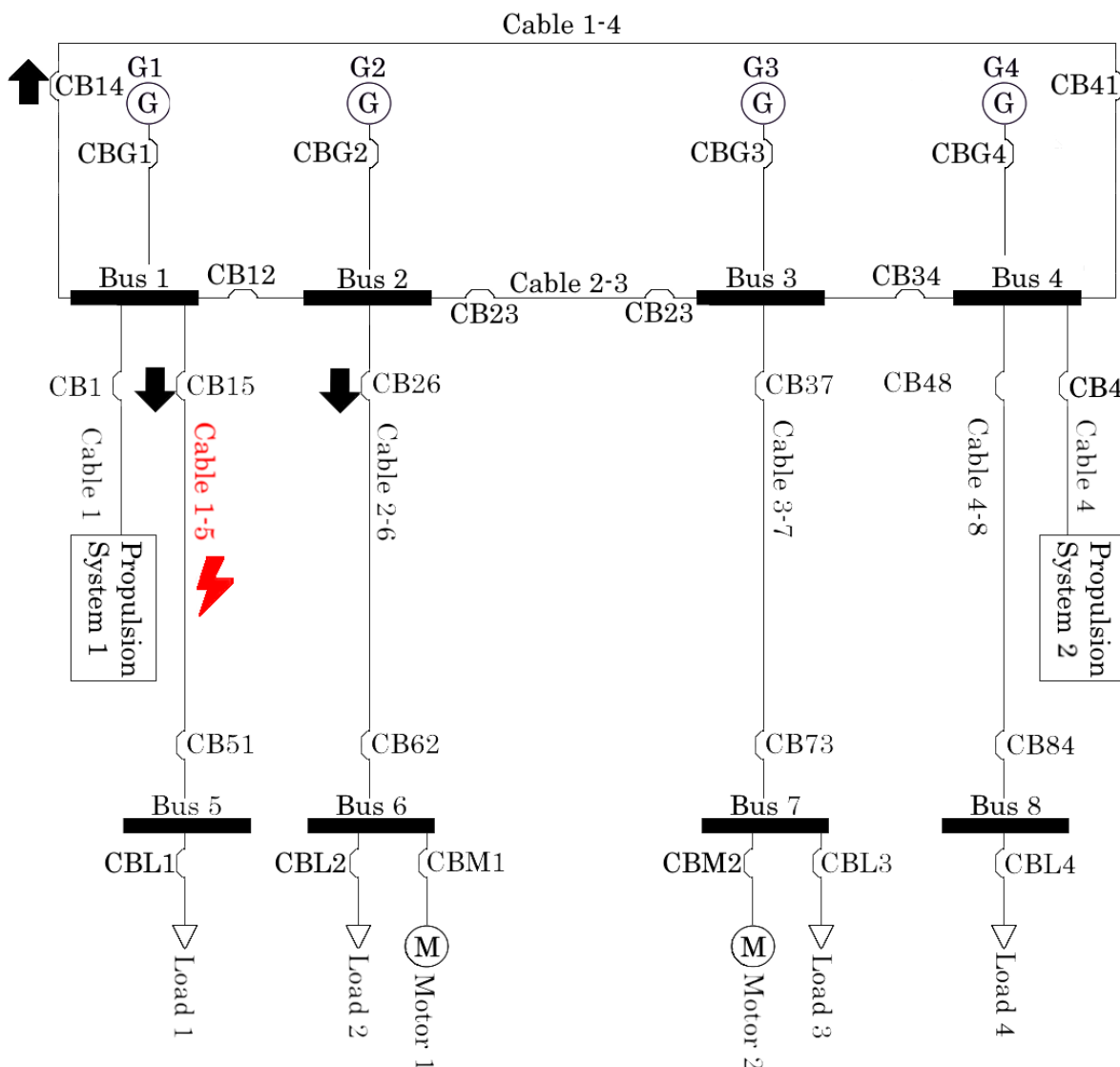


Figure 4.2: Location of the fault, CB14, CB15 and CB26, showing the defined forward direction of the corresponding relays, in the power system.

For a fault occurring at Cable 1-5, the expected bias of the relays is, that CB15 will be forward biased,

CB14 will be reverse biased due to fault current supplied by G3 and G4 and CB26 will be reverse biased due to fault current supplied by Motor 1. For this fault case, the system load is selected to be Motor dominant load, to illustrate the impact of the motors on the operation of CB26. The simulation is performed for both bolted PP and 3P faults.

4.2.1 Verification of Self-polarisation, I_x/V_x variant

Implementing the relay using a I_x/V_x self-polarisation method is the simplest implementation of any of the polarisation methods. That is because the input voltage is the measured phase voltages which in this case is the polarising quantity. Thus, to acquire the voltage angle, DFT is performed on the voltage waveform, assuming 60 Hz fundamental frequency, and the rest of the relay is exactly as described in Section 4.1. For this algorithm, the polarising angle for each phase is:

Current	Polarising angle
I_a	$I_a \angle - V_a \angle$
I_b	$I_b \angle - V_b \angle$
I_c	$I_c \angle - V_c \angle$

To test the relay, it is subjected to a voltage and current input obtained from the power system model described in Chapter 3. The relay and system settings are shown in Table 4.1. The fault is applied at $t = 20s$ and cleared after 0.2s.

Table 4.1: Simulation parameters and relay settings for the verification of the relay model using I_x/V_x self-polarisation.

Parameter	Setting
System Load	Motor Dominant load
Fault location	Cable 1-5
Polarisation	I_x/V_x
Intentional delay	SI IDMT
Pickup current	1.2 [pu]
RCA	-45°

Table 4.2: Results of I_x/V_x self-polarisation tests with faults at Cable 1-5. Magnitude and angle measurements in the table are made at $t=20.15s$. Green = forward bias, Red = reverse bias.

Relay Location	Fault Type	Phase A		Phase B		Phase C		Tripping delay [ms]
		I [pu]	Angle [°]	I [pu]	Angle [°]	I [pu]	Angle [pu]	
CB15	Bolted 3P	35.89	-11.829	35.88	-11.832	35.91	-11.816	34.6
CB14	Bolted 3P	3.534	167.997	3.532	168.002	3.535	169.018	No trip
CB26	Bolted 3P	0.3062	-27.31	0.3047	-27.018	0.307	-26.9159	No trip
CB15	Bolted PP	40.445	15.302	40.218	-133.976	0.252	0.095	39.8
CB14	Bolted PP	3.966	-164.606	3.974	46.015	0.008	55.630	No trip
CB26	Bolted PP	1.318	-112.065	1.940	-1.698	2.528	-52.358	No trip

The simulation results in Table 4.2, show that only CB15 would trip in this case for both a 3P and PP fault, as expected. The relay trips with a delay of 34.6 ms and 39.8 ms, for a 3P and PP fault respectively, which is a few ms longer than the minimum time delay of the relay. This is the case because the fault current observed through CB15 is larger than 10 pu and the relay operates with a DT delay of two cycles, ie. 33 ms. The tripping zone of the relay is defined from the RCA setting as -135° to 45° . Thus, CB14 does not trip despite seeing over-currents, because all phases are reverse biased in both fault cases. In the case of a 3P fault, CB26 is forward biased but with a low current, at the time of the measurement, but this is not the case throughout the fault period as illustrated in Figures 4.3 and 4.4.

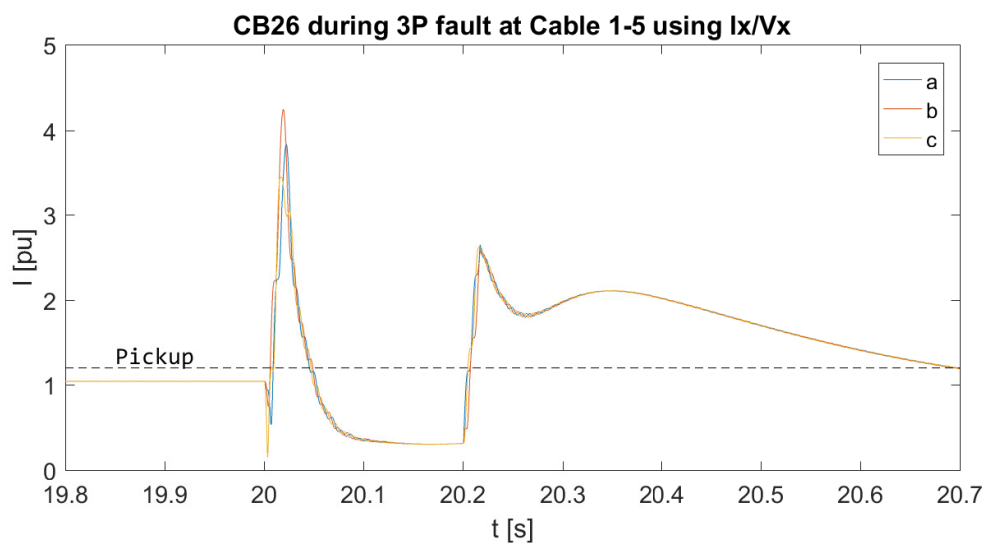


Figure 4.3: Current magnitude through CB26 during 3P fault at Cable 1-5.

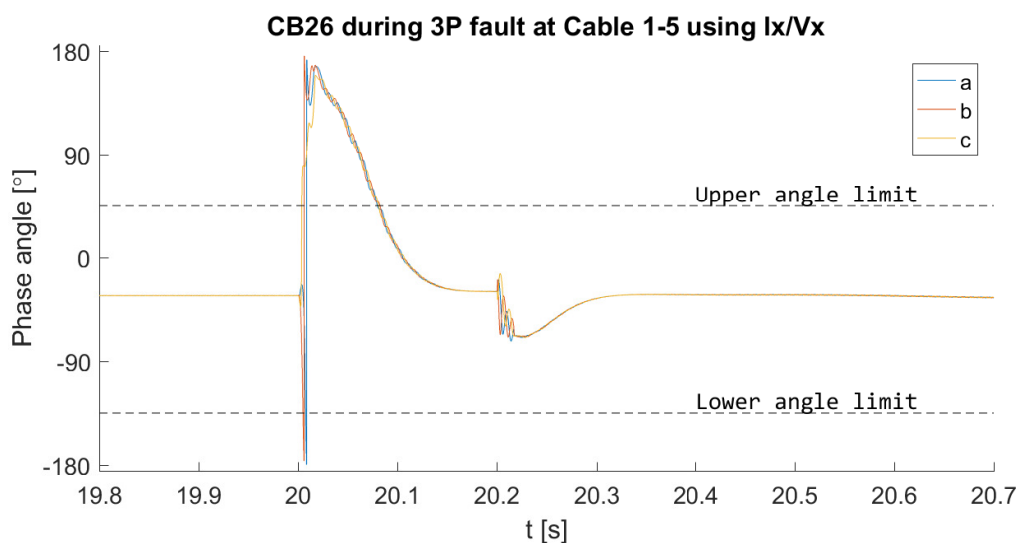


Figure 4.4: I_x/V_x polarising angle at CB26 during 3P fault at Cable 1-5.

For approximately 5 cycles following the fault, Motor 1 acts as a fault current source. However, during

this time the relay can detect that the current is reverse biased and thus will not trip, as can be observed in Figure 4.4. This illustrates that the fault current supplied by the motors will not cause false tripping of CB26 when using I_x/V_x polarisation method. It is notable, that following a fault the motors will be below rated speed and therefore draw additional current for some time. This current is forward biased through CB26 and thus will be detected by the algorithm as a fault. In this case, the relay does not trip due to the IDMT delay, because the current is around 2 pu which corresponds to a delay of approximately 10 s in this case.

In case of a PP fault a similar behaviour of the faulted phases, a and b, through CB26 can be observed in Figures 4.5 and 4.6. There is a current spike and the relay is reverse biased for the first few cycles following a fault. However, for the rest of the fault period, the motor remains operational and will draw overcurrents on all three phases including the healthy phase c. These currents are forward biased and will eventually cause the relay to trip if the fault is not cleared. In addition, relays are not necessarily reset when the fault cleared due to the same post-fault overcurrent as was shown for the 3P fault. In Figure 4.7 it is shown that the fault is detected continuously on phase c during and following the fault, but the relay does not trip, as is the intended behaviour. In this case, proper choice of IDMT delay is necessary to achieve selectivity.

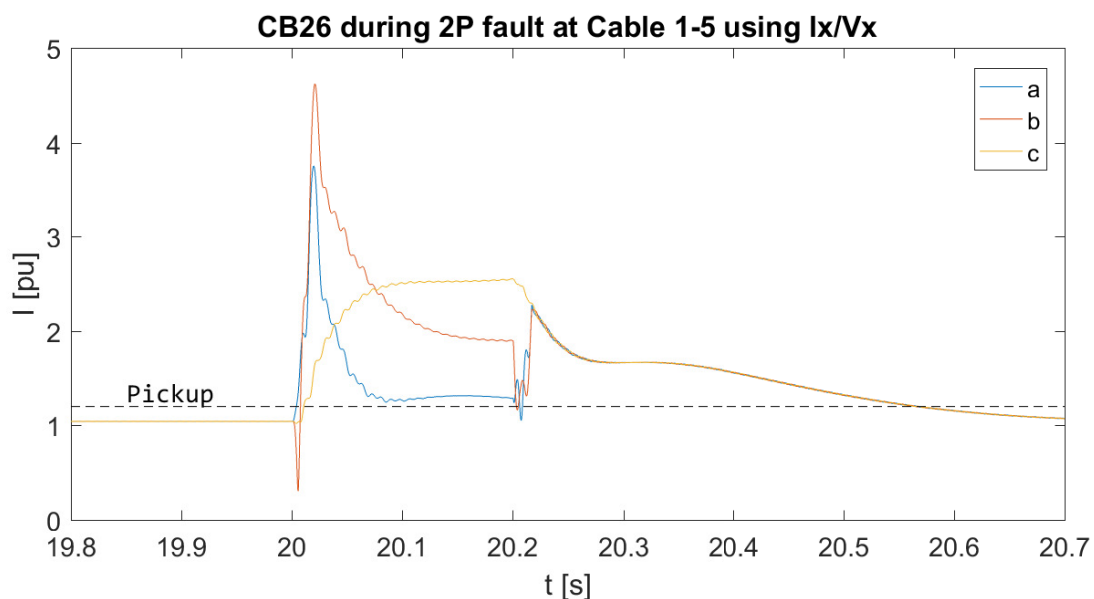


Figure 4.5: Current magnitude through CB26 during 2P fault at Cable 1-5.

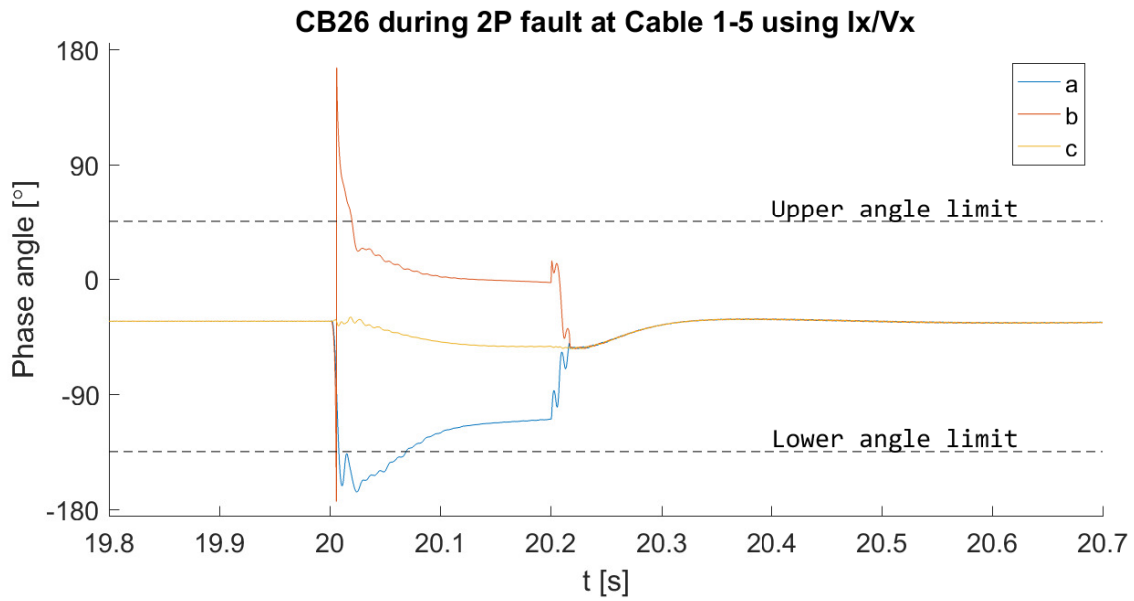


Figure 4.6: I_x/V_x polarising angle at CB26 during 2P fault at Cable 1-5.

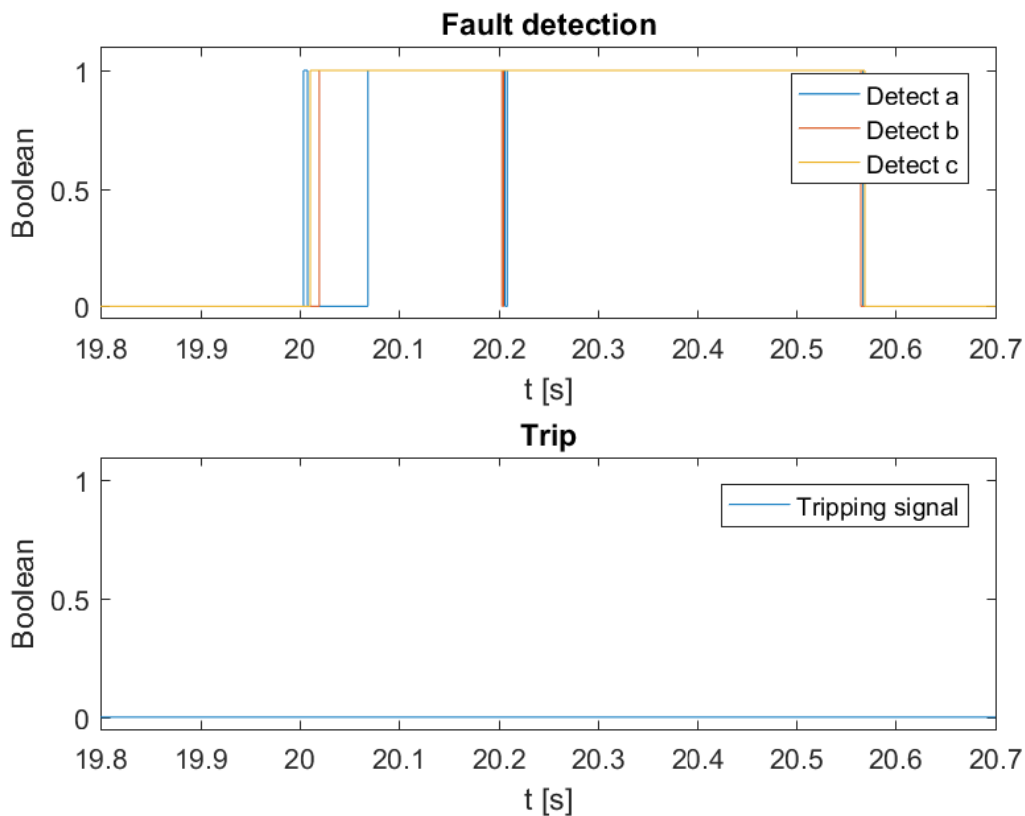


Figure 4.7: Boolean output of the fault detection algorithm before and after the delay.

For the shown fault cases the relay algorithm using I_x/V_x self-polarisation trips the relays selectively and with minimal time delay. Therefore the implementation of this algorithm in the simulation environment is verified and can be utilised for further studies. These initial simulations of the I_x/V_x

polarisation method indicate that for 3P faults the relay can determine the direction of the current well within the tripping or non-tripping zones. It is noted that for PP faults the polarising angles are close to the limits between the tripping and non-tripping zone and it is prudent to analyse the confidence of this polarisation method further.

4.2.2 Verification of self-polarisation, I_x/V_{xy} variant

A variation upon the self-polarisation method exists, in which the phase voltage is not used directly to determine the forward direction of the current. Instead, the polarising angle is defined as:

Current	Polarising angle
I_a	$I_a \angle - (V_a - V_b) \angle$
I_b	$I_b \angle - (V_b - V_c) \angle$
I_c	$I_c \angle - (V_c - V_a) \angle$

For the algorithm, this means that during the Voltage processing, the phase-to-phase voltage is obtained before DFT is performed. The RCA for this polarisation method is -90° and with this change to the algorithm, the verification of the relay operation is repeated. The relay and system settings are shown in Table 4.3 and the results are shown in Table 4.4.

Table 4.3: Simulation parameters and relay settings for the verification of the relay model using I_x/V_{xy} self-polarisation.

Parameter	Setting
System Load	Motor Dominant load
Fault location	Cable 1-5
Polarisation	I_x/V_{xy}
Intentional delay	SI IDMT
Pickup current	1.2 [pu]
RCA	-90°

Table 4.4: Results of I_x/V_{xy} polarisation method tests with faults at Cable 1-5. Magnitude and angle measurements in the table are made at $t=20.15s$. Green = forward bias, Red = reverse bias.

Location	Fault Type	Phase A		Phase B		Phase C		Tripping delay [ms]
		I [pu]	Angle [°]	I [pu]	Angle [°]	I [pu]	Angle [pu]	
CB15	Bolted 3P	35.891	-41.850	35.882	-41.831	35.907	-41.796	34.6
CB14	Bolted 3P	3.534	137.976	3.532	138.002	3.535	138.037	No trip
CB26	Bolted 3P	0.306	-57.331	0.3047	-57.017	0.307	-56.896	No trip
CB15	Bolted PP	40.445	-12.024	40.218	-148.628	0.252	-4.172	35.6
CB14	Bolted PP	3.966	168.067	3.974	31.364	0.008	51.362	No trip
CB26	Bolted PP	1.318	-139.391	1.940	-16.349	2.528	-56.625	No trip

The results of the simulations using I_x/V_{xy} self-polarisation show that the relays operate selectively and as expected for the chosen fault cases. CB15 trips for both fault types with minimum delay for

a fault Cable 1-5, while no other relay trips. CB26 is exposed to similar behaviour as those observed for the I_x/V_{xy} polarisation method in Section 4.2.1 as there is persistent forward-biased overcurrent through CB26 during a PP fault at Cable 1-5. The intended operation of the relay is verified and no significant differences are observed between the I_x/V_{xy} and I_x/V_x polarisation methods.

4.2.3 Verification of self-polarisation, I_{xy}/V_{xy} variant

A third variation of self-polarisation is implemented and verified for the defined fault cases. In this variation, I_{xy}/V_{xy} , the polarising angle is defined as:

Current	Polarising angle
I_a	$(I_a - I_b)\angle - (V_a - V_b)\angle$
I_b	$(I_b - I_c)\angle - (V_b - V_c)\angle$
I_c	$(I_c - I_a)\angle - (V_c - V_a)\angle$

For this algorithm, the Current and Voltage processing functions are changed such that the phase-to-phase voltage and the phase current difference is calculated before DFT is performed. These angles are then forwarded to the Angle difference calculation. The current magnitude is calculated by applying DFT to the phase current waveform as in the original algorithm. This algorithm is verified by repeating the simulation of relay operation using the settings in Table 4.5 and the results are shown in Table 4.6.

Table 4.5: Simulation parameters and relay settings for the verification of the relay model using I_{xy}/V_{xy} self-polarisation.

Parameter	Setting
System Load	Motor Dominant load
Fault location	Cable 1-5
Polarisation	I_{xy}/V_{xy}
Intentional delay	SI IDMT
Pickup current	1.2 [pu]
RCA	-45°

Table 4.6: Results of I_{xy}/V_{xy} polarisation method tests with faults at Cable 1-5. Magnitude and angle measurements in the table are made at $t=20.15s$. Green = forward bias, Red = reverse bias.

Location	Fault Type	Phase A		Phase B		Phase C		Tripping delay [ms]
		I [pu]	Angle [°]	I [pu]	Angle [°]	I [pu]	Angle [pu]	
CB15	Bolted 3P	35.891	-11.836	35.882	-11.823	35.907	-11.820	34.6
CB14	Bolted 3P	3.534	167.993	3.532	168.013	3.535	168.011	No trip
CB26	Bolted 3P	0.306	-27.248	0.3047	-26.852	0.307	-27.144	No trip
CB15	Bolted PP	40.445	-11.946	40.218	-148.470	0.252	21.523	37.2
CB14	Bolted PP	3.966	168.096	3.974	31.422	0.008	-158.290	No trip
CB26	Bolted PP	1.318	157.520	1.940	-33.789	2.528	-72.941	No trip

For this fault case, the relay operates as intended as only CB15 trips within the time frame of the

fault, for both fault cases. During 3P faults, the I_{xy}/V_{xy} algorithm operates similarly to the I_x/V_x algorithm as described in Section 4.2.1, as the relay correctly detects the direction of fault currents supplied by both motors and generators, and the relay trips selectively with minimal delay of 34.6 ms. However, during the PP fault this polarisation method detects that one of the faulted phases, a and b, is forward biased while the other is reverse biased in both CB14 and CB15. The polarising angles are illustrated in Figures 4.8 and 4.9. In this case, the reason CB15 trips while CB14 does not is the difference in current magnitude illustrated in Figures 4.10 and 4.11. This occurrence where one faulted phase is forward biased while the other is reverse biased is possible for all self-polarisation methods as described in Section 2.2.2 because the angle difference between the faulted phases becomes close to 180° and the polarising angles will likely be in different tripping-zones.

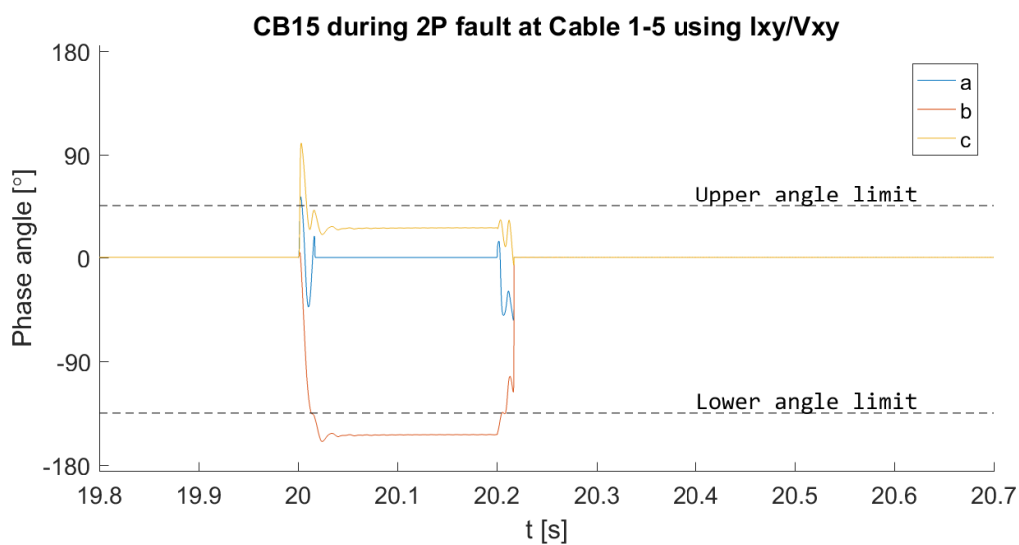


Figure 4.8: I_{xy}/V_{xy} polarising angle at CB15 during 2P fault at Cable 1-5.

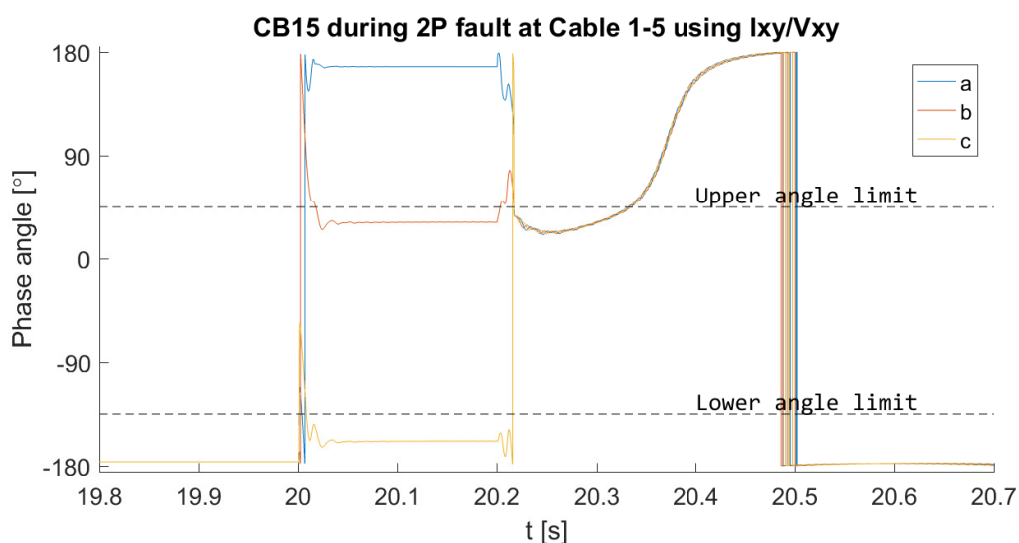


Figure 4.9: I_{xy}/V_{xy} polarising angle at CB14 during 2P fault at Cable 1-5.

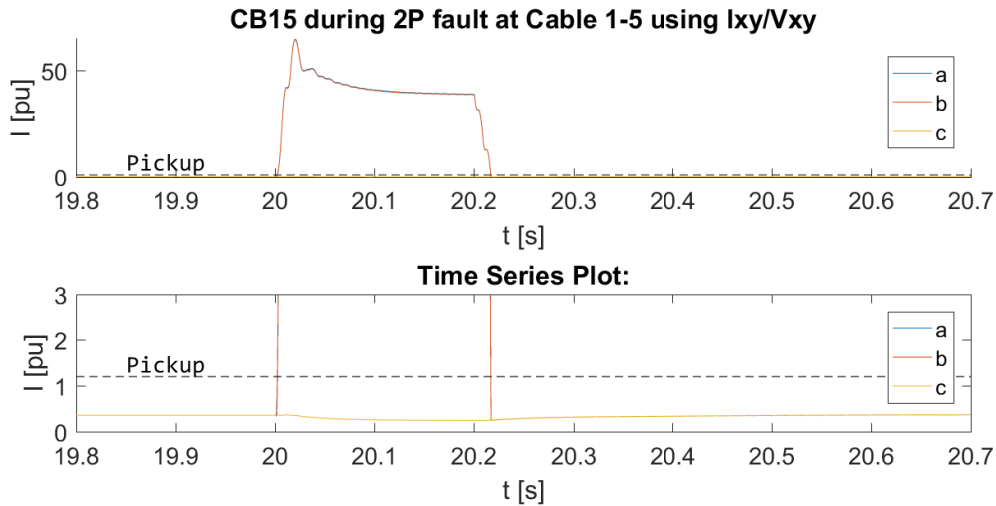


Figure 4.10: Current magnitude at CB15 during 2P fault at Cable 1-5.

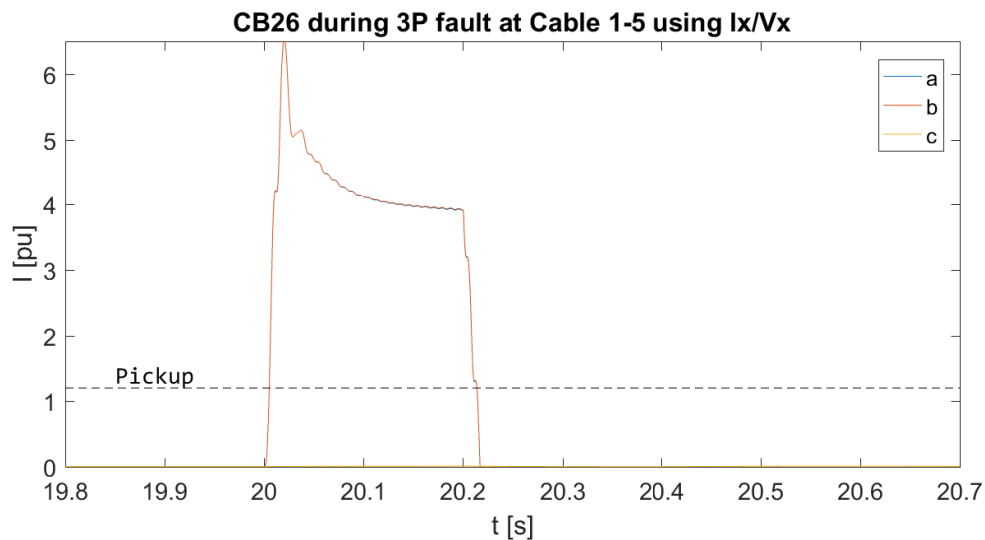


Figure 4.11: Current magnitude at CB14 during 2P fault at Cable 1-5.

The intended operation of the I_{xy}/V_{xy} algorithm is verified for this fault case, however, for PP faults it is illustrated that this algorithm may not have a reliable directional component and is functionally an ANSI-51, time-delayed overcurrent, relay. These cases can occur for I_x/V_x and I_x/V_{xy} polarisation methods as well, though that was not the case for the chosen fault cases. This result is notable, as it could limit the possible applications of this polarisation method.

4.2.4 Verification of Positive sequence polarisation, I_1/V_1

Positive sequence polarisation is implemented in the relay where the polarising angle is the angle between the positive sequence current and the positive sequence voltage as shown below. In this algorithm, the Voltage and Current processing are changed such that DFT is performed and

subsequently sequence transformation is performed. Notably, the positive sequence components are balanced by definition and the polarising angle for each phase will be equal. As such the angle needs to be computed only once, rather than for each phase. It also means that the relay cannot determine forward bias on a phase by phase basis, but only whether the relay is forward- or reverse biased. The verification of relay operation is repeated for this simulation using the settings in Table 4.7 and the results are shown in Table 4.8.

Current	Polarising angle
I_a	$I_1 \angle -V_1 \angle$
I_b	$(I_1 \angle - 120^\circ) - (V_1 \angle - 120^\circ)$
I_c	$(I_1 \angle + 120^\circ) - (V_1 \angle + 120^\circ)$

Table 4.7: Simulation parameters and relay settings for the verification of the relay model using positive sequence polarisation.

Parameter	Setting
System Load	Motor Dominant load
Fault location	Cable 1-5
Polarisation	I1/V1
Intentional delay	SI IDMT
Pickup current	1.2 [pu]
RCA	-45°

Table 4.8: Results of positive sequence polarisation method tests with faults at Cable 1-5. Magnitude and angle measurements in the table are made at $t=20.15s$. Green = forward bias, Red = reverse bias.

Location	Fault Type	Phase A		Phase B		Phase C		Tripping delay [ms]
		I [pu]	Angle [°]	I [pu]	Angle [°]	I [pu]	Angle [pu]	
CB15	Bolted 3P	35.891	-11.826	35.882	-11.826	35.907	-11.826	34.6
CB14	Bolted 3P	3.534	168.006	3.532	168.006	3.535	168.006	No trip
CB26	Bolted 3P	0.306	-27.081	0.3047	-27.081	0.307	-27.081	No trip
CB15	Bolted PP	40.445	-54.597	40.218	-54.597	0.252	-54.597	35.6
CB14	Bolted PP	3.966	125.077	3.974	125.077	0.008	125.077	No trip
CB26	Bolted PP	1.318	-25.624	1.940	-25.624	2.528	-25.624	No trip

Using positive sequence polarisation, the relays operate as intended as CB15 is the only tripped relay for the duration of the fault for both fault cases. The relays trip with a delay of 34.6 ms and 35.6 ms for a 3P and PP fault respectively, which is close to the minimum possible delay. Observing the polarising angle at CB14 the polarising angles in both fault cases are far from the tripping zone defined between -135° and 45° . For CB15, which is forward biased, the polarising angles are well within the defined tripping zone. The initial simulations indicate that positive sequence polarisation is reliable in determining the bias of the relay. In the case of the fault current supplied by the motor, the polarising angle CB26 during a PP fault is illustrated in Figure 4.12. It is observed that the bias of the relay is

correctly determined in this case as well as the relay is reverse biased for a few cycles following the fault when the motor is supplying fault current. The intended operation of the relay using positive sequence polarisation is verified for the chosen fault cases.

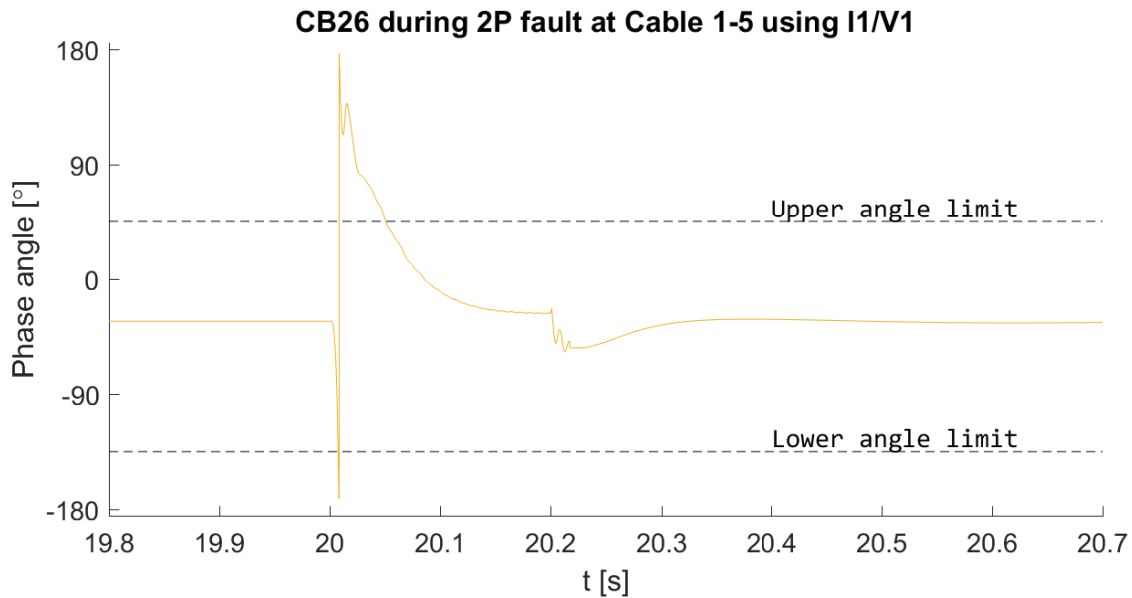


Figure 4.12: I1/V1 polarising angle at CB26 during 2P fault at Cable 1-5.

4.2.5 Verification of Cross-polarisation, I_x/V_{yz}

The final algorithm implemented in the relay is cross-polarisation in which the polarising angle is the angle between the phase current and the phase-to-phase voltage of the remaining phases, as shown below.

Current	Polarising angle
I_a	$I_a \angle - (V_b - V_c) \angle$
I_b	$I_b \angle - (V_c - V_a) \angle$
I_c	$I_c \angle - (V_a - V_b) \angle$

In this algorithm, the Voltage processing function is changed such that the phase-to-phase voltage is calculated and then transposed to the correct phase before DFT is applied. The verification of relay operation is then repeated using the settings in Table 4.9 and the results of the simulation are shown in Table 4.10.

Table 4.9: Simulation parameters and relay settings for the verification of the relay model using cross-polarisation.

Parameter	Setting
System Load	Motor Dominant load
Fault location	Cable 1-5
Polarisation	I _x /V _{yz}
Intentional delay	SI IDMT
Pickup current	1.2 [pu]
RCA	45°

Table 4.10: Results of cross-polarisation method tests with faults at Cable 1-5. Magnitude and angle measurements in the table are made at t=20.15s. Green = forward bias, Red = reverse bias.

Location	Fault Type	Phase A		Phase B		Phase C		Tripping delay [ms]
		I [pu]	Angle [°]	I [pu]	Angle [°]	I [pu]	Angle [pu]	
CB15	Bolted 3P	35.891	78.131	35.882	78.210	35.907	78.181	34.6
CB14	Bolted 3P	3.534	-102.042	3.532	-101.956	3.535	-101.985	No trip
CB26	Bolted 3P	0.306	62.650	0.3047	63.024	0.307	63.081	No trip
CB15	Bolted PP	40.445	31.215	40.218	21.834	0.252	142.126	35.6
CB14	Bolted PP	3.966	-148.694	3.974	-158.173	0.008	-162.339	No trip
CB26	Bolted PP	1.318	-96.152	1.940	154.113	2.528	89.672	No trip

For cross-polarisation the intended operation of the relays is verified, as only CB15 trips within the duration of the fault for both fault cases. The tripping zone for this polarisation method is defined between -45° and 135° . For both fault cases, CB14 and CB15 are well within the non-tripping or tripping zone respectively, indicating that the directional element is reliable for the faulted phases. As for CB26 during a PP fault, phase C is forward biased with a magnitude of 2.528 pu. Using SI IDMT this corresponds to a delay of 0.871 s, thus if the fault persists the relay will trip. The faulted phases are reverse biased for the duration of the fault, as is illustrated in Figure 4.13 and while this does not change the tripping of the relays in this fault case compared to the previous polarisation methods, notably, each other polarisation method used detected at least one of the faulted phases in forward direction at CB26 during the PP fault. This may be an advantage to using cross-polarisation, but further analysis is required.

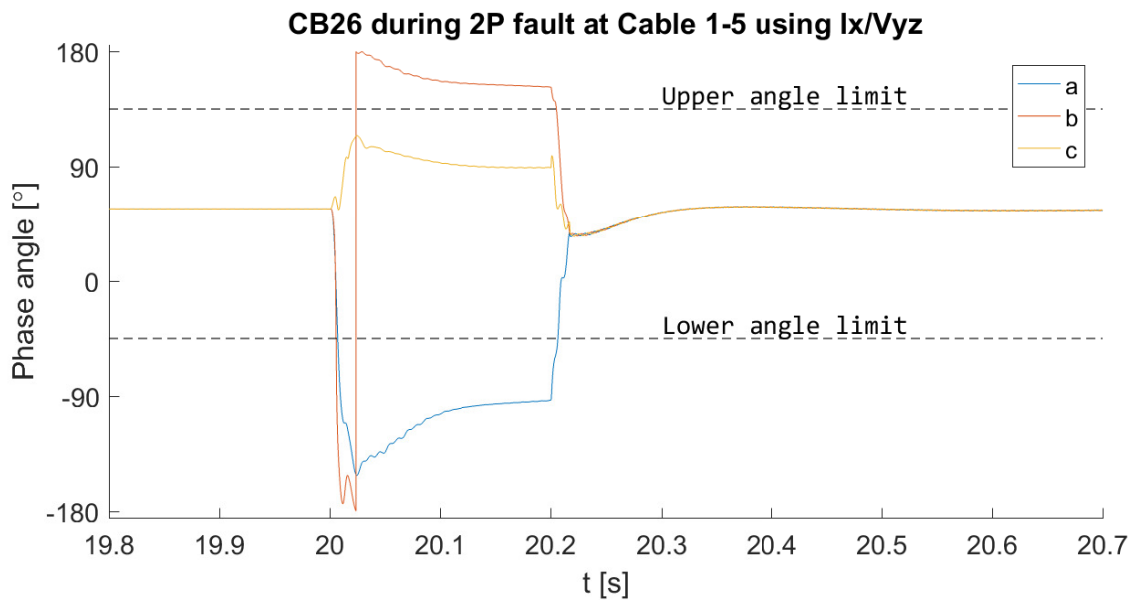


Figure 4.13: I_x/V_{yz} polarising angle at CB26 during 2P fault at Cable 1-5.

4.3 Summary

In this chapter, the relay is modelled in a simulation environment and the implemented ANSI-67 algorithm is explained in detail. The algorithm is then verified for a simple fault case in the modelled power system, for each polarisation method. The preliminary simulations show that each polarisation method is able to selectively trip the correct relay for the chosen fault cases and the correct operation of the algorithm is therefore verified. However, it is also illustrated that depending on system parameters cases may exist where self-polarisation methods lose their directional element during PP faults, which warrants further investigation. The initial simulations indicate that positive-sequence-polarisation and cross-polarisation may both be reliable methods of determining the current direction, for the relevant fault types.

5 | Result validation

In this chapter, an experimental setup is outlined with the purpose of validating the modelled relay algorithm. The setup is verified, while errors and discrepancies are quantified. The validity of conclusions drawn based on the relay model is then discussed.

5.1 Experimental setup

The experimental setup incorporates a physical relay which is provided by DEIF A/S for this purpose. The relay is an MVR-215, which is a medium voltage relay that is commercially used. This relay contains several programmed protection functions, but for these tests, only ANSI-67 is enabled. The ANSI-67 algorithm in the provided relay is based on positive sequence polarisation. As such, only the results of the modelled positive sequence algorithm is compared to the experimental results.

A real-time test of the relay is performed by utilising an OMICRON CMC-356. The Omicron can output current and voltage waveforms from COMTRADE files, which are generated using the power system model described in Section 3.1 on page 22. The current and voltage waveforms in this system model are acquired directly from the system and include no scaling as the CTs and VTs are not modelled. In a real system, the relay will receive the secondary side voltage and current of the measurement transformers. Furthermore, the current and voltage magnitudes in the system are higher than the hardware ratings of both the Omicron and the relay. Thus, the Omicron scales the imported waveforms to be within its hardware limits. By choosing the scaling ratios in the Omicron settings, the CTs and VTs can be emulated in the experimental setup. The CT ratio is 600:1 and the VT ratio is 20:1. The resulting experimental setup is outlined in Figure 5.1. The physical devices are shown in Figures 5.2, 5.3 and 5.4.

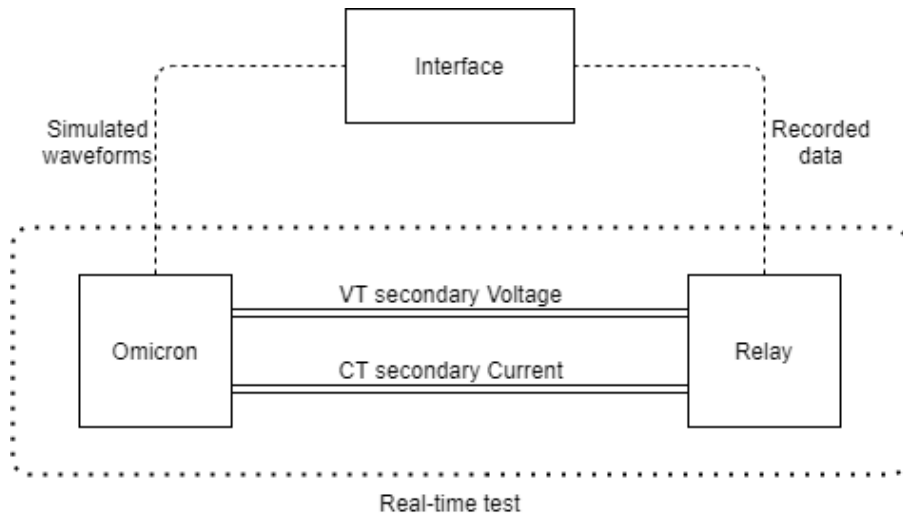


Figure 5.1: Outline of experimental setup.



Figure 5.2: DEIF MVR-215.



Figure 5.3: OMICRON CMC-356.



Figure 5.4: Experimental setup at Aalborg University

The figure illustrates that the simulated waveforms can be imported by the Omicron in preparation for a test, while recorded data from the test can be exported from the relay after a test. During a test, the voltage and current are generated by the Omicron and picked up by the relay in real-time. The current and voltage waveforms are simulated with a constant sampling frequency of 10 kHz. At this resolution, the Omicron can playback up to 3 seconds of data. As a result, each test is run for 1 second before the moment of the fault and 2 seconds after. The relay records data for 2 seconds before and after a trigger, which is configured to be the moment of the fault. The data can be both analogue and digital signals in the relay. The analogue signals are the phase currents and voltages, which are sampled at 64 samples pr. cycle, corresponding to 3840 Hz at a system frequency of 60 Hz. The digital signals are sampled at 200 Hz and can be system frequency, tripping signals and sequence components.

To validate the operation of the relay model in the modelled power system, a test case is chosen. As only one physical relay is available for testing, a single relay is chosen as the object of the relay model validation. The relay is R26, which controls CB26 located at the Bus 2 terminal of Cable 2-6 in the power system. Thus, the voltages used in the relay are the simulated phase voltages at Bus 2 and the phase currents at the Bus 2 terminal of Cable 2-6. To test the operation of this relay it will be exposed to a forward and reverse biased fault current. The relay is tested for both PP and 3P faults and the resulting 4 test cases are outlined in Table 5.1.

Table 5.1: Test cases for experimental validation of relay.

Test name	Fault type	Fault location
Reverse 2P	Bolted PP	Bus 2
Reverse 3P	Bolted 3P	Bus 2
Forward 2P	Bolted PP	Cable 2-6
Forward 3P	Bolted 3P	Cable 2-6

5.2 Verification of experimental setup

To comment on the results of the experimental tests, the operation of the experimental setup is verified. The generation of input signals for the relay, by using an Omicron is investigated by measuring the output of the Omicron during tests. In addition, the relay data recording should be verified, but the validation of the relay operation will be based solely on the fault detection signal of the relay, which needs no further verification other than the tests defined in Table 5.1, the results which are discussed later in this chapter.

The playback function of the Omicron is verified by comparing the simulated voltage and current waveform with the measured output of the Omicron. Phase A is measured during the Forward 3P

test, using the relay disturbance recorder. The measured signal and the simulated waveform including CT scaling are shown in Figures 5.5.

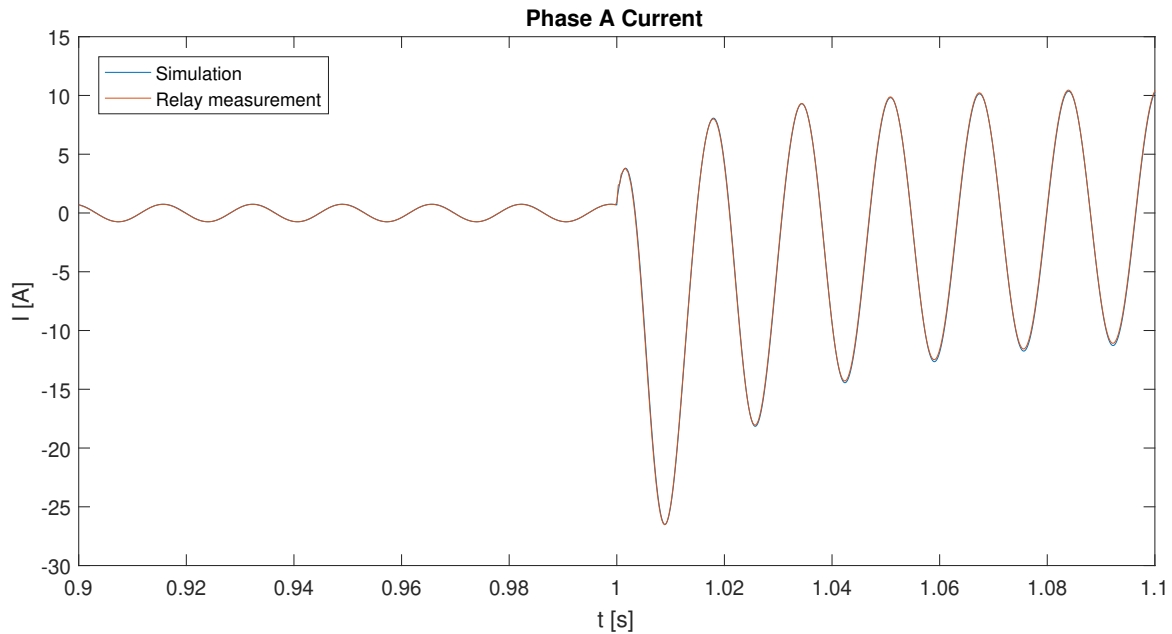


Figure 5.5: Recorded and simulated phase A current during Forward 3P test.

The figure illustrates that the measured signals correspond to the simulated signals at the moment of the fault. The current measurement of the relay has an error in magnitude of approximately 0.13%. These errors are within the accuracy ratings of the hardware. The relay current measurement inaccuracy is $<0.5\%$ or <15 mA, while the Omicron current output inaccuracy is 12.8 mA + 0.05% [28, p43,29, p43]. The signal errors are similar for the voltage. Thus, the playback function of the Omicron is verified as there is complete overlap between the simulated current waveform and the current recorded by the relay.

5.3 Validation of Relay Operation

To validate the correct operation of the modelled relay, the physical and modelled relay are each subjected to the tests defined in Table 5.1 and the timing of the "Start" is then compared. The Start signal is the moment the fault is detected, starting the intentional time delay.

5.3.1 Reverse PP Fault

The results of the Reverse 2P test is shown in Figure 5.6.

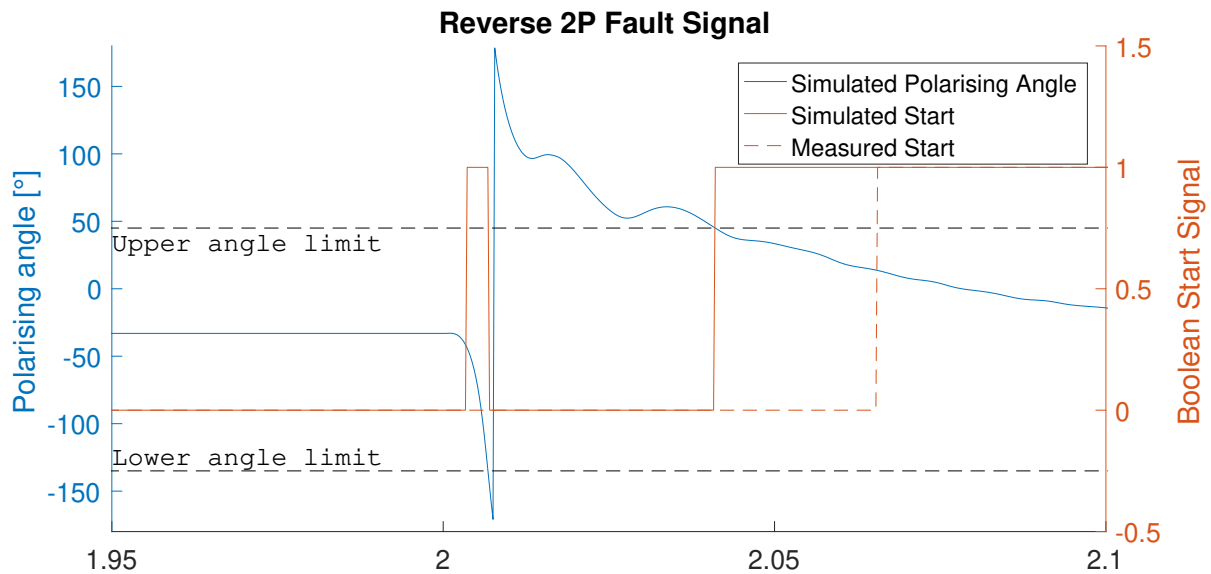


Figure 5.6: Reverse 2P test polarising angle, along with start signals.

During the Reverse 2P test the Start signal of the modelled relay becomes high for approximately 1 period immediately following the fault. This happens because it takes a minimum of 1 period to estimate the phase angle and the current then becomes reverse biased. This has no practical impact because the signal is too short for the relay to trip. The comparable start signals become high at 41 ms and 66 ms following the fault for the modelled and experimental signal, respectively. The relays trip at these times because the reverse biased current of the motor has dropped to a magnitude where the current through the relay is once again forward biased, but at a lower magnitude. The delay of 25 ms is partially accounted for by the resolution of the recorded data from the relay which has a sample time of 5 ms. That still means that at least 20 ms of delay is caused by differences in phase estimation or computational delay. The differences in phase estimation can be both measurement inaccuracy and calculation delay, however, regardless of the cause, the 10 to 25 ms second delay is not likely to make a significant impact on the correct operation of the relay and the modelled relay is validated for this case.

5.3.2 Reverse 3P Fault

In Figure 5.7 the results of the Reverse 3P test is shown. In this test, neither relay detects a fault, as intended for a reverse fault. The correct operation of the modelled relay is therefore validated for this case.

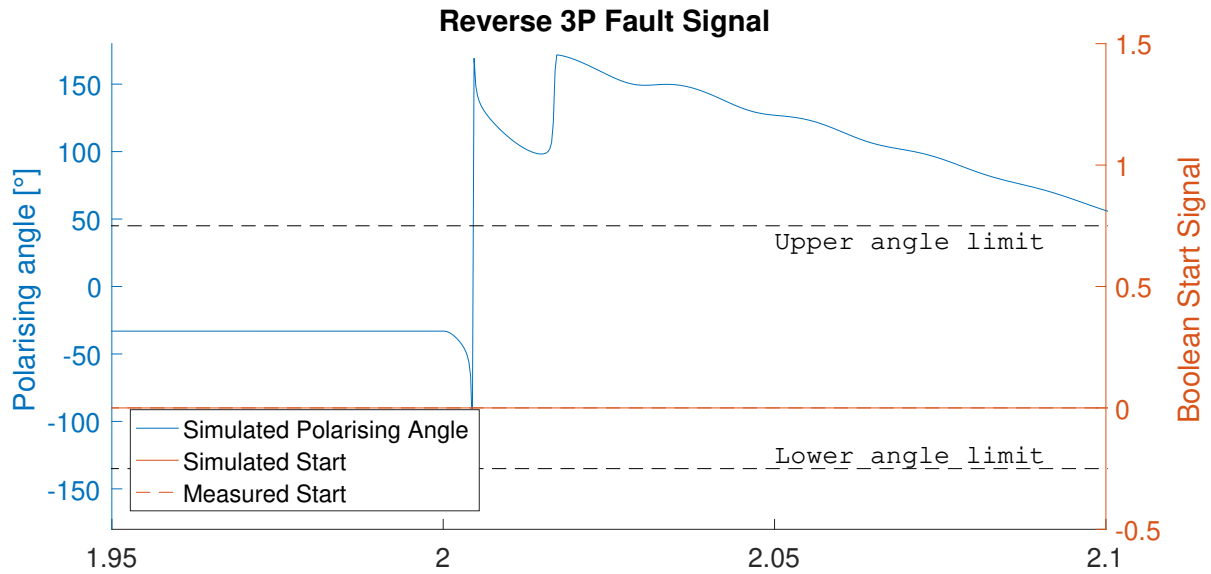


Figure 5.7: Reverse 3P test polarising angle, along with start signals.

5.3.3 Forward PP and 3P Fault

The results of the forward biased fault case are shown in Figure 5.8 and 5.9. For the Forward 2P test the experimental setup detects the fault 5 ms delayed compared to the model, while the delay is 10 ms for the Forward 3P test. In both cases, up to 5 ms of the delay can be accounted for by the resolution of the recorded Start signal. For the forward faults it relays are forward biased throughout the test, and as a result, the delay in the experimental setup compared to the modelled relay is minimal and the relay model is validated for these cases. In addition, during the 3P faults, the phase voltages in the test are at a magnitude where the relay switches from using the measured voltage angle to the voltage memory. It is shown that for these fault cases the use of voltage memory has no adverse effect on the reliability of the relay polarisation.

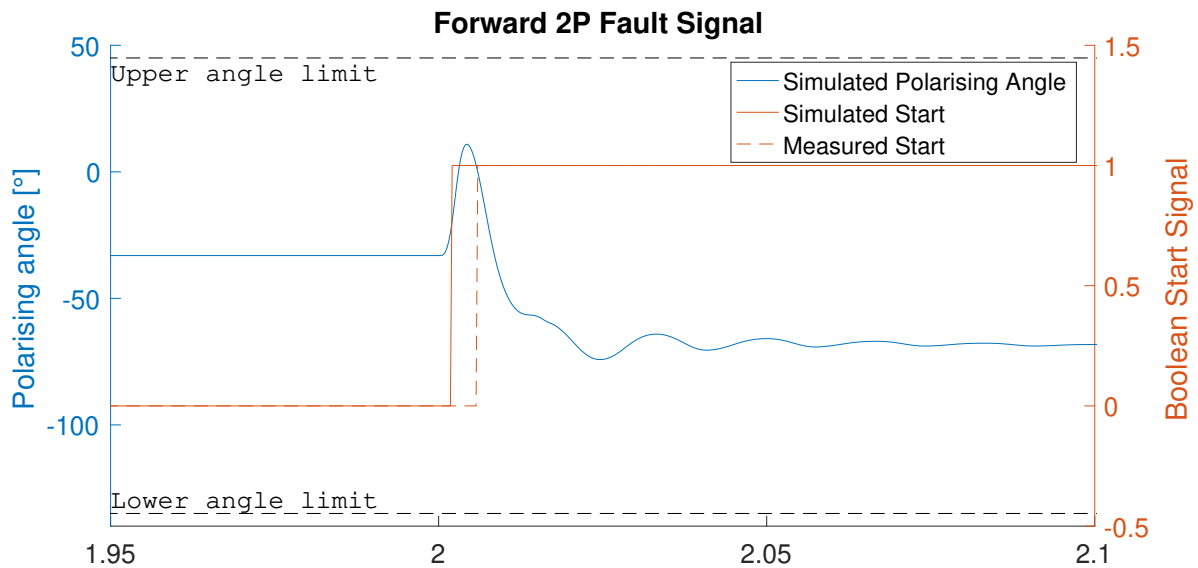


Figure 5.8: Forward 2P test polarising angle, along with start signals.

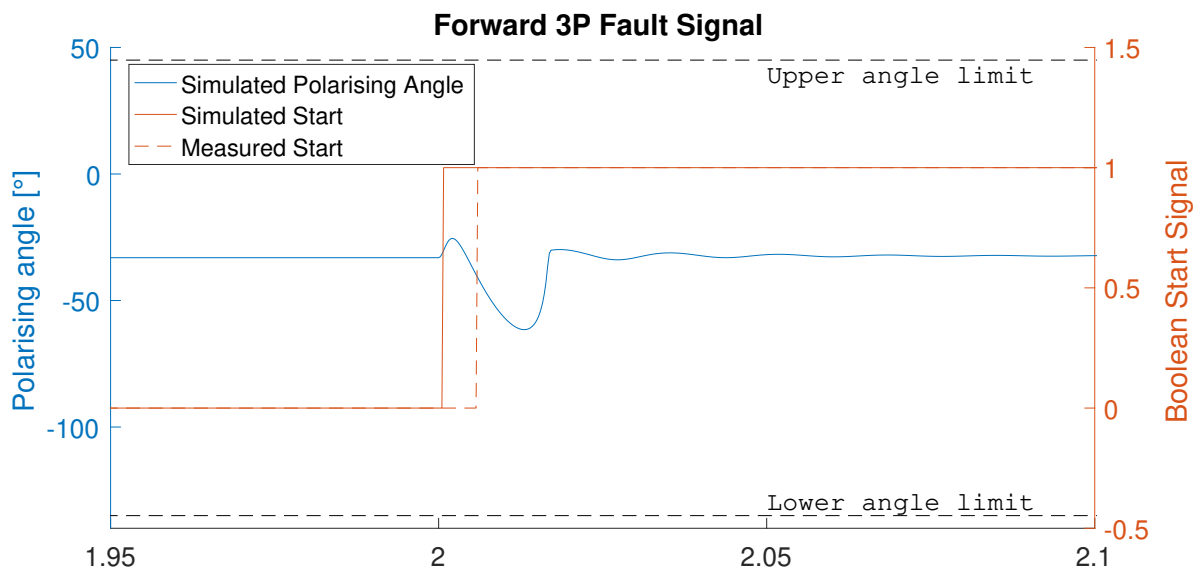


Figure 5.9: Forward 3P test polarising angle, along with start signals.

The delays in the operation of the real relay compared to the modelled relay is likely caused by computational delay, as it is observed that a large change in angle adds to the delay. However, it is observed that the longest delay in these fault cases is 25 ms which is unlikely to cause faulty operation of the relay, as a typical time grading delay will be 150 to 300 ms. The relays are observed to pick up the same faults and the relay model is considered validated against the real relay. Thus, the expected operation of the MVR215 relay is also verified.

5.4 Summary

In this chapter an experimental setup is outlined, using a physical relay provided by DEIF A/S and tested using an OMICRON CMC-356. The operation of the modelled relay is then validated by comparison the to results of the real relay. The results show that the fault detection of the modelled relay acts similarly to the real relay for the chosen fault cases, and it is unlikely that the modelled relay will trip in cases where the real relay would not, or vice versa. It is also observed that the real relay detects the fault slower than the modelled relay, likely due to computational delay, and it can be concluded that the operation of the modelled relay is validated, provided that an added delay of up to 25 ms does not make a significant difference to the correct operation of relays.

6 | Impact of polarisation methods on power system protection

The purpose of this chapter is to evaluate each investigated polarisation method and its uses in a protection scheme for the modelled power system. This is done by proposing a protection scheme for the power system and then quantifying the impact of frequency deviation, fault impedance and system load on each polarisation method. Then the proposed protection scheme is analysed and the performance of each polarisation method is discussed in the context of the proposed protection scheme.

6.1 Protection scheme

A protection scheme can be developed for the modelled power system using time grading and RB. To use RB a forward direction in the loop is defined and the direction of relays shown in Figure 6.1.

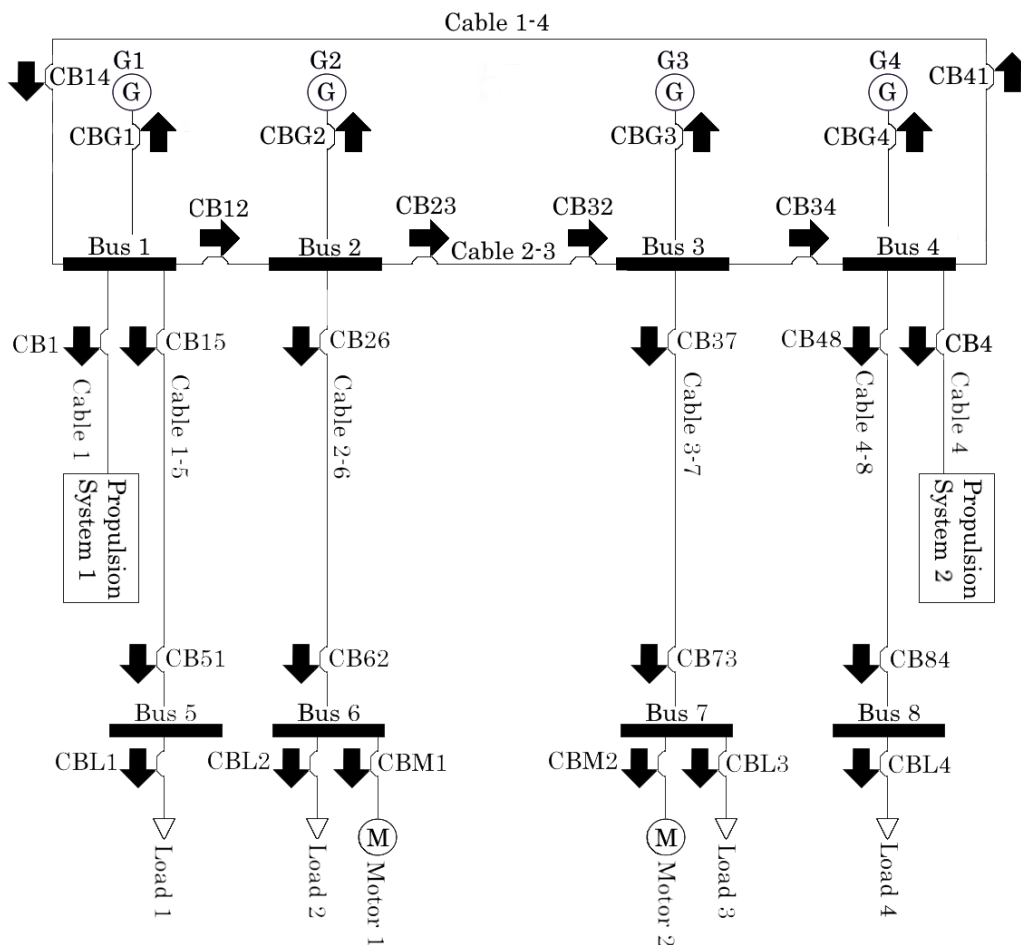


Figure 6.1: Maritime power system with forward direction indication of each relay.

To ensure selective tripping in case of a fault reverse relay blocking and interlocked CBs is utilised according to Table 6.1. E.g. if CB14 is picking up the fault then CB41 cannot trip, but if CB41 trips then so does CB14. For this protection scheme to function, forced tripping signals must take precedence over blocking signal. With this logic communication delays are minimised as each relay only needs to monitor the state of its neighbouring relays and there is no need to transfer information through chains of devices. In addition, tripping in the loop is selective without the use of additional time grading, which should result in fast tripping for faults in the loop. An example of the performance of this protection scheme for a fault in the loop is shown in Figure 6.2.

In this example, if the correct polarisation of relays is assumed, CB14 will be reverse biased while CB41 will be forward biased. CB41 will trip and as a result, CB14 will also trip due to CB interlocking, clearing the fault. This action needs no time delay other than an IDMT delay to ensure the correct polarisation of the relays. During the fault, it is not obvious what the bias of the remaining relays in the loop will be i.e. CB12, CB23, CB32 and CB34, however when examining the tripping logic it is apparent that this does not matter because it can be assumed that CB23 and CB32 will have the same bias. If they are reverse biased CB12 will also be reverse biased and none of them will trip while CB34 will be blocked by the bias of CB41. If CB23 and CB32 are forward biased then all the remaining relays will be blocked. Thus, the protection will trip selectively for faults in the loop, provided the relay reliably detect the direction of the fault current. However, the protection scheme becomes more complex when considering feeder faults. An example case is given for at fault at Bus 6 in Figure 6.3.

In this example, CB12, CB26 and CB62 are all forward biased, while CB23 is reverse biased. This means that CB12 is not blocked by the described logic and will likely trip Bus 2, leading to the unnecessary disconnection of generator G2. Thus, additional tripping logic must be introduced and in this protection scheme time grading can be utilised. The ends of each feeder need not be time graded i.e. the loads, however working backwards through the series connection to the loads, each additional CB increases the time grading. The duration of time grading is usually based on the rated speed of CB, but in this system model the CBs are ideal components. The duration of time grading is arbitrarily chosen to be 150 ms and the resulting time grading is shown in Table 6.2.

Table 6.1: Logic of RB in the loop and interlocked CBs in the power system.

Associated CB	Received signal	Relay action
CB14	Trip CB41	Trip
	Start CB12	Block
CB41	Trip CB34	Trip
	Start CB14	Block
CB34	Trip CB32	Trip
	Start CB41	Block
CB32	Trip CB 23	Trip
	Start CB 34	Block
CB23	Trip CB12	Trip
	Start CB32	Block
CB12	Trip CB14	Trip
	Start CB23	Block

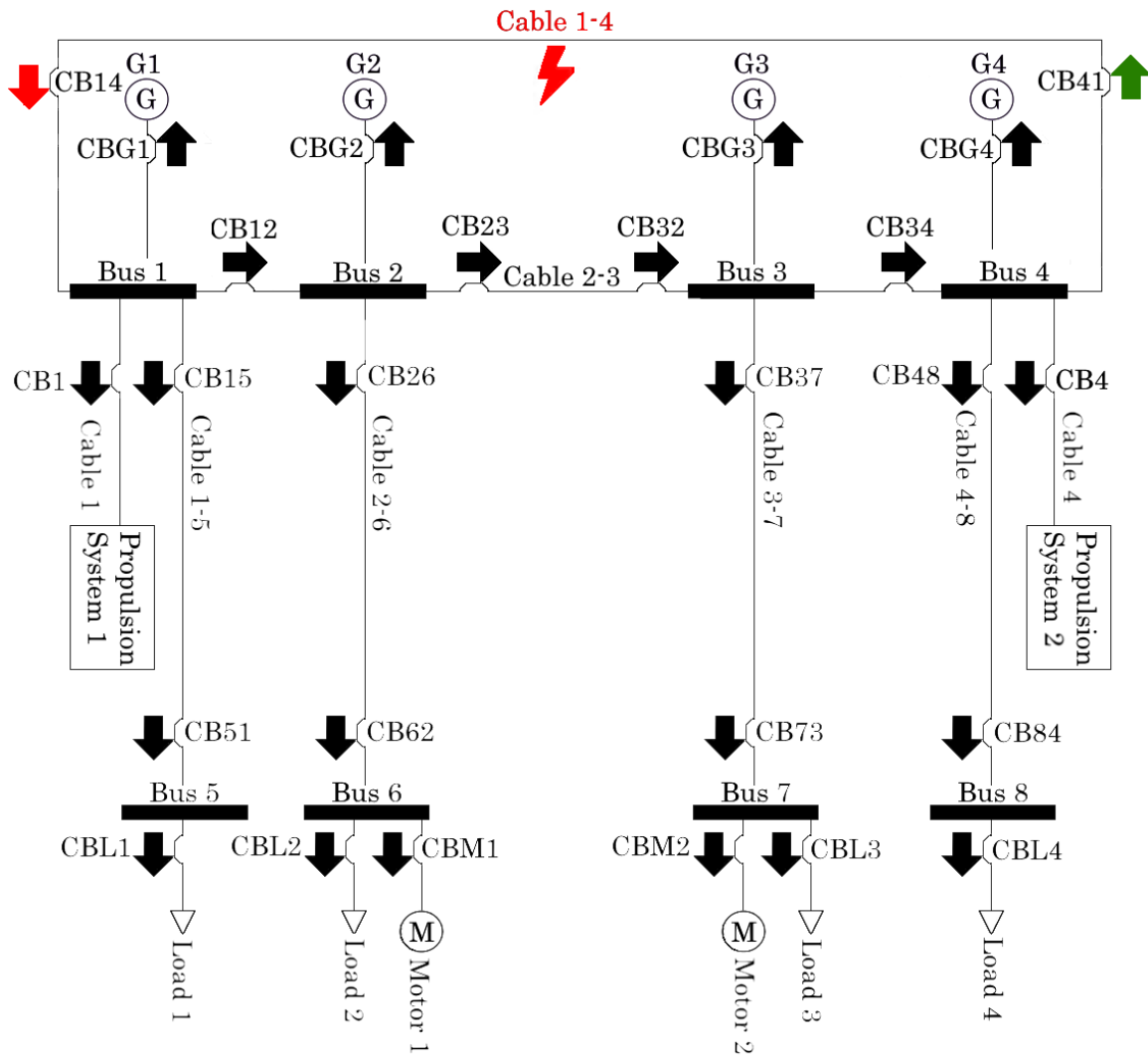


Figure 6.2: Example of protection scheme for a fault at Cable 1-4.

Table 6.2: Time grading of relays.

Associated CB	Time grading nr.	Absolute delay
CB51, CB62 CB73, CB84	1	150 ms
CB15, CB25 CB37, CB48	2	300 ms
CB14, CB12 CB32, CB34	3	450 ms

Adding time grading to the protection scheme allows for selective tripping for any fault location in the system, but adds to the tripping delay, especially in the case of faults on the MSBs. Each relay in the loop with a forward direction towards a busbar now has the longest time grading in the system. A protection scheme that can ensure selective tripping of faulted components has been proposed, utilising

6.2.1 Frequency deviation

In maritime power systems, the system will likely operate at frequencies deviating from the nominal frequency for some periods of time. Therefore it is prudent to quantify the effect of frequency deviation on the phase angle estimation of the relay to ensure the correct operation of the relays during these periods. It should be noted that there are several options for methods of phase angle estimation in relays, but in the modelled relay DFT is performed with a constant sampling time of 0.26 ms, corresponding to approximately 64 samples/cycle at 60 Hz. As this test is related to the phase estimation method and the phase estimation method is the same for all polarisation methods, the choice of polarisation method in this test is inconsequential.

The test is performed by applying voltage and current signals to the relay model using I_x/V_x self-polarisation. The voltage and current signals are applied in the range of 55 Hz to 65 Hz, as this is typically the allowable frequency range for generator protection settings in maritime power systems. The resulting polarising angles are shown in Figure 6.4. The graph shows that at nominal frequency the polarising angle is stable at 5.65° and as the frequency deviates, the polarising angle begins to deviate and oscillate. As the frequency deviates within a relatively large range of 10 Hz, the maximum difference in polarising angle is approximately 2.8° .

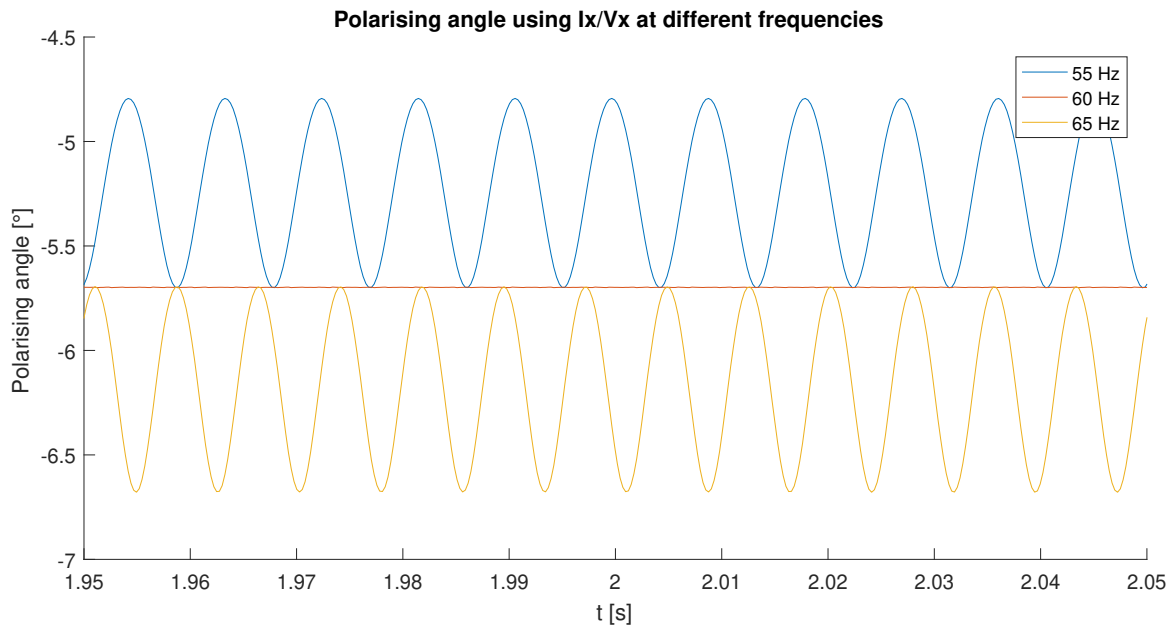


Figure 6.4: Polarising angles at different system frequencies for I_x/V_x polarisation.

When utilising DFT with constant sampling time at a frequency different from the nominal frequency, phase angle deviation will accumulate at a rate proportional to the difference in frequency. This will make the phase angle estimate of a single quantity unreliable. The reason this does not appear to

be an issue relay model and polarising angle error remains constant at a constant frequency, is that the current and voltage have synchronous sampling. This means that the accumulated phase angle deviation of the current and voltage are equal, and since the polarising angle is the difference between two quantities, the phase angle deviation is nullified. Synchronous sampling is common practice in commercial relays as well and is used in the MVR-215 utilised in previous tests. Thus, provided synchronous sampling is utilised, it is unlikely that a change in system frequency will cause incorrect polarisation of directional relays.

6.2.2 Fault impedance

In this test, fault cases will be examined with varying fault impedance for each polarisation method. The purpose of this is to quantify the impact of fault impedance on polarising angle for each method and assess the impact of fault impedance on the reliability of the relay.

For cables faults, the angle of the SC impedance is substantially smaller than the angle of the source impedance and the impact of the X/R ratio of the fault impedance on the fault current angle will be negligible. Thus, the fault impedance can be approximated as being purely resistive [30, p. 110]. Three fault impedance levels are defined for these tests. Low fault impedance will be approximately zero and will serve as a basis for comparison to the impact of the fault impedance. Medium fault impedance is 2Ω as this is a common estimate of arcing faults in cables at medium voltages [30]. High fault impedance is 20Ω , which is included to illustrate the impacts of a large range of fault impedances, but it is not a realistic case.

Impact of Fault Impedance on Positive Sequence Polarisation.

A PP fault is applied to the Cable 1-4 in the power system model described in Section 3.1 on page 22 with a Varied load case and the test is repeated for each fault impedance. The fault occurs at $t=20s$. Cable 1-4 is chosen as the fault location for this test because it is nearly unloaded during normal operation. As a result the relays at the cable only see the fault current and any impact of different fault impedances can be observed in isolation. The voltage and current data are applied to the relay model described in Section 4.1 on page 40 and repeated for each polarisation method. The polarising angle of the relay controlling CB41 when using positive sequence polarisation is illustrated in Figure 6.5. CB41 should be forward biased during a fault at Cable 1-4, based on the protection scheme defined in Section 6.1.

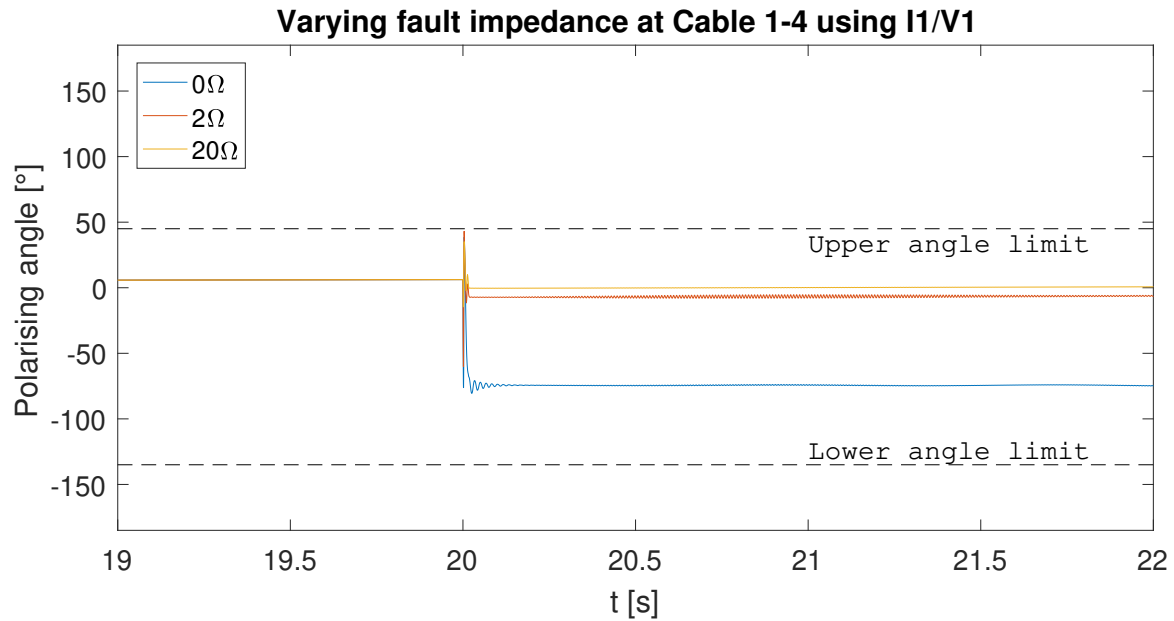


Figure 6.5: Polarising angles at different fault impedances using positive sequence polarisation at the relay controlling CB41 during PP fault at Cable 1-4.

Observing the polarising angle when using positive sequence polarisation it becomes clear that as the fault resistance increases the polarising angle approaches zero, as the fault current becomes more resistive. Regardless of fault impedance, the polarising angle is well within the angle limits and the relay is forward biased as expected. While having a significant impact on the polarising angle, fault impedance has no impact on the reliability of a relay using positive sequence polarisation during PP faults.

Impact of Fault Impedance on Self-Polarisation.

The test is repeated for each variant of self-polarisation but the results are similar for each case and so only one variant is discussed here I_x/V_{xy} variant. The results of the remaining tests can be found in Appendix C. The polarising angles of phase A during a PP fault between phase A and B, when using I_x/V_{xy} polarisation can be observed in Figure 6.6 while the polarising angle of phase B can be observed in Figure 6.7.

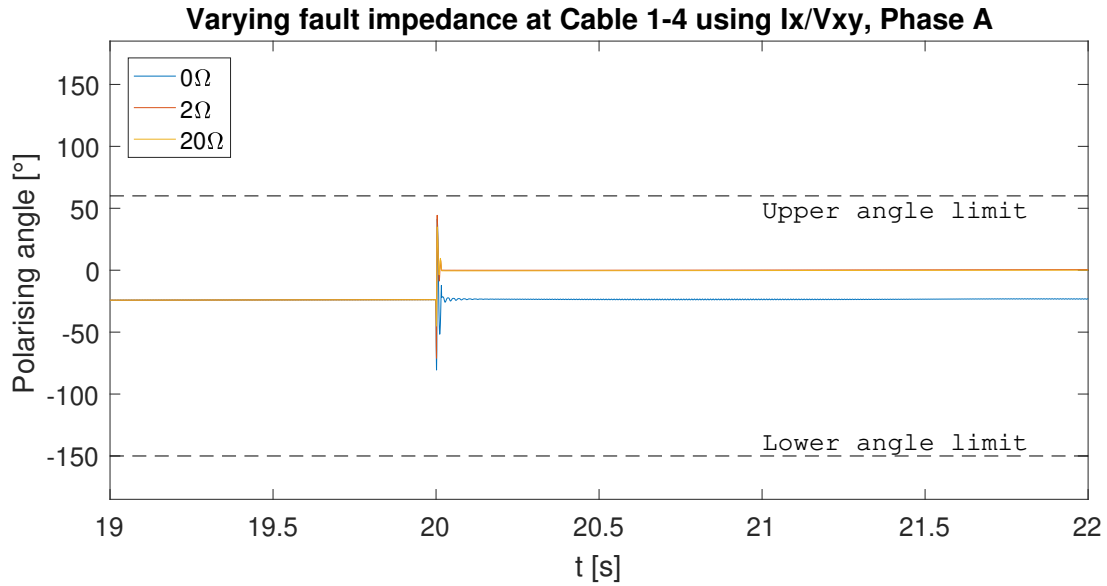


Figure 6.6: Polarising angles of phase A at different fault impedances using I_x/V_{xy} polarisation at the relay controlling CB41 during PP fault at Cable 1-4.

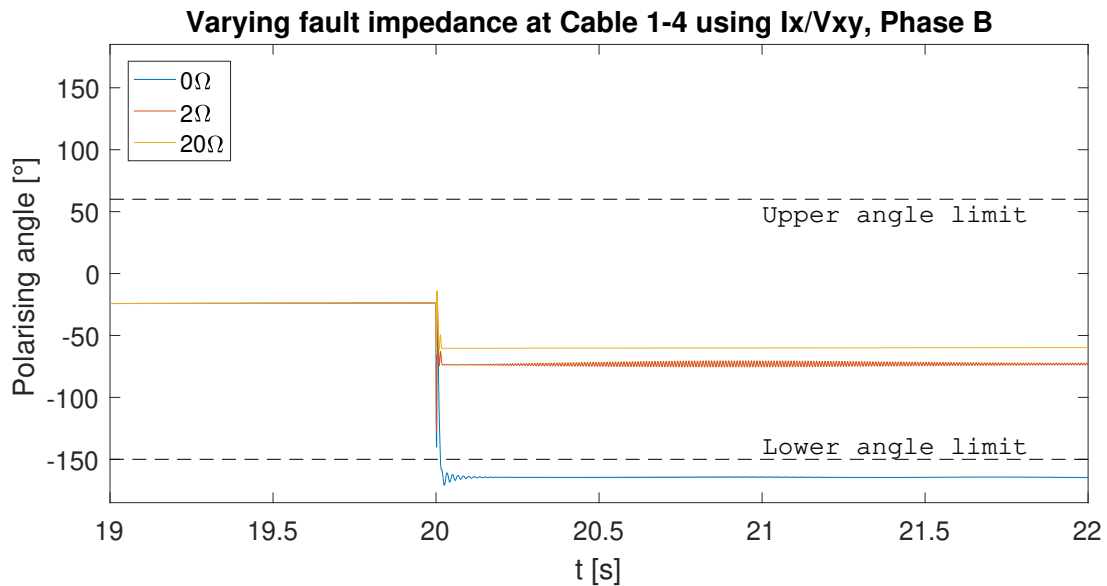


Figure 6.7: Polarising angles of phase A at different fault impedances using I_x/V_{xy} polarisation at the relay controlling CB41 during PP fault at Cable 1-4.

It is notable in Figure 6.6 and 6.7, that the relay is not directional at low fault impedance because one of the faulted phases is forward biased while the other is reverse biased. This is caused by the large angle difference between the polarising angle of the two phases which is inherent to all self-polarisation methods during PP faults. It is therefore remarkable that for larger fault impedances the angle difference between the polarising angle of phases A and B is reduced and the relay correctly detects the forward bias of the fault current for both the faulted phases. The reverse is also true for reverse biased faults which can be found in Appendix C and as a result, the performance of self-polarisation methods is improved at higher fault impedances.

Impact of Fault Impedance on Cross-Polarisation.

The test is repeated for cross-polarisation and the polarising angles of phase A during a PP fault between phase A and B, when using cross-polarisation can be observed in Figure 6.8 while the polarising angle of phase B can be observed in Figure 6.9.

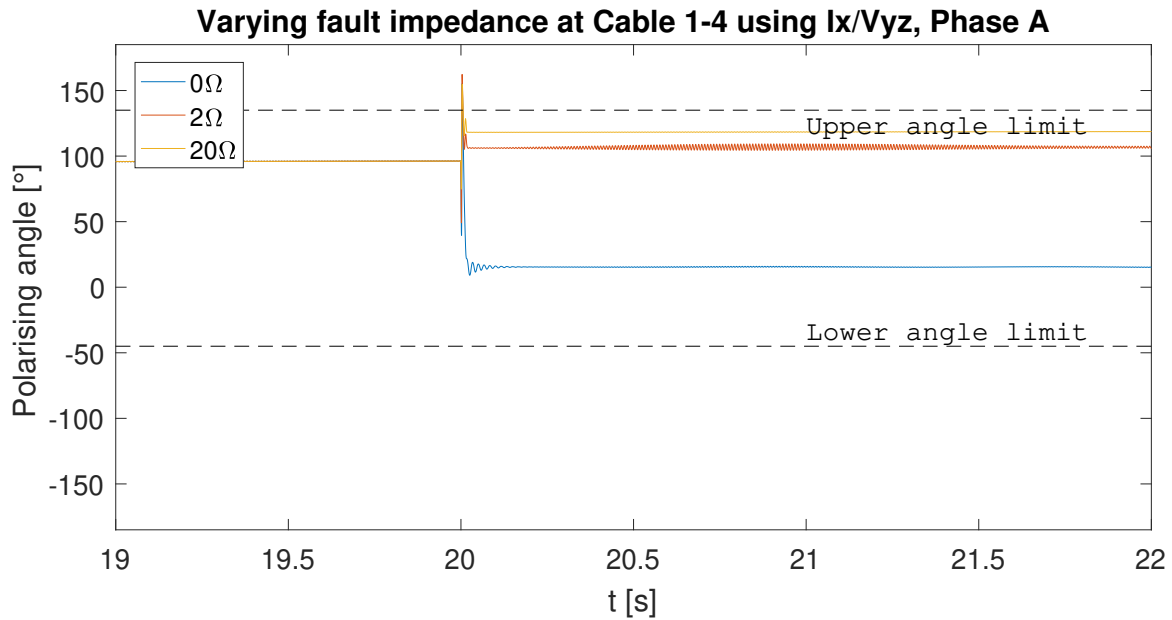


Figure 6.8: Polarising angles of phase A at different fault impedances using cross-polarisation at the relay controlling CB41 during PP fault at Cable 1-4.

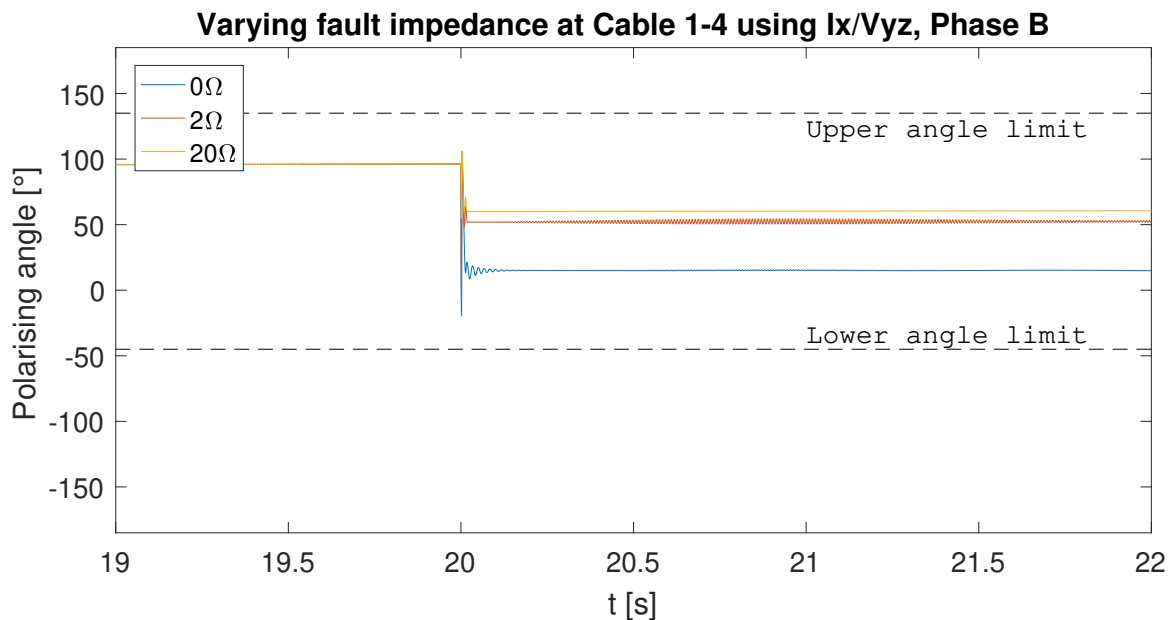


Figure 6.9: Polarising angles of phase B at different fault impedances using cross-polarisation at the relay controlling CB41 during PP fault at Cable 1-4.

In the case of cross-polarisation the polarising angles of the faulted phases during PP faults is by definition equal, provided the fault impedance is zero, which is also observed in the low impedance test case. At higher fault resistances the fault current becomes more resistive, while the difference between the voltage angles of the faulted phases increases. As a result, the polarising angle of one phase, in this case, phase B, approaches 60° while the angle of the other polarising angle approaches 120° . These polarising angles are still within the limits of being forward biased as expected, however, it is noteworthy that one polarising angle approaches the limit between forward and reverse biased, which is 135° for the default relay settings. While no single parameter investigated in this report has been shown to introduce a possible error 15° , it may be possible for some situations that cross-polarisation is not reliable for these relay settings. It is therefore prudent to assess whether erroneous detection of fault current detection can occur in a real relay using cross-polarisation for high impedance PP faults. It is also possible to change the RCA used for cross polarisation and this option is discussed further in Section 6.3.2.

In addition to each of the tests shown for PP faults, the same tests are done for 3P faults. The results of these test are shown in Appendix C, and show that changes in fault impedance have no significant impact on any of the polarisation methods during 3P faults.

6.2.3 System loading

In this test, fault cases are examined during a varied system load, a thruster dominant system load and a motor dominant system load. The purpose of this is to quantify any impacts the system loading has on the polarisation methods.

A bolted PP fault is applied to the Cable 2-6 in the power system model described in Section 3.1 on page 22. The fault occurs at $t=20s$ and the test is repeated for each system load. The system loads are Varied load, Motor dominant load and Thruster dominant load. Cable 2-6 is chosen as the fault location for this test because it supplies one of the motor loads, the size of which varies in the load cases. Thus, observing a fault in cable 2-6 will illustrate the impacts of varying the load current magnitude compared to the fault current. The voltage and current data are applied to the relay model described in Section 4.1 on page 40 and repeated for each polarisation method. The polarising angle of the relay controlling CB26 when using positive sequence polarisation is illustrated in Figure 6.10. CB26 should be forward biased during a fault at Cable 2-6, based on the protection scheme defined in Section 6.1.

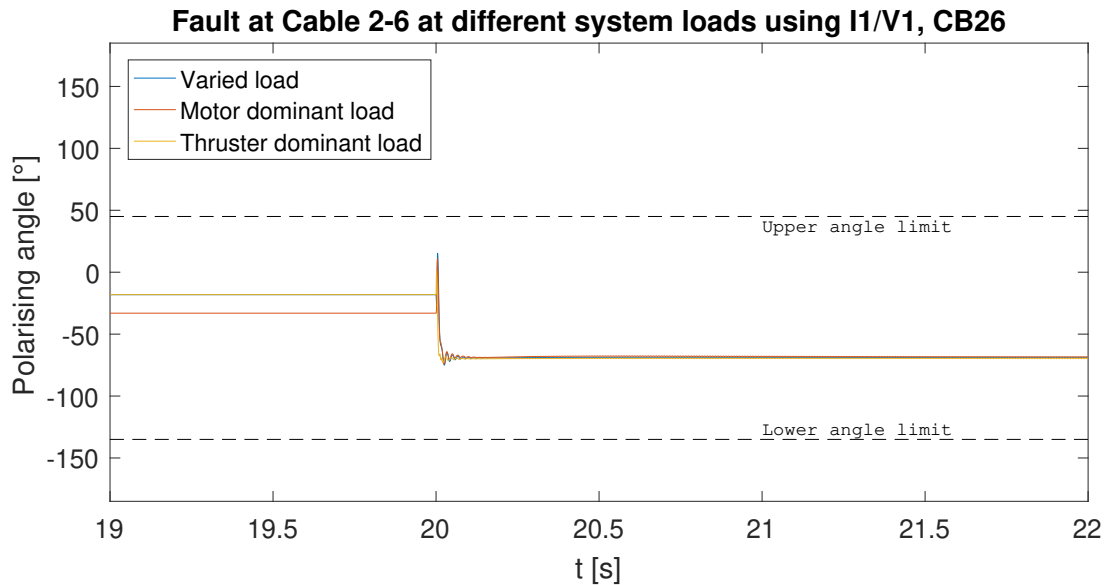


Figure 6.10: Polarising angles at different system loads using positive sequence polarisation at the relay controlling CB26 during PP fault at Cable 2-6.

The graph illustrates that before the fault, the polarising angle is higher in the case of a Varied or Thruster dominant load, compared to a Motor dominant load. This is expected, as CB26 is located such that the current supplying M1 is measured and the motor is largely an inductive component. However, during the fault, the measured current is mainly the fault current which is mostly unaffected by the size of the loads and as a result, the polarising angle is approximately equal for each load case. Figures 6.11 and 6.12 show similar results in the case of self- and cross-polarisation. Additional results including 3P fault cases are included in Appendix C. The load seems to have no impact on the polarising angle and the loads need not be considered when choosing a polarisation method.

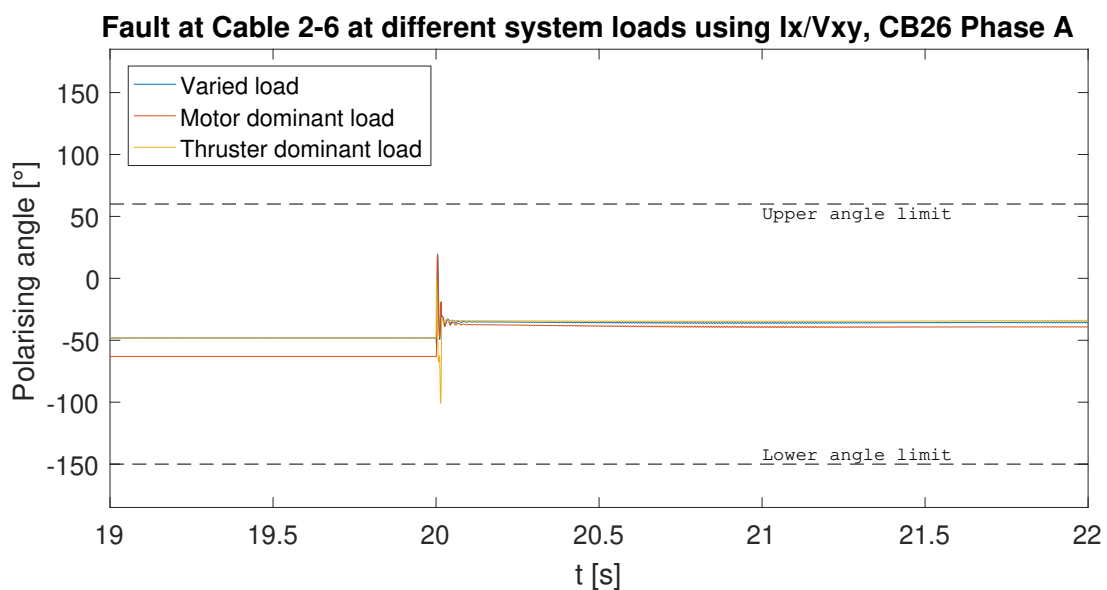


Figure 6.11: Polarising angles at different system loads using I_x/V_{xy} polarisation at the relay controlling CB26 during PP fault at Cable 2-6

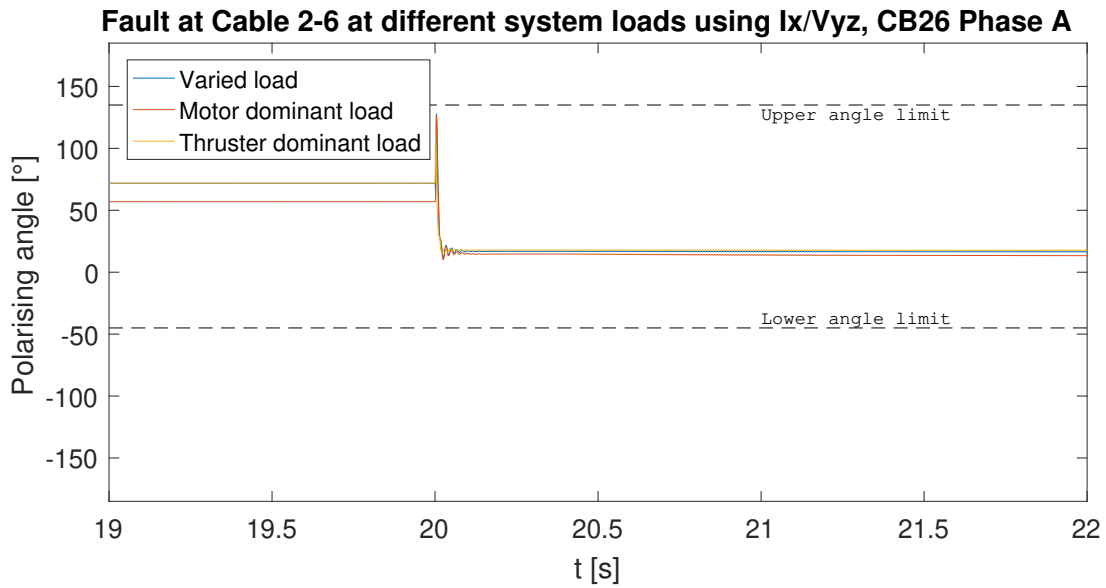


Figure 6.12: Polarising angles at different system loads using I_x/V_{yz} polarisation at the relay controlling CB26 during PP fault at Cable 2-6

While the system load has a negligible impact on the polarisation of the relay, it is still prudent to investigate whether the system load has any impact on the operation of the relays. Therefore, the pickup time of the relay controlling CB26 is investigated for each load case. The phase B current and the relay pickup time at CB26 when using positive sequence polarisation is illustrated in Figure 6.13. Due to the difference in system load, the rise time of the fault currents is different for each load case. However, for each load case the relay still picks up the fault within approximately 2 ms of each other and it is unlikely that the load case will have any impact on the correct operation of the relays.

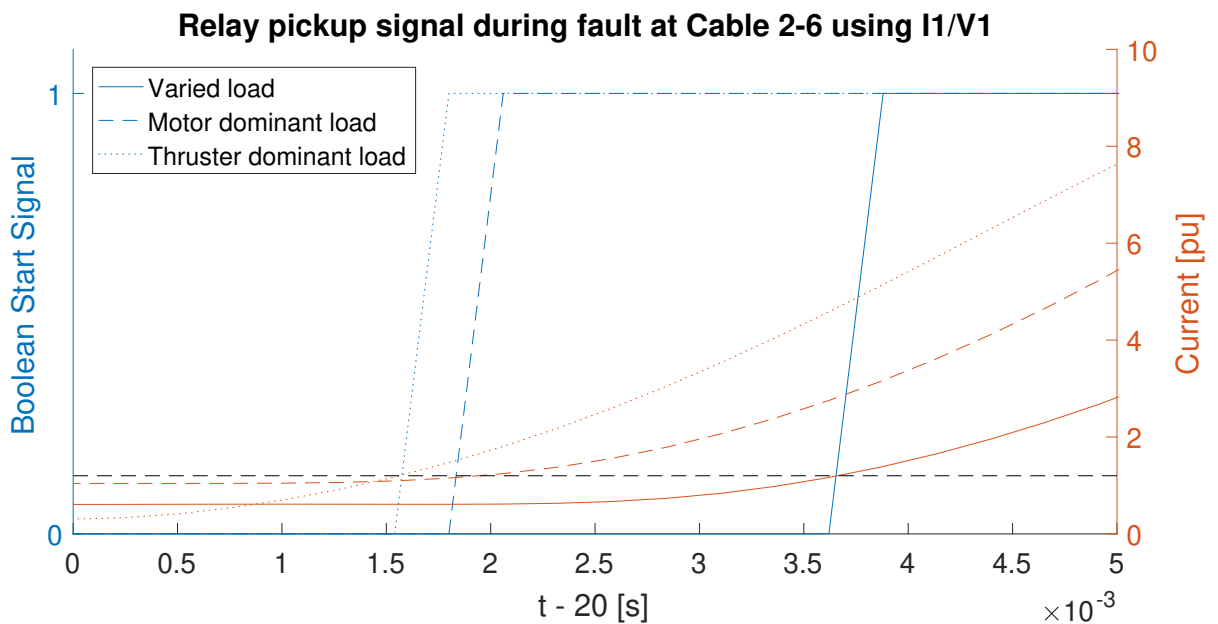


Figure 6.13: Difference in pickup time at different loads for relay controlling CB26 during PP fault at cable 2-6 using positive sequence polarisation.

6.3 Considerations in relay protection of maritime power systems

Based on the proposed protection scheme and the results of relay simulations, additional considerations on relay operation and protection of maritime power systems can be made. In this section, the impacts of ground faults on relay operation is considered and some assumption on relay settings is discussed and reevaluated. Finally, the proposed protection scheme is discussed in the context of maritime power systems by considering the effects of variable generation and system configuration on the performance of the protection scheme.

6.3.1 Ground faults

In this report, an analysis of relay performance during PP and 3P is performed. However, it is relevant to consider the operation of the modelled relay during other fault cases and ensure that the relay algorithms do not cause false tripping. Thus, the modelled relay is exposed to a PG fault and a PPG fault. Using the modelled system, the fault is applied at Cable 1-4 while observing the relay operating CB41. A comparison of PPG fault and the PP fault is shown for current magnitude in Figure 6.14 and the polarising angle using positive sequence polarisation in Figure 6.15.

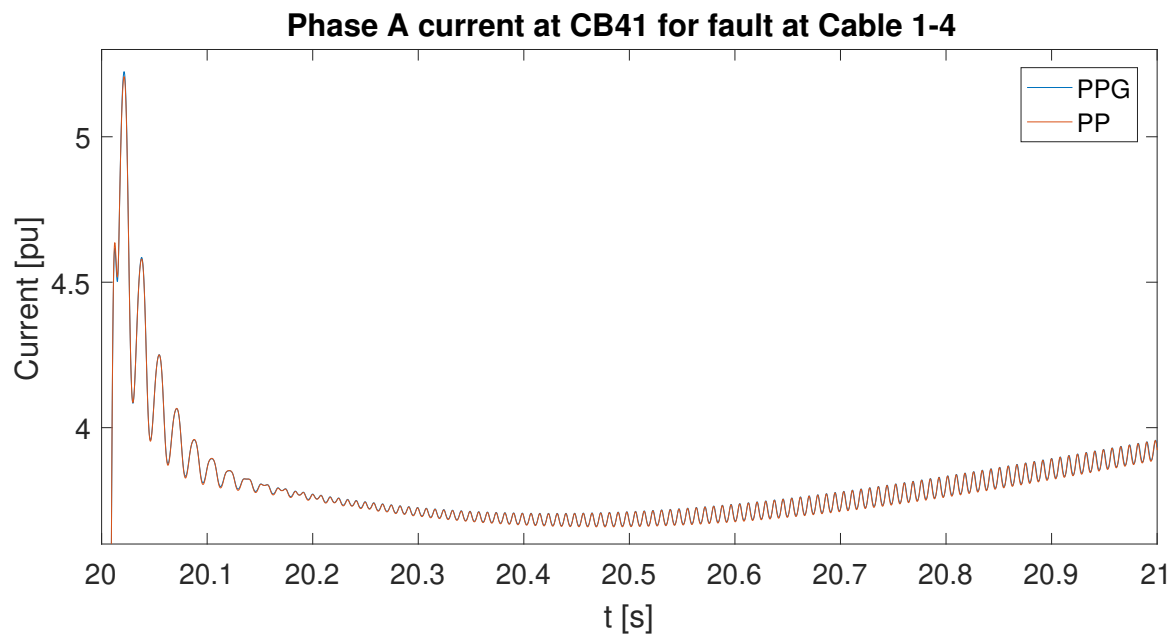


Figure 6.14: Polarising angles at different fault impedances using positive sequence polarisation at the relay controlling CB41 during PP fault at Cable 1-4.

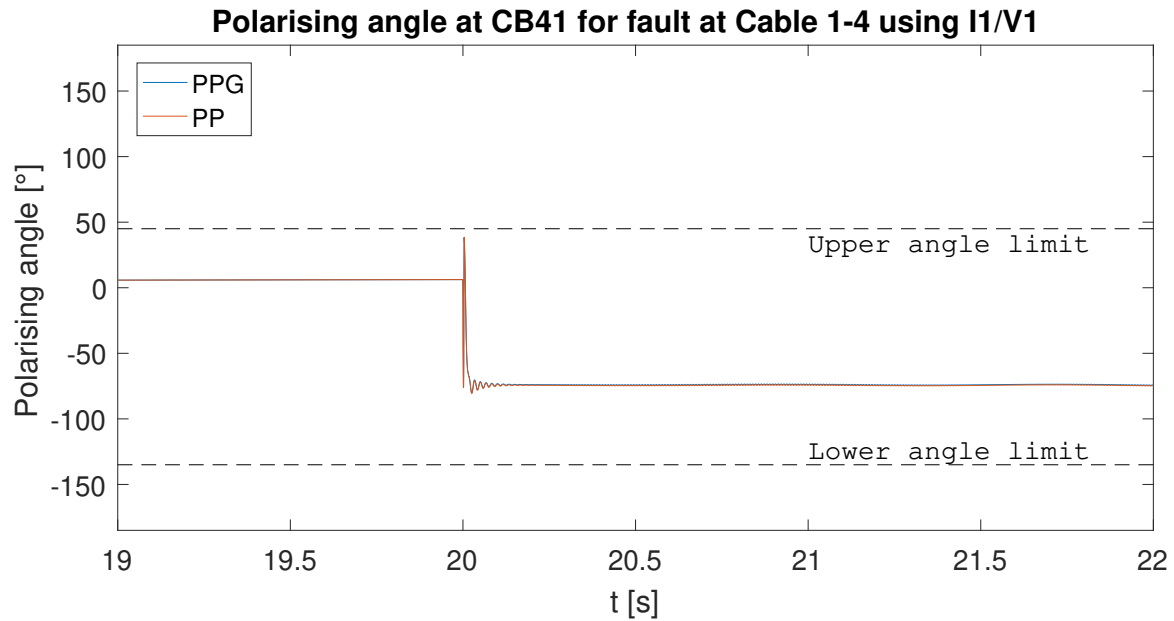


Figure 6.15: Polarising angles at different fault impedances using positive sequence polarisation at the relay controlling CB41 during PP fault at Cable 1-4.

Observing the current magnitude of phase A during a PPG fault and a PP fault it is apparent that the fault currents are practically equal. This is the case in the modelled power system due to the high resistance grounding of the generators causing a low ground fault current, and it is likely to be the case in maritime power systems in general. As a result, the polarising angle difference in the two fault cases is less than 0.5° . It is therefore expected that during PPG faults the relays will operate as though the fault was a PP fault, and correctly detect the current direction.

The fault current can also be observed during a PG fault in Figure 6.16. In this case, an increase in phase current magnitude of approximately 0.02 pu can be observed. It is noted that this increase occurs in Cable 1-4 which is unloaded during normal operation, and a fault current of this magnitude would be practically undetectable by the relay in a loaded cable. At this current magnitude, it can be expected that the relay will not detect PG faults in the power system, and other protection methods may be utilised for PG faults, such as ANSI-67N, directional earth fault protection.

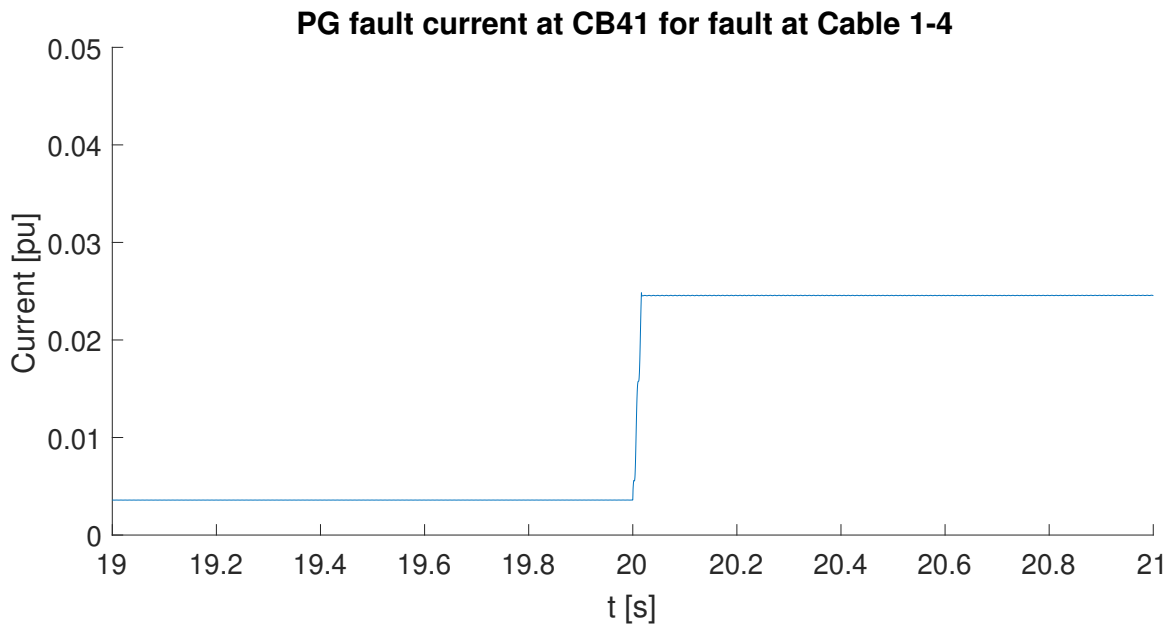


Figure 6.16: Polarising angles at different fault impedances using positive sequence polarisation at the relay controlling CB41 during PP fault at Cable 1-4.

6.3.2 Assumptions on RCA of polarisation methods

During the analysis of polarisation methods in this report, each polarisation method utilises the RCA values for each method that is commonly found in textbooks. While these generally hold true, it is relevant to consider whether a more suitable RCA can be determined for maritime power systems specifically. In the tests performed in this report, there has been no reason to reconsider the RCA of -45° for positive sequence polarisation, as each forward biased fault has been well within the defined tripping zone, and the reverse is true for reverse biased faults. In the case of self-polarisation, several RCAs can be defined, due to its variants. However, for each variant of self-polarisation, a case is shown in this report where one or more polarising angles are close to the limits of the tripping zone. This could lead one to reevaluate the RCA in these cases, but due to the difference in the polarising angles of the faulted phases during PP fault, even small changes to the RCA will cause the incorrect operation of the relay using self-polarisation in some fault cases.

Finally, in the case of cross-polarisation, for most of the shown fault cases, there has been no reason to reconsider the choice of RCA, however, in cases with high fault impedance it is observed that the polarising angle can approach the upper bounds of the tripping zone. At the same time, none of the shown fault cases has polarising angles close to the lower bounds of the tripping zone. This begs the question of whether the RCA for cross-polarisation can be changed to increase reliability. Based on the results in this report, the RCA can be increased by up to 45° before it will have an adverse effect on the relay operation, but finding a more suitable RCA for maritime power systems between 45° and

90° requires further analysis which is not included in this work.

6.3.3 Variable Generation

In maritime power system generation is modular and power demand is highly variable. As a result, a different number of generators can be connected at different times, and it is prudent to consider how this might impact a protection scheme. Considering the modelled power system with four generators connected in a loop. In case two or three generators are connected, there will be little or no impact on the directional setting of the proposed protection scheme because that is one of the benefits of connecting the generators in a loop. In addition, there is no reason a variable number of generators will have a significant impact on the performance of polarisation methods. However, when the number of generators changes so does the available SC power. Variance in SC power can lead to varying tripping times for the relays, especially in fault cases with significant fault impedance. This can lead to loss of coordination through time grading. Thus, when developing a protection scheme for a maritime power it must be assessed whether the SC current will be sufficiently higher than the load current, that the relay can operate with a single set of IDMT parameters. If this is not the case, then to utilise time grading reliably in a protection scheme, the relays IDMT setting must be updated, when a change in the number of connected generators occur.

6.3.4 Open main switchboard busbar loop

The modelled power system has the generators connected in a loop, and while this is the default state of the system, a protection scheme must take into account a situation in which the loop is opened. Using the proposed protection scheme while cable 2-3 is disconnected, it will become apparent that Bus 3 is no longer protected, and in case of changes to the number of connected generators, the protection scheme will need to change more drastically. Thus, when a CB is tripped in the loop, either deliberately or tripped by a relay, the relay settings must be updated. One solution would be to define the forward direction of each relay in the loop towards the opening in the loop, as illustrated in Figure 6.17. Reverse relay blocking would no longer be utilised, while interlocked pairs of CBs and time grading should be able to ensure reliable tripping. This would also require the use of bidirectional relays at CB14 and 41 in order to protect the Cable 1-4. Thus, CB14 and CB41 will trip regardless of the current direction, but they will have a longer time grading when reverse biased compared to forward bias. This method will add additional time grading and slow the operation of relays in some fault cases particularly, the relays performing cable protection in the loop.

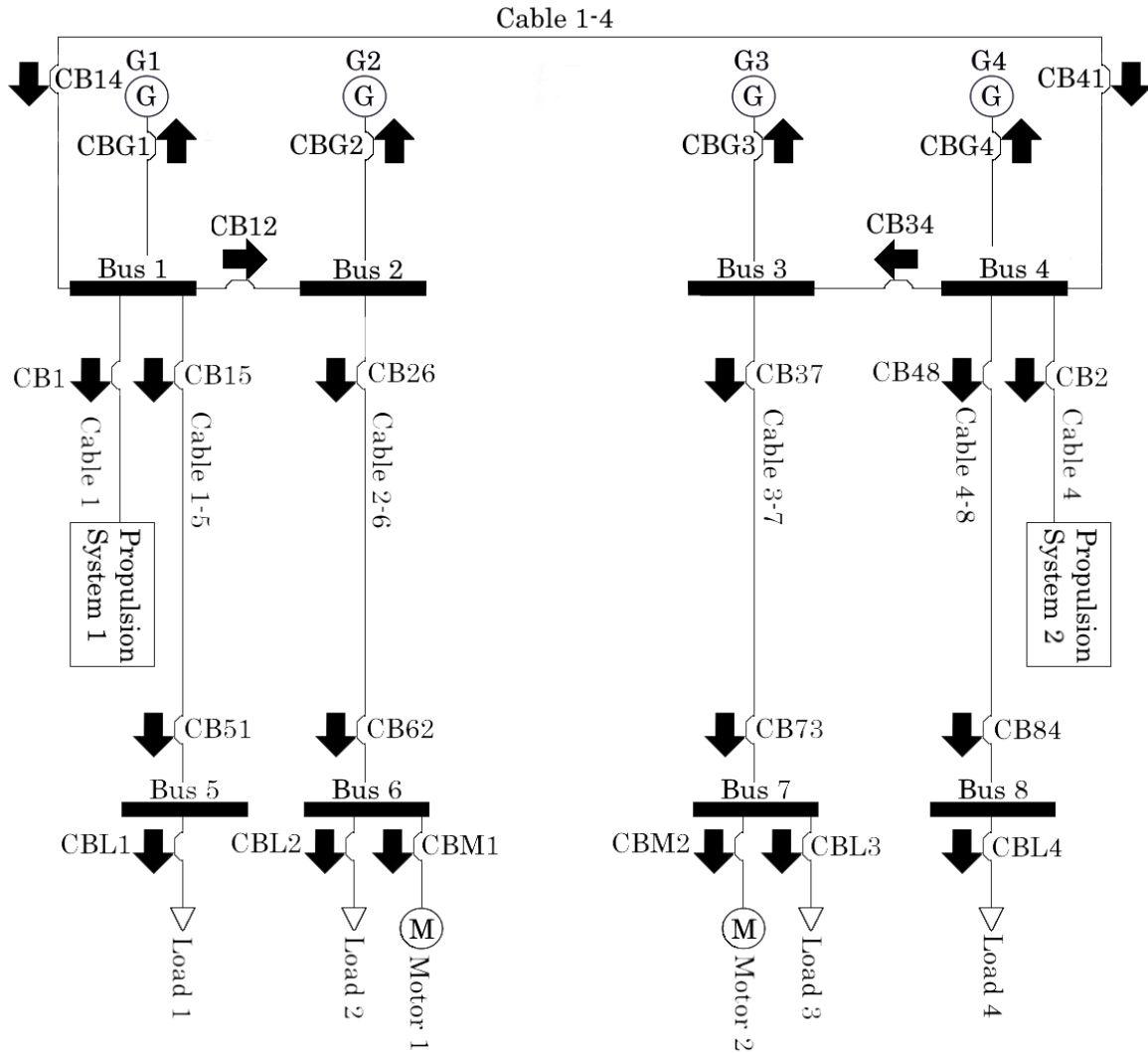


Figure 6.17: Relay forward directions in power system with open generator loop.

6.4 Summary

In this chapter a protection scheme for the maritime power system model is devised utilising RB, CB interlocking and time grading. Then the impacts of several parameters on the operation of relays is quantified. This includes, fault impedance, system loading, fault types and variable system frequency. The results of this is that positive sequence polarisation and cross-polarisation are identified as reliable polarisation methods for all of the examined cases. Then, the protection scheme is examined during changes to the system configuration using redundant connections. The main challenge to the development of fast, selective protection schemes is identified as changes to the system configuration.

7 | Conclusion

In this chapter, the main points of interest of this report are summarised and the contributions of the work performed in this thesis are clarified. Then, further studies on the subject of maritime power system protection are proposed and outlined. Before this, the main conclusions of this thesis will be made, based on the objectives of this report.

7.1 Thesis Summary

The main objectives of this thesis as defined in Chapter 1 are:

- Review a set of ANSI-67 algorithms and analyse the utilised polarisation methods for main switchboard busbar protection in closed-ring-multiple-infed configurations.
- Investigate the operation of relays utilising ANSI-67 in a benchmark maritime power system in a simulation environment and validate relay models in an experimental setup.
- Evaluate the performance of various polarisation methods for ANSI-67 protection and analyse their impact on the development of protection schemes for closed-ring-multiple-infed maritime power systems.

In this report, a 8-bus closed-ring-multiple-infed maritime power system model is developed and used to simulate fault cases in the power system. A relay model is developed containing 5 variations of ANSI-67 algorithms to compare the performance of polarisation methods. One of the algorithms is validated in an experimental setup using a real relay provided by DEIF A/S. The performance of the modelled relay is then tested through simulations and the results are analysed, to review and investigate the performance of polarisation methods in maritime power systems

The ANSI-67 protection algorithms to be reviewed are based on three polarisation methods which are investigated in this thesis, with some additional variants of the methods. The methods are self-polarisation, cross-polarisation and positive sequence polarisation.

Self-polarisation cannot be recommended for most considered cases. In its simplest implementation, it will not be reliably directional during phase-to-phase faults. Accurate detection of current direction when using any variant of self-polarisation relies on the existence of a minimum fault impedance, which cannot be guaranteed during bolted faults. While other methods may be applied to increase the

reliability of self-polarisation methods, this would provide no apparent benefit over other polarisation methods, and as such, there is no reason to increase the complexity of the algorithm.

It can be concluded that the positive sequence polarisation and cross-polarisation algorithms, both perform reliably for all investigated fault cases and with pickup times of less than one period of the system frequency. The only differences in the operation of positive sequence polarisation, compared to cross-polarisation, that may be significant is in the case of phase-to-phase faults with high fault impedance. It is possible that cross-polarising relays may operate too close to the angle limits of its tripping zone to be reliable, but this has not been definitively shown in this report. There may be simple solutions such as adjusting the characteristic angle for cross-polarisation. In conclusion, both cross-polarisation and positive sequence polarisation are suitable options for ANSI-67 protection in maritime power systems.

In general, the choice of polarisation method is not significantly different in a maritime power system compared to land-based power systems. The factors in a maritime power system that could be assumed to have an impact on polarisation methods are variable system frequency, variable short-circuit power, large penetration of motor loads or short cable distances, however, this report shows that these impacts are small or negligible in the operation of the individual relays. When comparing maritime power systems to land-based power systems, the main difference in ANSI-67 protection is related to the protection scheme, rather than the polarisation methods.

Even with reliable directional relays, developing a protection scheme for a closed-ring-multiple-infed maritime power system is challenging. In this report, an example of such a protection scheme is proposed utilising directional fault detection for reverse relay blocking to increase selectivity and reduce tripping time. However, the protection scheme still relies on conventional time grading, which may be too slow in some cases in maritime power systems applications. As such further analysis and development of the protection schemes is required.

In conclusion, all objectives of this thesis have been successfully achieved, as two suitable polarisation methods have been identified and implemented in a relay model. The relay model has been validated experimentally, and the directional OC algorithms are evaluated in the context of protection schemes for closed-ring-multiple-infed maritime power systems by means of simulation studies.

7.2 Main Contributions

The main contributions of this work are:

- reviewing commercially available polarisation methods for directional OC protection in the context of maritime power systems.
- developing a generic closed-ring-multiple-infed maritime power system model, for fault dynamic studies.
- developing and validating a relay model containing several directional OC protection algorithms.
- sensitivity analysis of directional OC based protection schemes for maritime applications in respect to speed, selectivity and reliability.

7.3 Future work

While some conclusions can be made based on the studies described in this report, it is evident that further studies on the subject of relay protection in maritime power systems are required. This report suggests the following areas of study to continue the work done in this thesis.

Analysis of protection schemes and accurate modelling of communication and computational delays. In this report, the reliability of relay polarisation methods is assessed in order to use them in protection schemes for maritime power systems. A protection scheme is proposed for closed-ring-multiple-infed configurations, and while the proposed protection scheme should be reliable and selective when tripping, it relies on communication between relays and time grading. Therefore, it may be too slow for some use cases in maritime power systems. In order to improve the proposed protection scheme, a study should be performed of the practical requirements for speed of operation of the relay, which can be done through literature and collaboration with the maritime industries. In addition relay models should be improved to include practical computational delays, if applicable, as well as communication delays. If this is done, then studies on the improvement of protection schemes may be performed by considering more complex intercommunication between relays.

Impact of system grounding on relay operation. The power system model utilised in this report relies on high resistance grounding to reduce ground fault currents. While this is a common methodology in maritime power systems it is not the only relevant one. To further the study of relay protection and to develop protection schemes for maritime power systems, ungrounded power systems should be considered. While no significant difference in the use of polarisation methods can be expected based on a change in grounding method, there may be fault cases in ungrounded power systems that require attention in a protection scheme. Cases that require further analysis are restriking arcs and

intermittent earth faults. A study of the effects of intermittent earth faults on relay protection would require either data from a real-world occurrence or increased complexity of the power system model.

Improve relay model and phase measurement method. The relay models utilised in these studies can be further improved by more accurately representing the phase measurement methods utilised in commercial relays and modelling the voltage memory, typically used in such relays. In this context, it would also be prudent to examine whether any circumstance in maritime power systems compared to the land-based system, has an impact on the choice of the phase measurement method.

Bibliography

- [1] Robert E. Hebner, Fabian M. Uriarte, Alexis Kwasinski, Angelo L. Gattozzi, Hunter B. Estes, Asif Anwar, Pietro Cairoli, Roger A. Dougal, Xianyong Feng, Hung-ming Chou, Laurence J. Thomas, Manisa Pipattanasomporn, Saifur Rahman, Farid Katiraei, Michael Steurer, M. O. Faruque, Mario A. Rios, Gustavo A. Ramos, Mirrasoul J. Mousavi, and Timothy J. Mccoy. Technical cross-fertilization between terrestrial microgrids and ship power systems. *Journal of Modern Power Systems and Clean Energy*, 4(2):161–179, 05 2015. Copyright - The Author(s) 2016; Last updated - 2016-04-26.
- [2] T. J. McCoy. Electric ships past, present, and future [technology leaders]. *IEEE Electrification Magazine*, 3(2):4–11, 2015.
- [3] Espen Skjong, Rune Volden, Egil Rødskar, Marta Molinas, Tor Johansen, and Joseph Cunningham. Past, present and future challenges of the marine vessel’s electrical power system. *IEEE Transactions on Transportation Electrification*, 2, 04 2016.
- [4] P. Ghimire, D. Park, M. K. Zadeh, J. Thorstensen, and E. Pedersen. Shipboard electric power conversion: System architecture, applications, control, and challenges [technology leaders]. *IEEE Electrification Magazine*, 7(4):6–20, 2019.
- [5] D. T. Hall. *Practical marine electrical knowledge*. UK: Witherby & Co Ltd., 1999.
- [6] Willem Maes. *Marine Electrical Knowledge*. Antwerp Maritime Academy, 2012.
- [7] Cătălin Iosif Ciontea. *Utilisation Of The Ratios Of Symmetrical Components In Electrical Protection*. PhD thesis, Aalborg University (AAU), 2018.
- [8] Det Norske Veritas Germanischer Lloyd. *Dnv rules for classification of ships july 2016*. <https://www.dnvg1.com/rules-standards/index.html>., Accessed 22/05/2021.
- [9] Moni Islam, Kamal Garg, Pat Patel, and Saurabh Shah. Protection system design ship and offshore vessels — an overview. In *Industry Applications Society 60th Annual Petroleum and Chemical Industry Conference*, pages 1–7, 2013.
- [10] MacAngus-Gerrard, Geoff. *Offshore Electrical Engineering Manual*. Elsevier Science & Technology, proquest ebook edition, 2017. <https://www.proquest.com/ebooks-offline/offshore-electrical-engineering-manual/docview/2308444>

- [//ebookcentral.proquest.com/lib/aalborguniv-ebooks/detail.action?docID=5166112](http://ebookcentral.proquest.com/lib/aalborguniv-ebooks/detail.action?docID=5166112),
Accessed 26/05/2021.
- [11] Yanfeng Gong, Yan Huang, and Noel N. Schulz. Integrated protection system design for shipboard power system. *IEEE Transactions on Industry Applications*, 44(6):1930–1936, 2008.
- [12] DEIF A/S. *Designer’s Handbook: Medium Voltage Relay MVR 200 series*.
<https://www.deif.dk/produkter/mvr-200-series/>, Accessed 22/05/2021.
- [13] Schneider Electric. *Directional phase overcurrent protection in Easergy P3 relays*.
- [14] Relion ABB. *630 series, Technical manual*.
- [15] Christophe Prévé. *Protection of Electrical Networks*. ISTE Ltd, 1st edition, 2006. ISBN-10: 1-905209-06-1.
- [16] ABB. *Distribution Automation Handbook, Section 8.2: Relay Coordination*.
- [17] C. Russel Mason. *The Art & Science of Protective Relaying*. Wiley, 1956. ISBN-10:0471575526.
- [18] B. Li, X. Yu, and Z. Bo. Protection schemes for closed loop distribution network with distributed generator. In *2009 International Conference on Sustainable Power Generation and Supply*, pages 1–6, 2009.
- [19] B. Polajžer, M. Pintarič, M. Rošer, and G. Štumberger. Protection of mv closed-loop distribution networks with bi-directional overcurrent relays and goose communications. *IEEE Access*, 7:165884–165896, 2019.
- [20] Mnguni MES, Tzoneva R. Comparison of the operational speed of hard-wired and iec 61850 standard-based implementations of a reverse blocking protection scheme. *Journal of Electrical Engineering and Technology[Internet]*, 2015. Available from:
<http://dx.doi.org/10.5370/JEET.2015.10.3.740>.
- [21] Mathworks®. Marine full electric propulsion power system. simscape r2016b.
<https://se.mathworks.com/help/releases/R2016b/physmod/sps/examples/marine-full-electric-propulsion-power-system.html>. Accessed 27/12/2020.
- [22] Ieee recommended practice for excitation system models for power system stability studies. *IEEE Std 421.5-2016 (Revision of IEEE Std 421.5-2005)*, pages 1–207, 2016.
- [23] Schneider electric. *Medium Voltage Variable Speed Drive ATV6000 - 6.6 kV - 1000 kVA*.
<https://www.se.com/us/en/product/ATV6000C100A6666NA3/>

- medium-voltage-variable-speed-drive-atv6000---6.6-kv---1000-kva/, Accessed 22/01/2020.
- [24] Irving M Gottlieb. *Practical Electric Motor Handbook*. Newnes, electronic edition edition, 1997.
- [25] M. Taleb, M. Akbaba, and E. A. Abdullah. Aggregation of induction machines for power system dynamic studies. *IEEE Transactions on Power Systems*, 9(4):2042–2048, 1994.
- [26] Thomas J. Overbye J.Duncan Glover. *Power System analysis and design*. Cengage Learning, 6st SI eddition edition, 2016. ISBN-13: 978-1-305-63618-7.
- [27] ABB. *The MV/LV transformer substations (passive users)*.
https://new.abb.com/docs/librariesprovider27/default-document-library/abb-transformerstations_ebook.pdf?sfvrsn=2, Accessed 06/01/2020.
- [28] OMICRON electronics. *CMC 356 User Manual*. Version CMC356.AE.4,
<http://userequip.com/files/specs/6011/CMC%20356%20User%20Manual.pdf>, Accessed 26/05/2021.
- [29] DEIF A/S. *Data Sheet: Medium Voltage Relay MVR 200 series*.
<https://www.deif.dk/produkter/mvr-200-series/>, Accessed 26/05/2021.
- [30] Gerhard Ziegler. *Numerical Distance Proteciton, Principles and Applications*. Publicis Publishing, 2011.
- [31] nexans. *6-36kV Medium Voltage Underground Power Cables*. <https://www.nexans.co.uk/UK/files/Underground%20Power%20Cables%20Catalogue%2003-2010.pdf>, Accessed 07/01/2020.
- [32] Prabha Kundur. *Power System Stability and Control*. Mcgraw-Hill inc., 1st edition, 1993. ISBN: 0-07-035958-X.

A | Model Parameters

Diesel Generator

Table A.1: Diesel generator and governor parameters

Genset parameter	Value
Rated Power [MVA]	4.5
Rated Voltage [kV]	6.6
Pole pairs	4
Rated frequency [Hz]	60
Stator Resistance [pu]	0.011
Stator Reactance [pu]	0.15
d-axis synchronous reactance [pu]	1.05
q-axis synchronous reactance [pu]	0.7
zero-sequence reactance [pu]	0.15
d-axis transient reactance [pu]	0.35
d-axis subtransient reactance [pu]	0.25
q-axis subtransient reactance [pu]	0.325
d-axis transient open-circuit [s]	5.25
d-axis subtransient open-circuit [s]	0.03
q-axis subtransient open-circuit [s]	0.05
Inertia constant	3.525
Diesel generator time constant [s]	0.3
Governor time constant [s]	0.2
Excitation system	AC1A

Excitation system

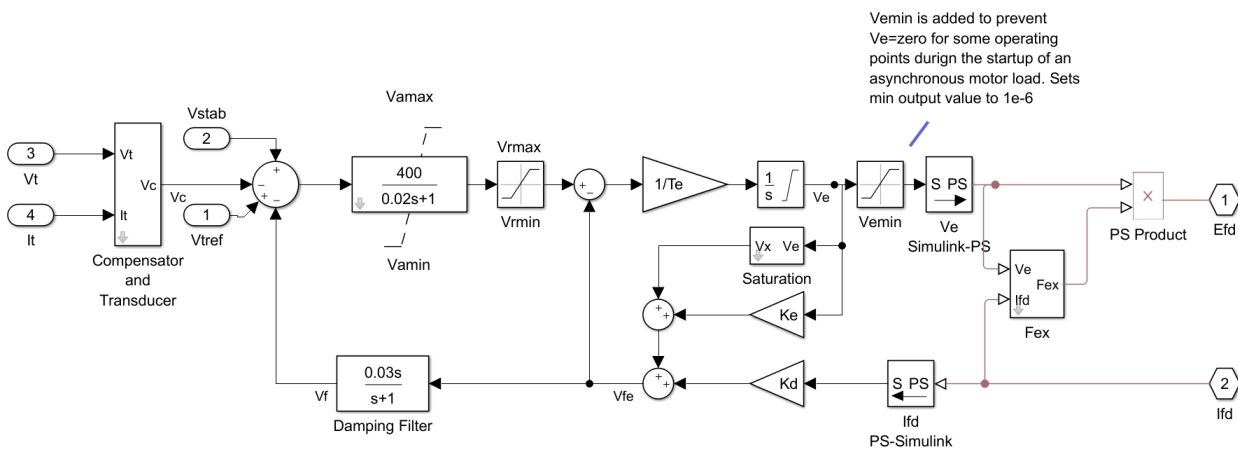


Figure A.1: Excitation control implementation in simulink with Excitation voltage limited to minimum 10^{-6}

Asynchronous motor

Table A.2: Squirrel cage induction motor parameters

Induction motor parameter	Value
Rated Power [MVA]	1.0
Rated Voltage [kV]	6.6
Pole pairs	5
Rated frequency [Hz]	60
Stator Resistance [pu]	0.0258
Stator Inductance [pu]	0.0930
Referred rotor resistance [pu]	0.0145
Referred rotor inductance [pu]	0.0424
Magnetizing inductance [pu]	1.7562
Stator zero-sequence inductance [pu]	0.0930

Cables

Table A.3: Line parameters for π -model cables based on [31, p. 27].

Cable	Rated current [A]	Specific Resistance [$\frac{\Omega}{km}$]	Specific Inductance [$\frac{mH}{km}$]	Specific Capacitance [$\frac{\mu F}{km}$]
3x150mm Cu	430	0.124	0.294	0.497
3x35mm Cu	175	0.524	0.376	0.293
Cable no.	Length [m]	Resistance [$m\Omega$]	Inductance [μH]	Capacitance/2 [nF]
1, 4, 1-4, 2-3	100	12.4	29.4	24.85
2-6, 3-7	200	24.8	58.8	49.7
1-5, 4-8	200	104.8	75.2	29.3

B | Aggregation of Parallel Asynchronous Motors

Verification of Simplified Motor Aggregation Method

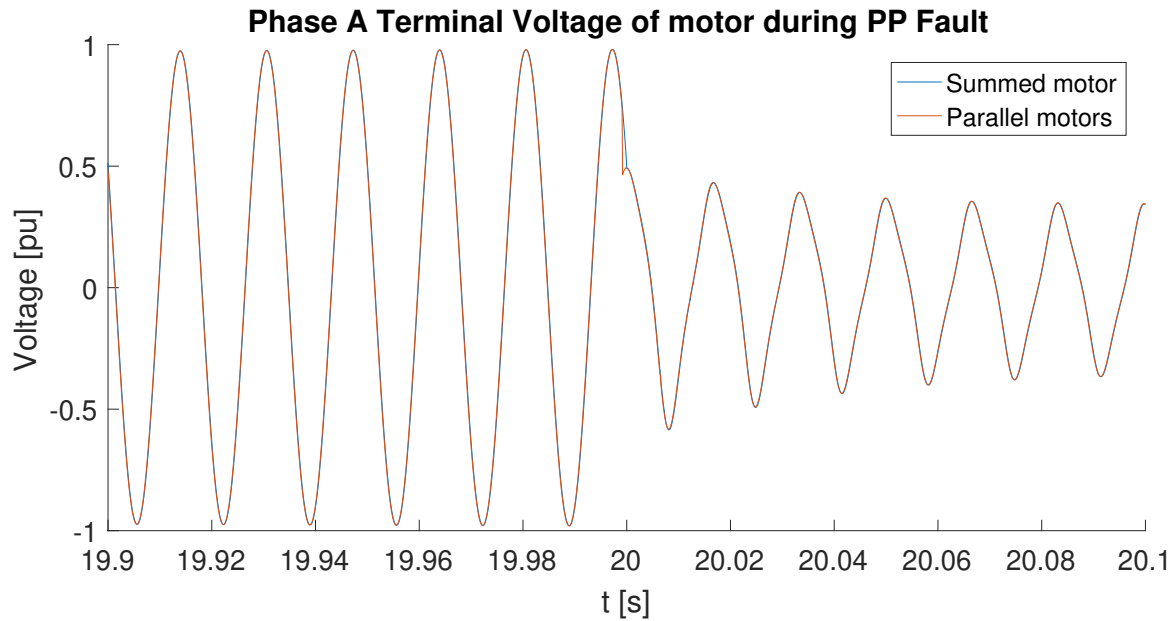


Figure B.1: Phase A voltage of busbar feeder, during PP fault. Summed motor is a single 2 MW motor, while parallel motors is two 0.5 MW motor and one 1 MW motor connected at the same busbar.

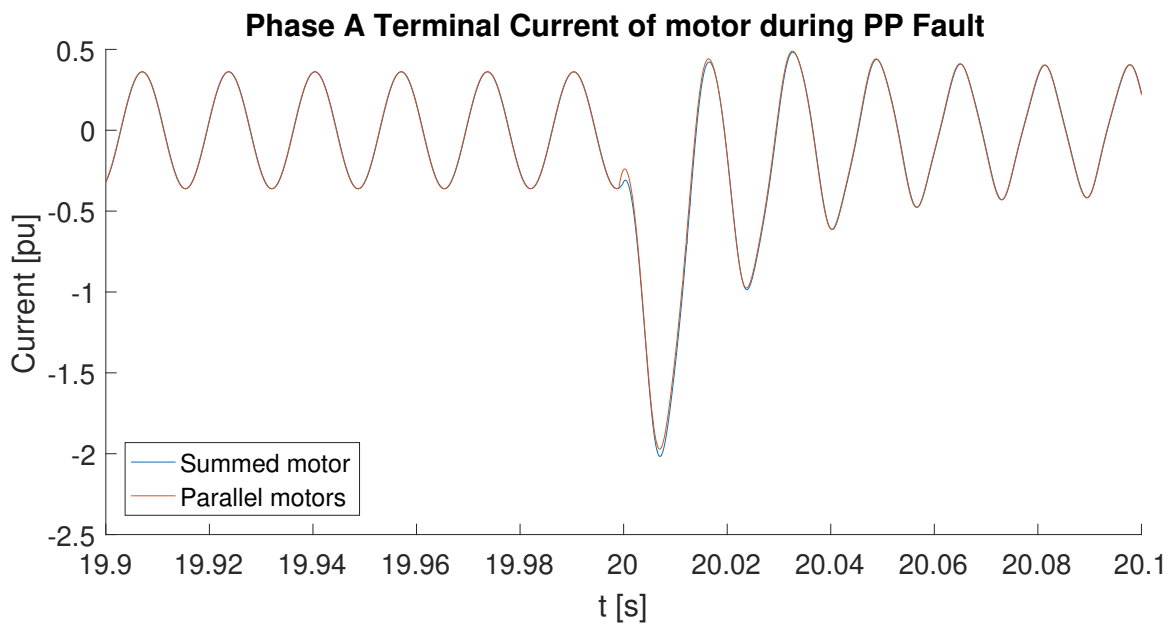


Figure B.2: Phase A current of busbar feeder, during PP fault. Summed motor is a single 2 MW motor, while parallel motors is two 0.5 MW motor and one 1 MW motor connected at the same busbar.

Aggregation of Different Asynchronous Motors

The transient and synchronous reactances of a single motor can be defined as[25, 32, pp301-302]:

$$X = \omega(L_s + L_m) \quad (\text{B.1})$$

$$X' = \omega(L_s + L_m - \frac{L_m^2}{L_r + L_m}) \quad (\text{B.2})$$

where L_s is the stator inductance, L_r is the referred rotor inductance and L_m is the magnetising inductance. Letting i be the index of the motors to be aggregated the equivalent transient reactance of motors in parallel can be determined as[25]:

$$X'_{eq} = \frac{1}{\sum \frac{1}{X'_i}} \quad (\text{B.3})$$

Given rotor voltages for the individual motors the rotor voltage of the equivalent machine can be determined and the synchronous reactance is found as[25]:

$$E'_{eq} \angle \delta_{eq} = X'_{eq} \sum \frac{E'_i \angle \delta_i}{X'_i} \quad (\text{B.4})$$

$$X_{eq} = \frac{X'_{eq} V \cos(\delta_{eq})}{-E'_{eq} + V \cos(\delta_{eq})} \quad (\text{B.5})$$

where V is the system voltage. Equation (B.5) is only valid when the terminal voltage of the motors is equal to the system voltage, which is a reasonable assumption in maritime power systems, due to short cables. The stator winding leakage reactance is now:

$$X_{ls,eq} = X_{eq} - \sqrt{X_{eq}(X_{eq} - X'_{eq})} \quad (\text{B.6})$$

The next aggregate parameter to be found is the rotor resistance R_{eq} . This is done based on the first transient torque peak of the aggregate motor. The first transient torque peak occurs 13 ms after motor start for all induction machines and therefore the first transient torque peak of the aggregate motor is simply the sum of the motors[25]. R_{eq} is determined by solving Equations (B.7) and (B.8).

$$T_{lr,eq} = \sum T_{lr,i} \quad (\text{B.7})$$

$$T_{lr,eq} (1 + \sqrt{1 + (\frac{2X_{ls,eq}}{R_{eq}})^2}) = T_{lr,i} (1 + \sqrt{1 + (\frac{2X_{ls,i}}{R_i})^2}) \quad (\text{B.8})$$

The final parameter to be determined is the inertia of the aggregate motor[25].

$$H_{eq} = \frac{\sum H_i \omega_i^2}{\omega_{eq}^2} \quad (\text{B.9})$$

Notice that $H_{eq} = \sum H_i$ in case the motors all operate at the same speed.

C | Additional Simulation Results

CB41 during PP fault at Cable 1-4, at varying fault impedance.

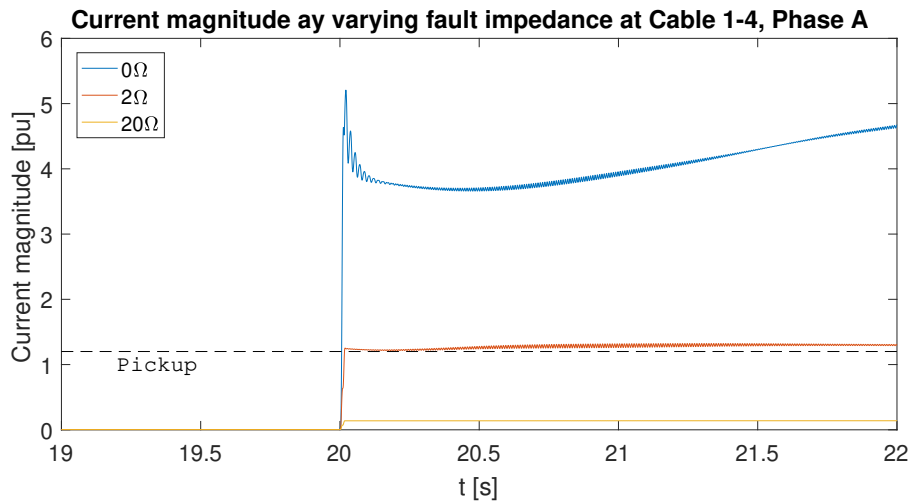


Figure C.1

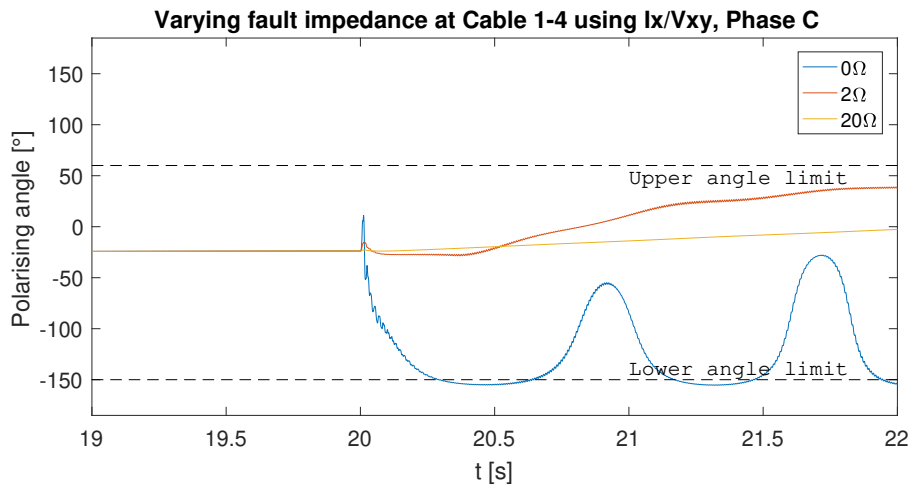


Figure C.2

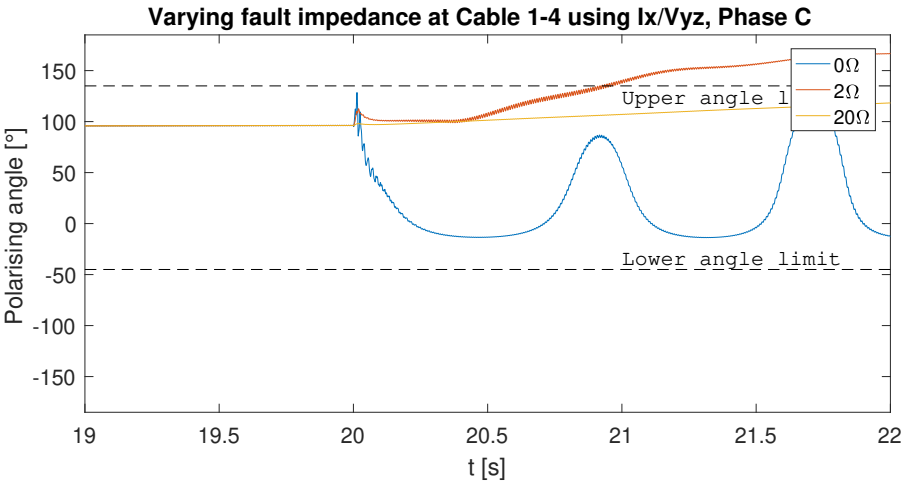


Figure C.3

CB41 during 3P fault at Cable 1-4, at varying fault impedance.

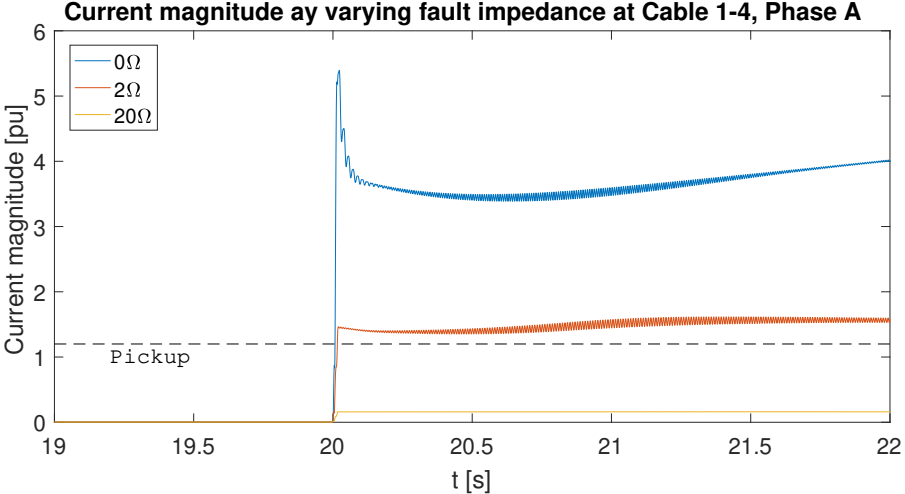


Figure C.4

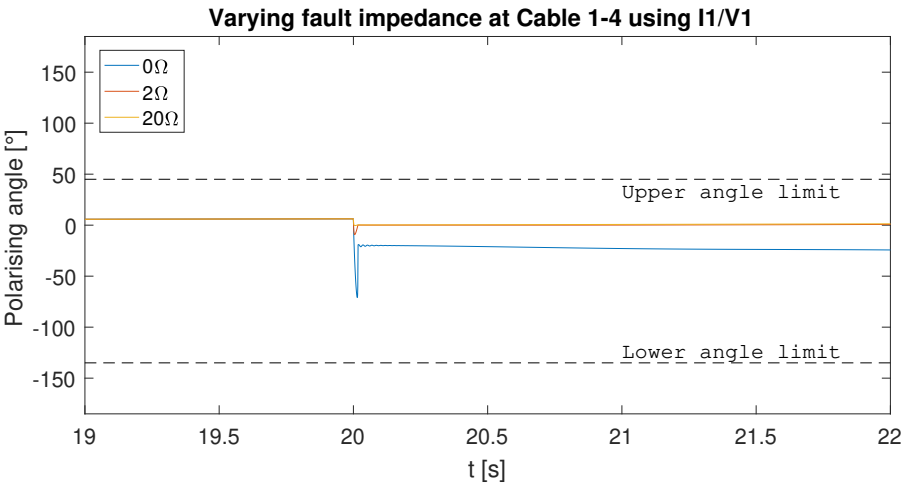


Figure C.5

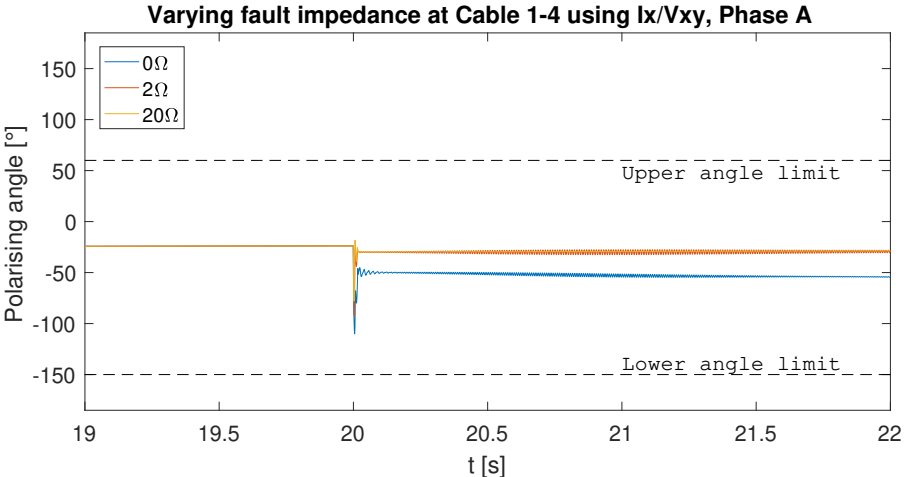


Figure C.6

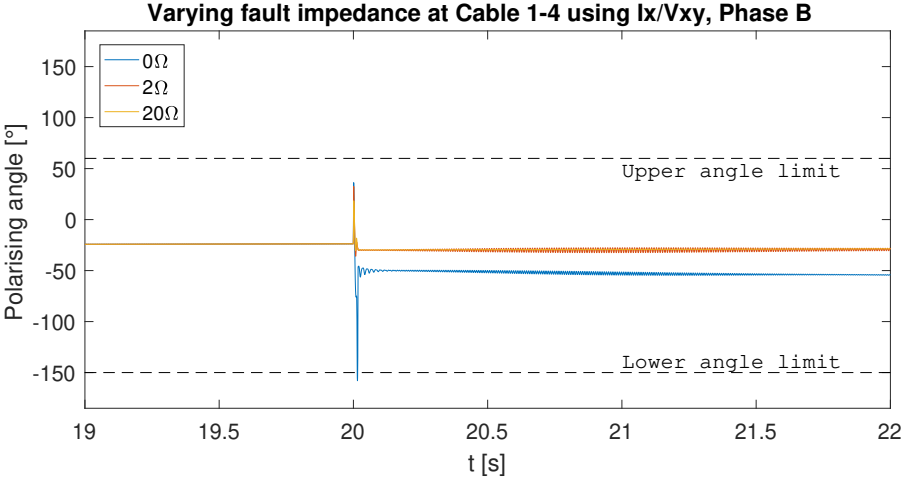


Figure C.7

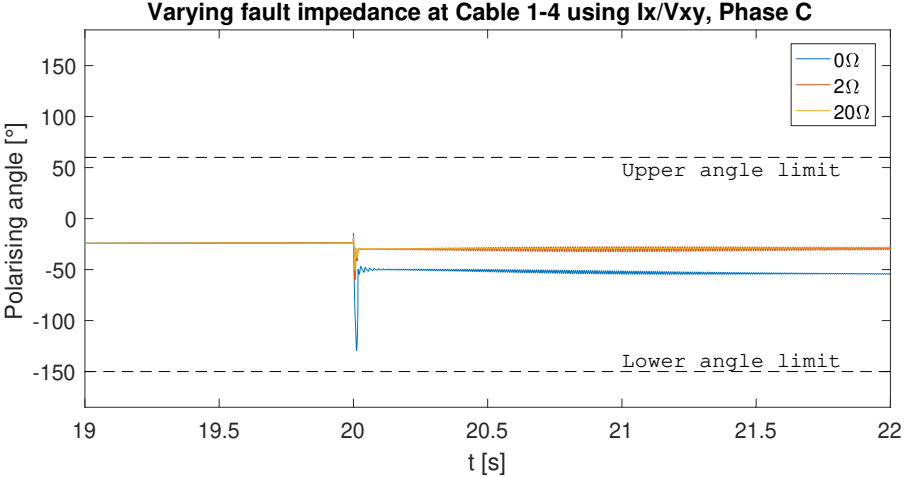


Figure C.8

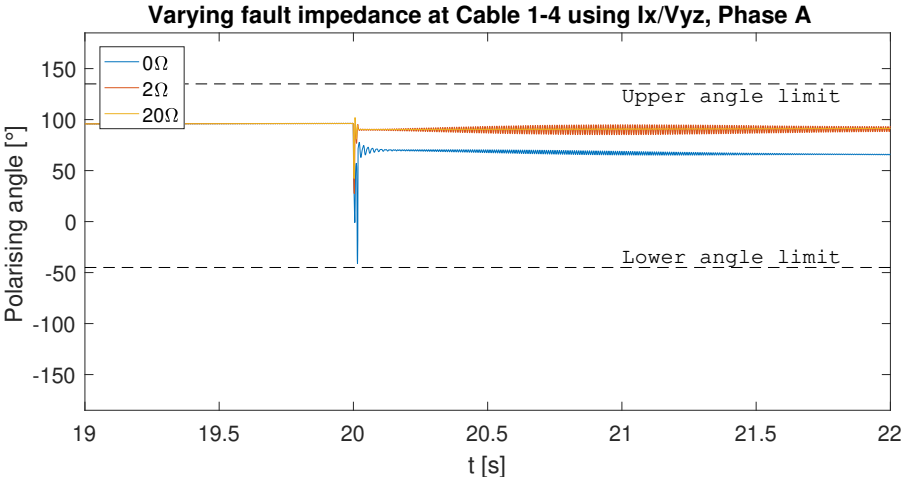


Figure C.9

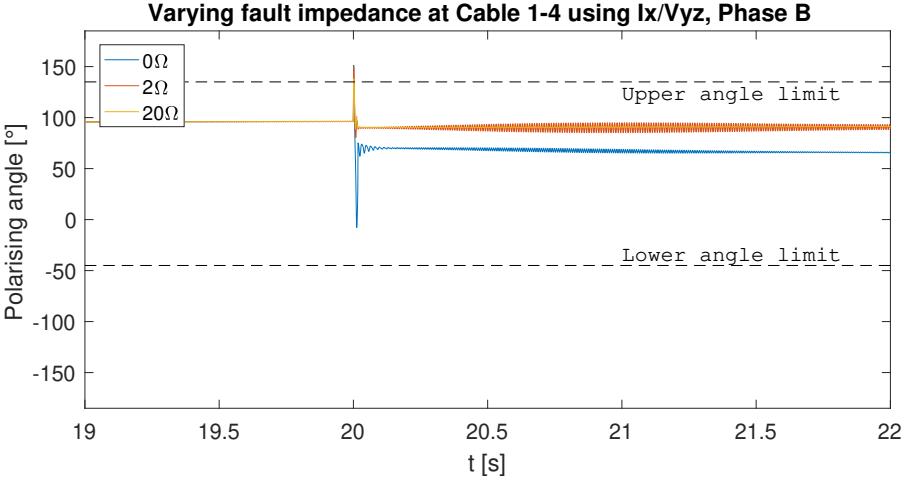


Figure C.10

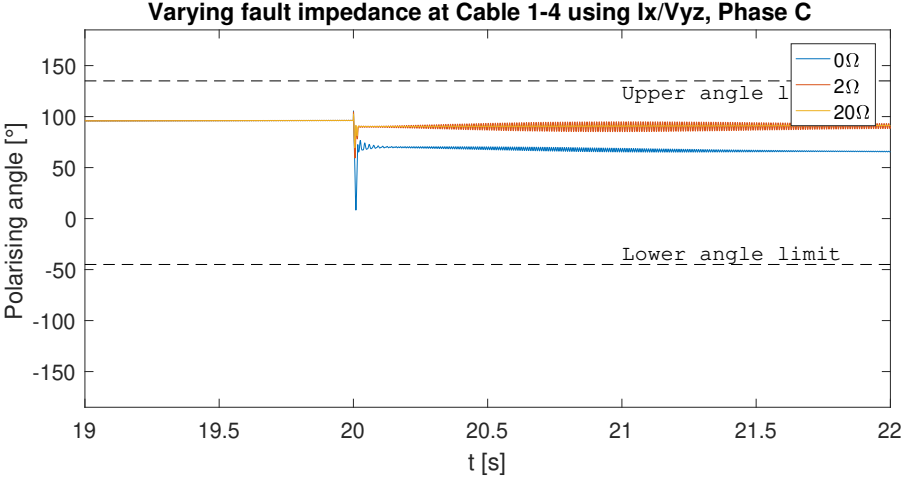


Figure C.11

CB14 during PP fault at Cable 1-4, at varying fault impedance.

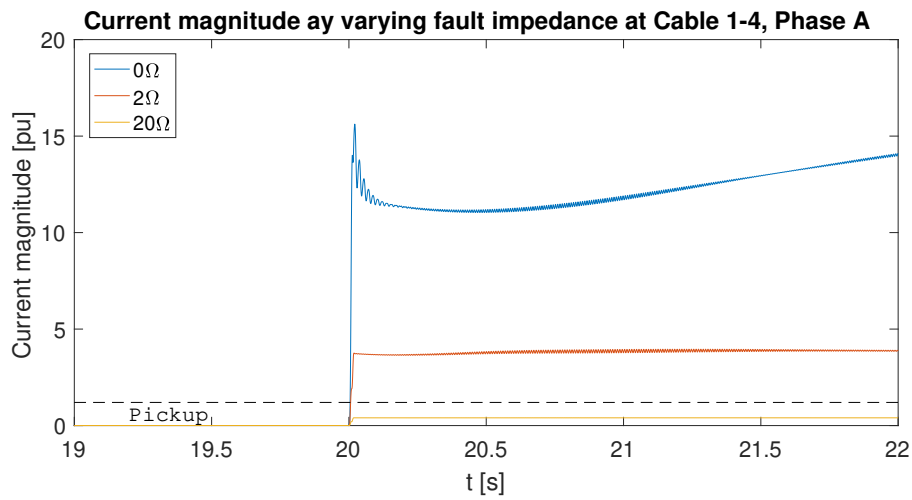


Figure C.12

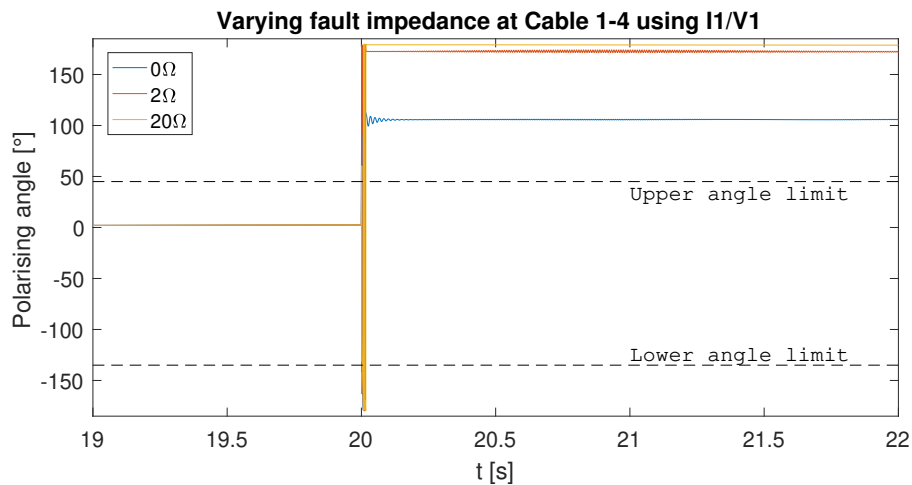


Figure C.13

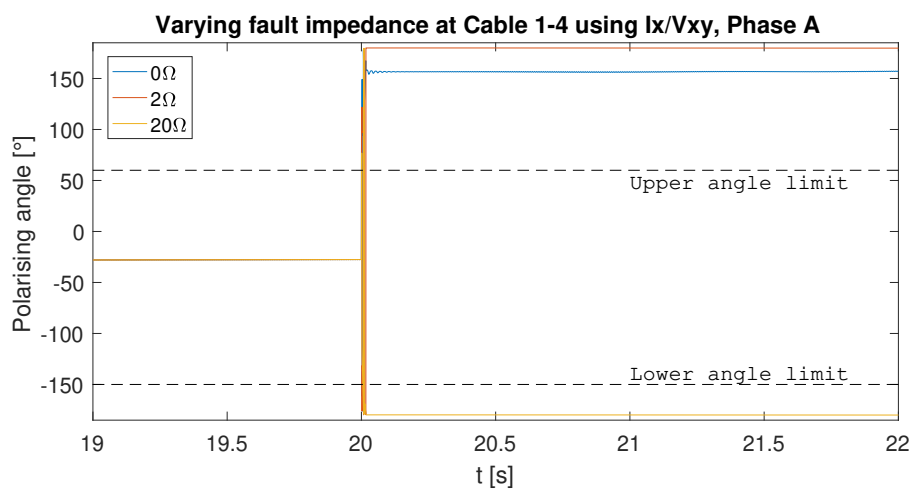


Figure C.14

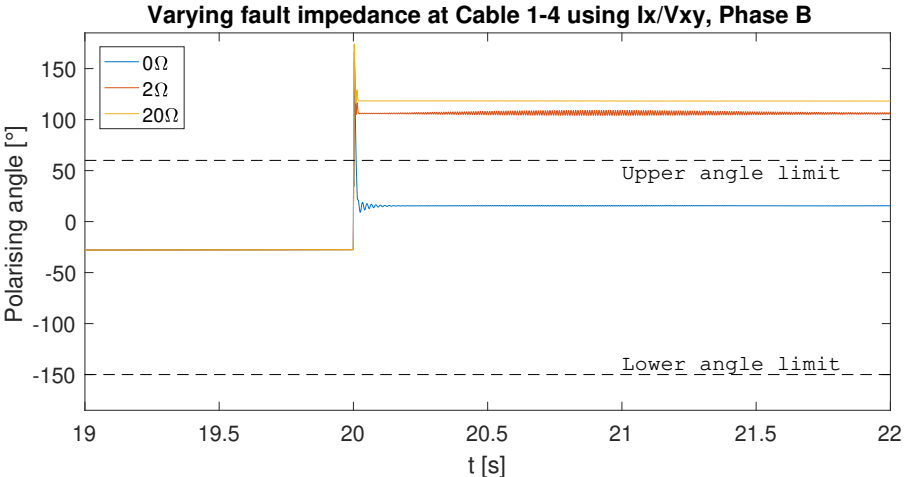


Figure C.15

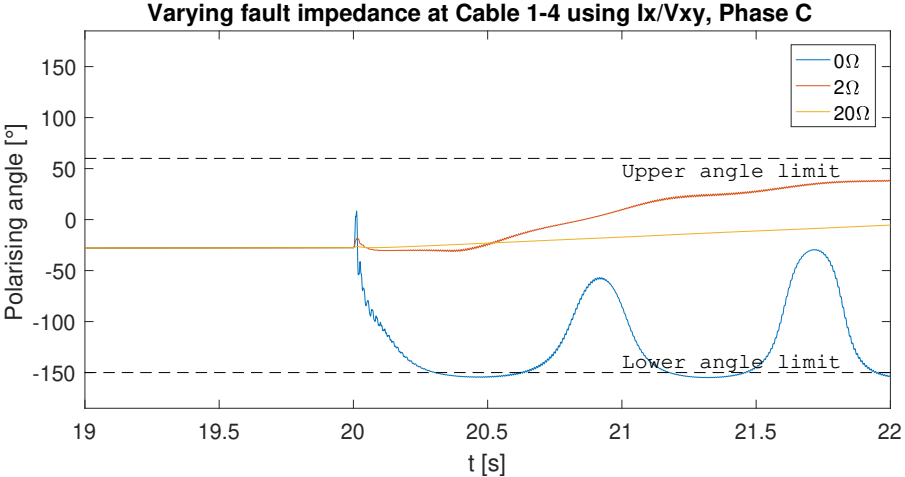


Figure C.16

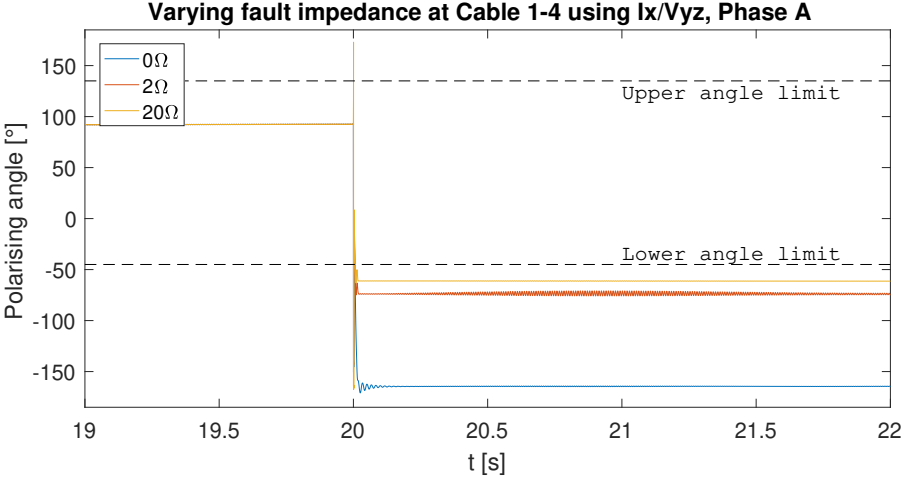


Figure C.17

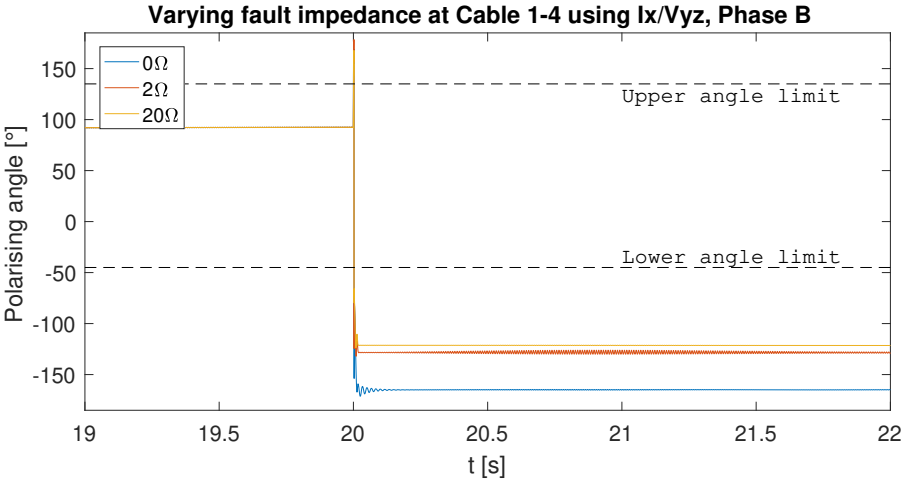


Figure C.18

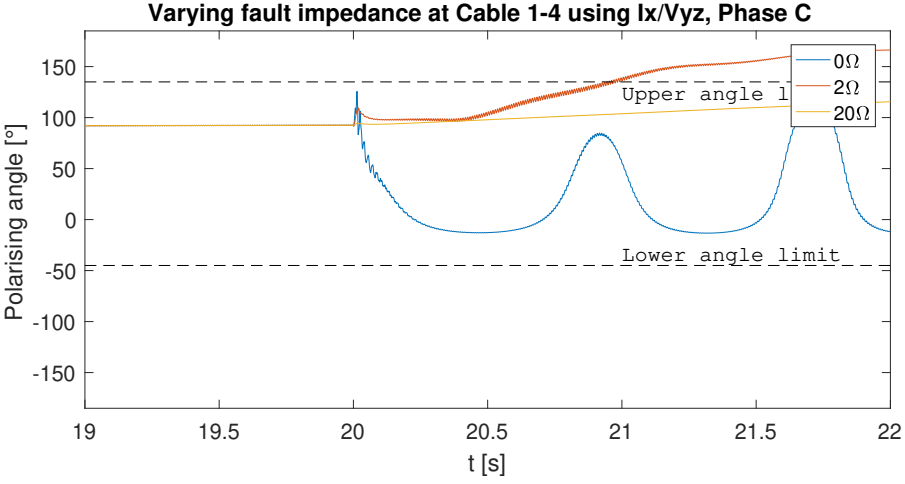


Figure C.19

CB14 during 3P fault at Cable 1-4, at varying fault impedance.

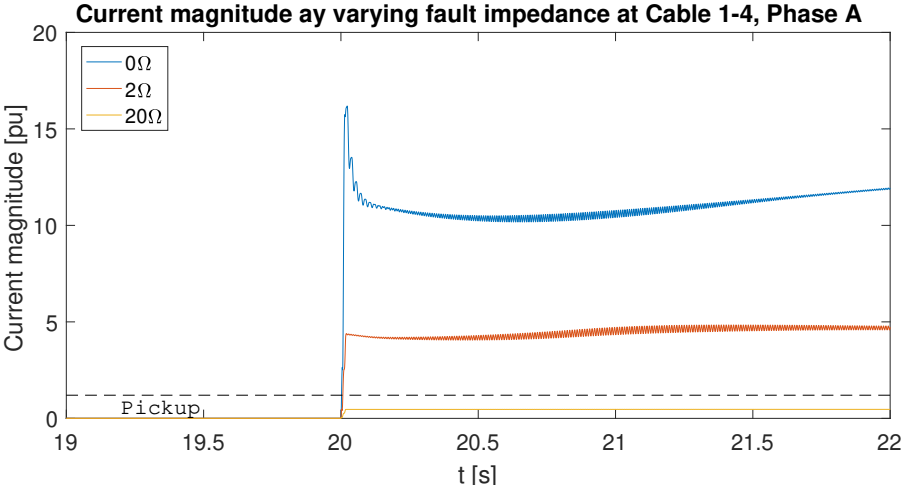


Figure C.20

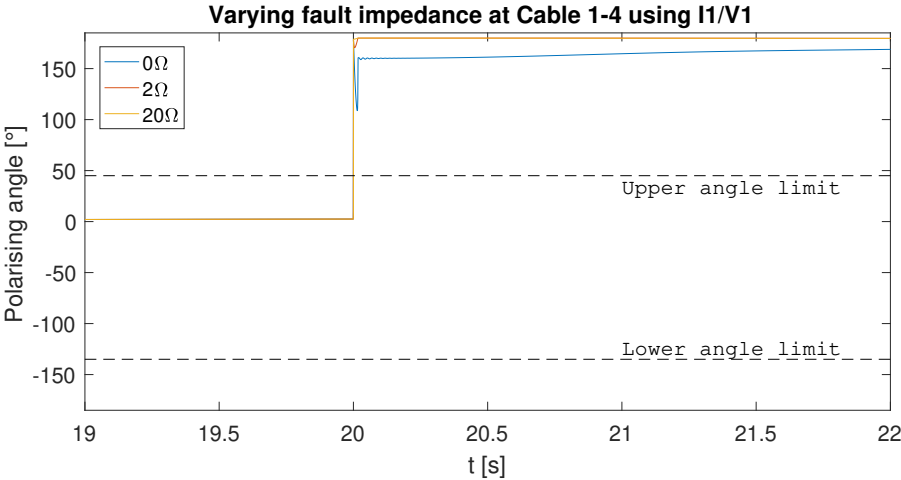


Figure C.21

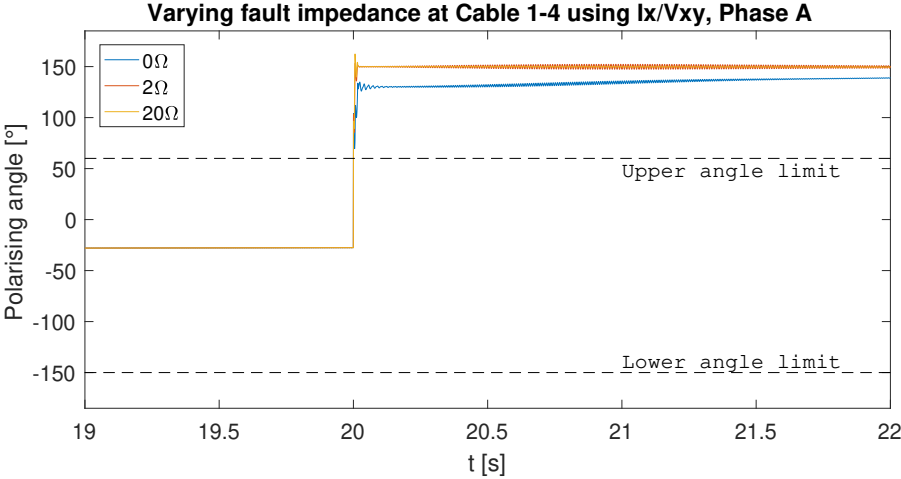


Figure C.22

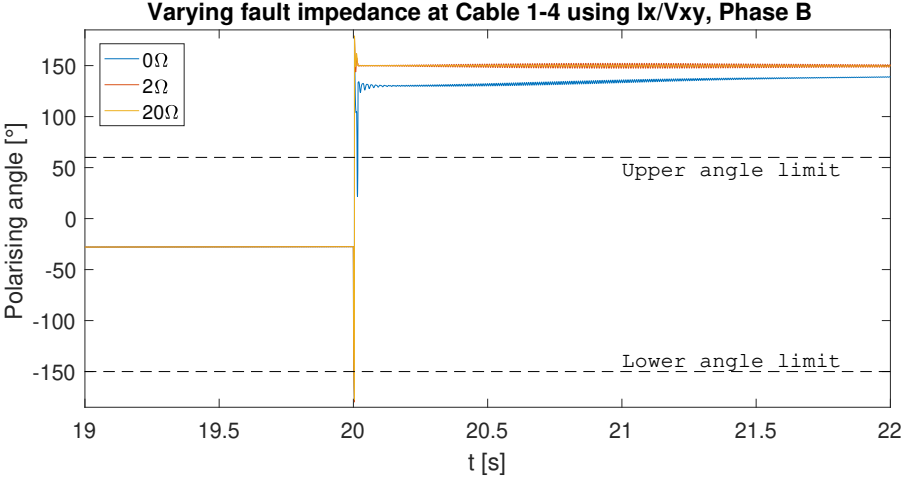


Figure C.23

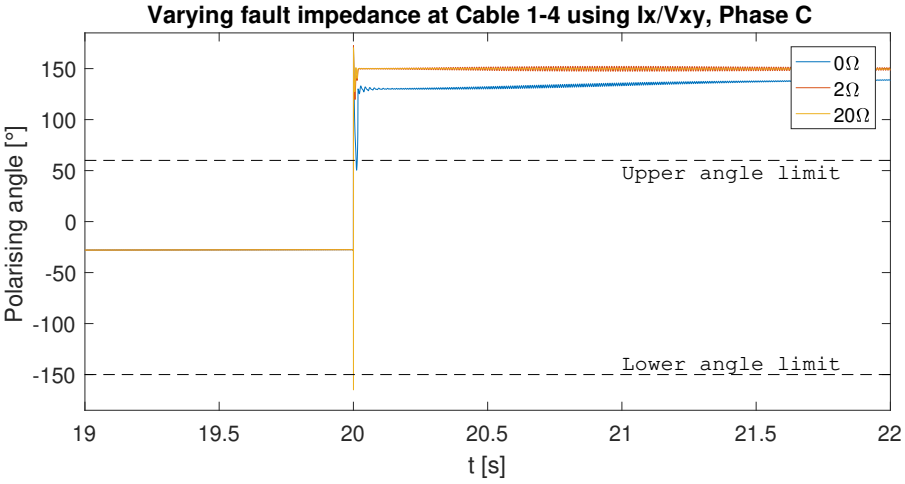


Figure C.24

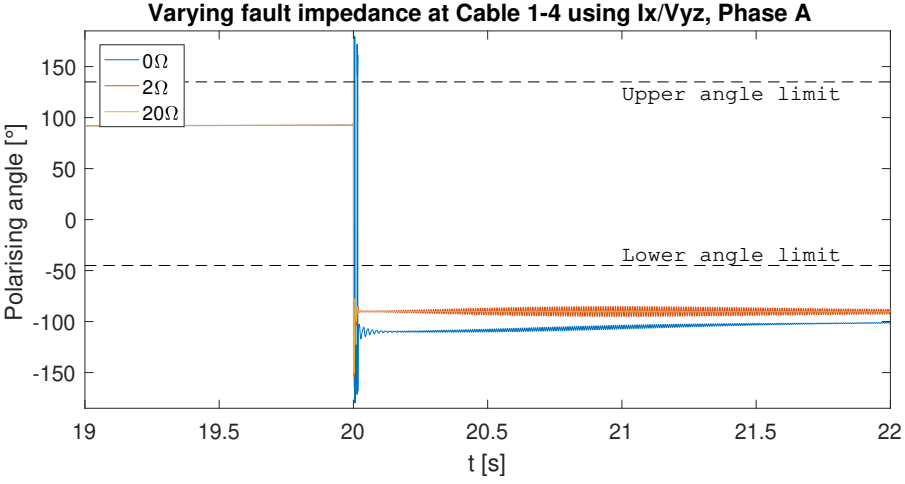


Figure C.25

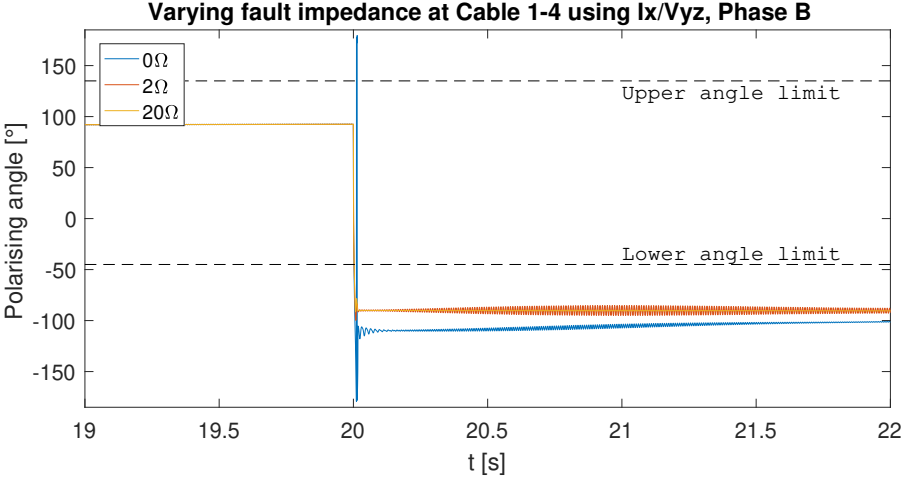


Figure C.26

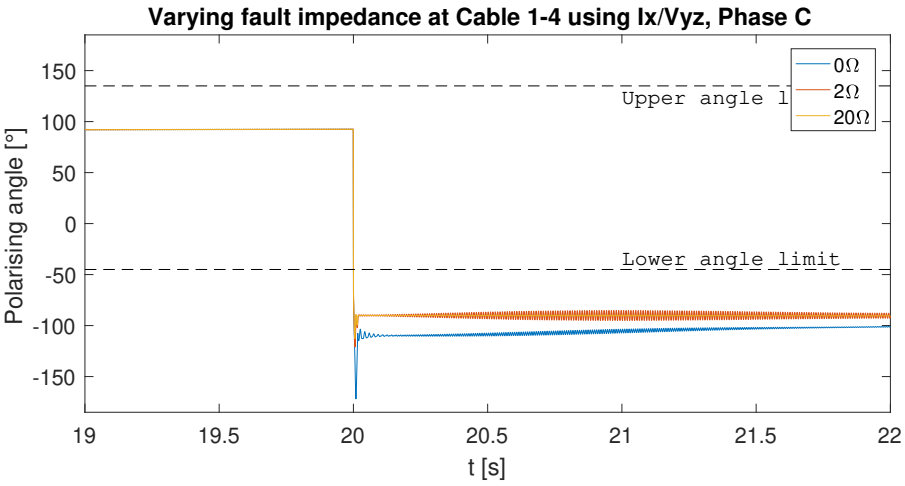


Figure C.27

CB26 during 2P fault at Cable 2-6, at different system loads.

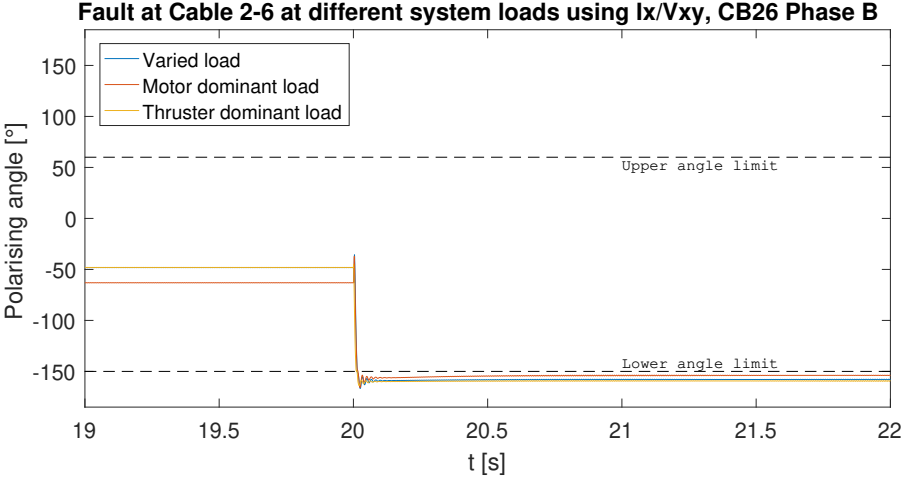


Figure C.28

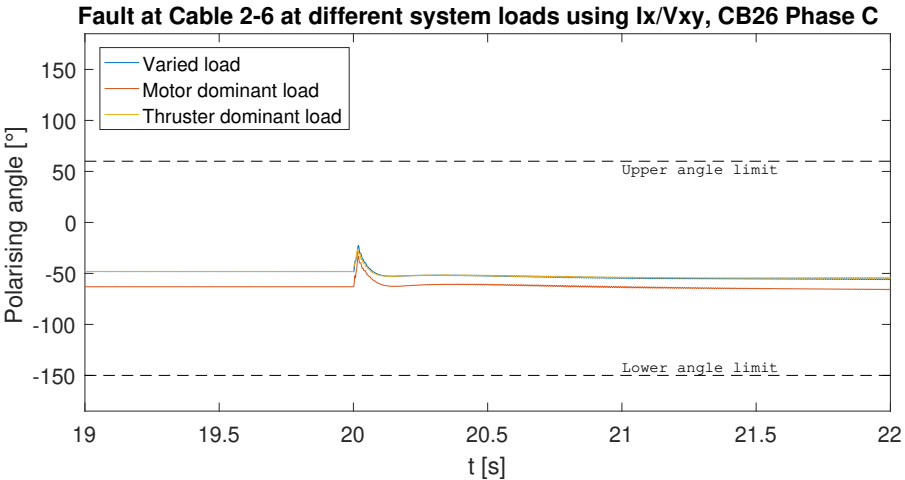


Figure C.29

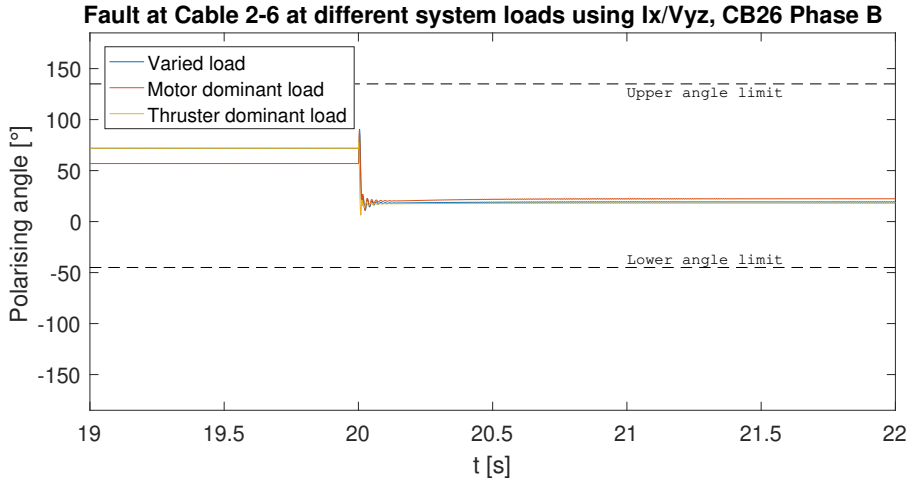


Figure C.30

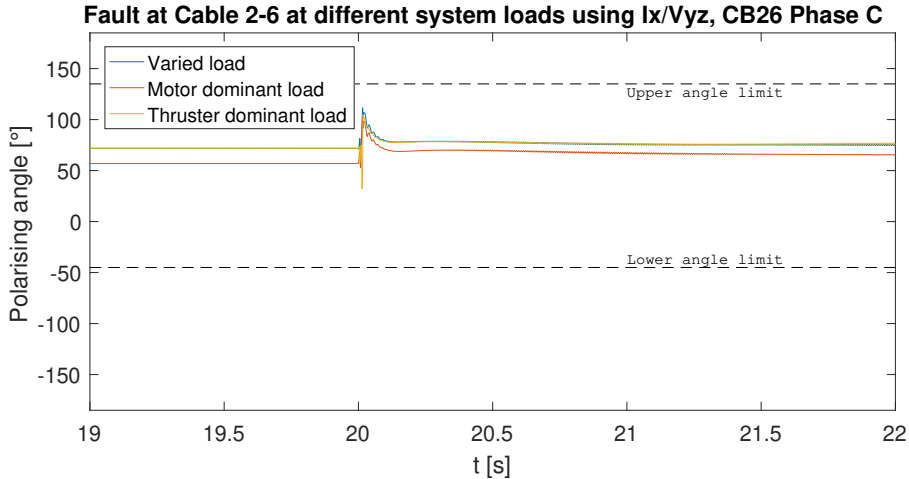


Figure C.31

CB26 during 3P fault at Cable 2-6, at different system loads.

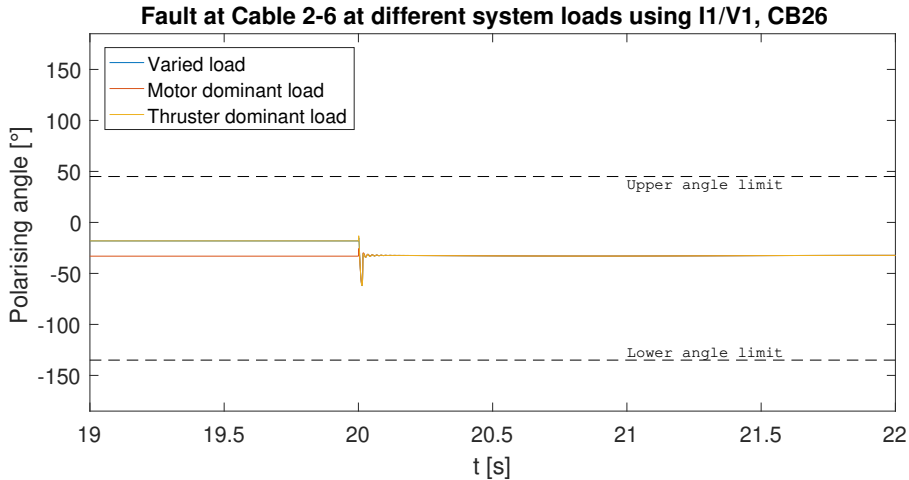


Figure C.32

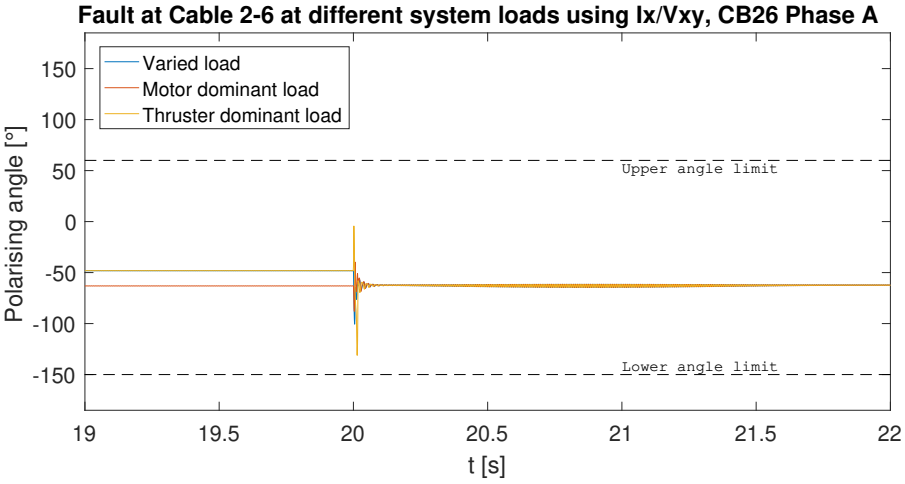


Figure C.33

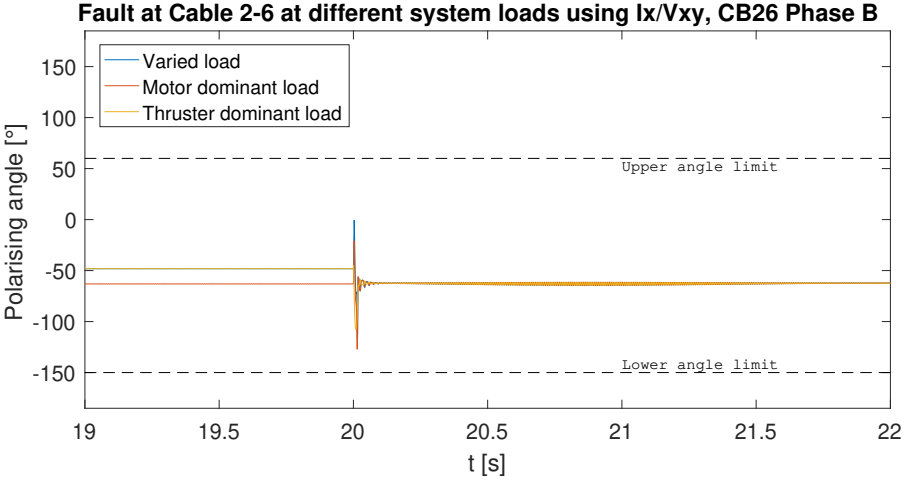


Figure C.34

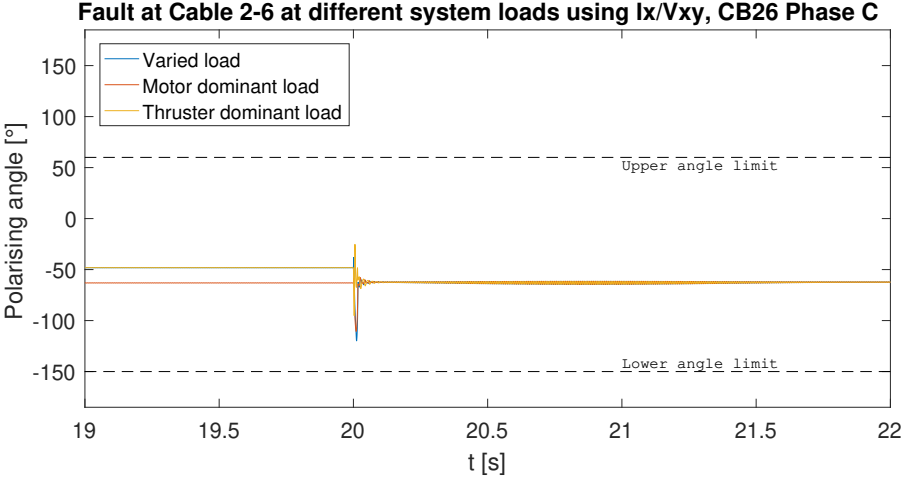


Figure C.35

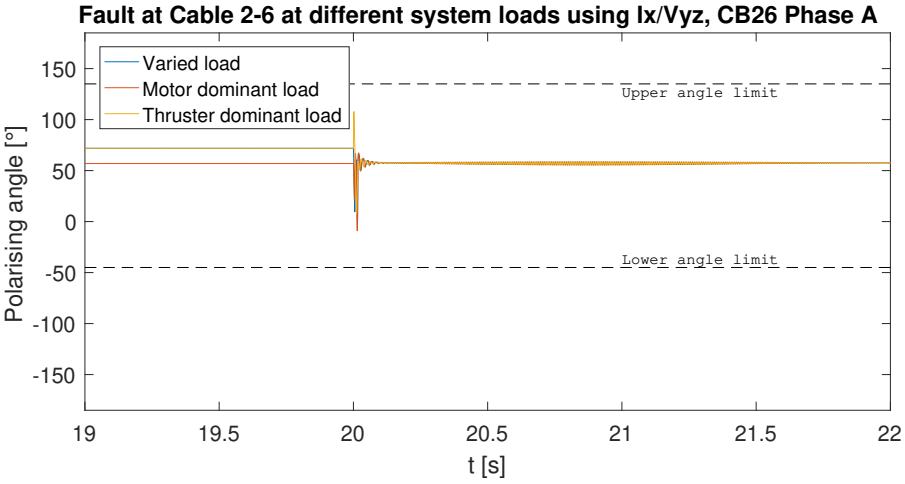


Figure C.36

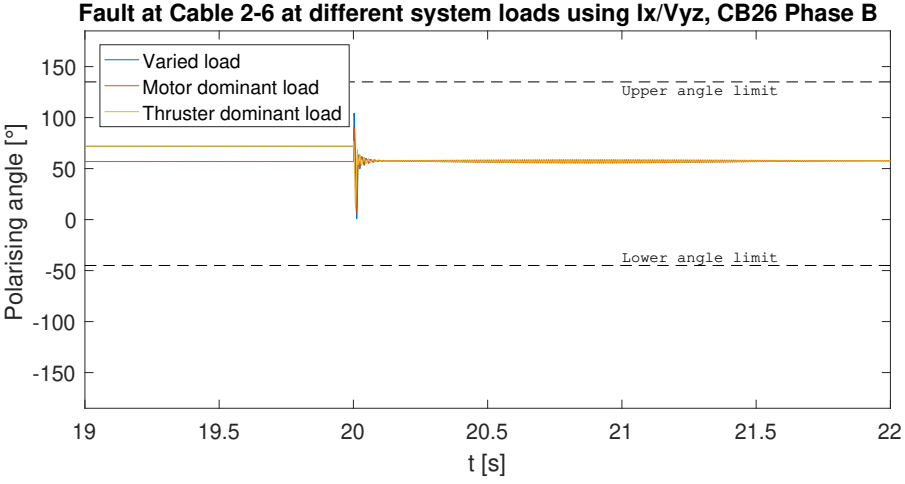


Figure C.37

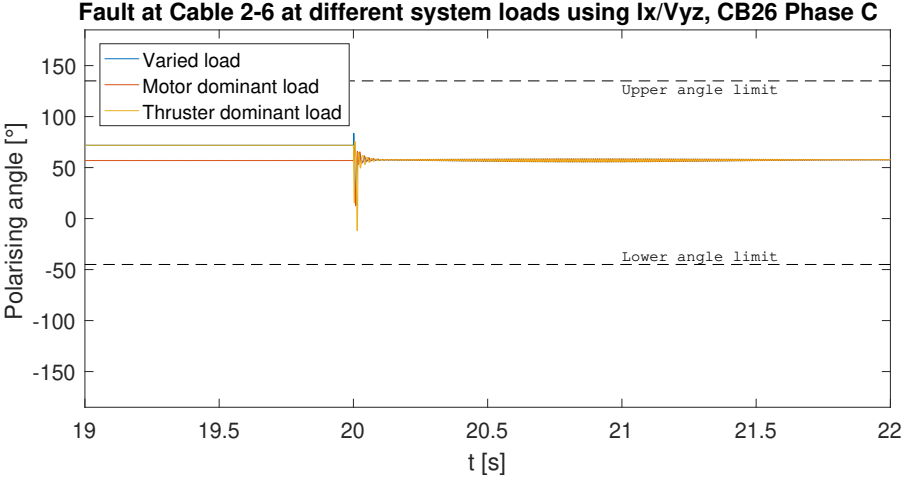


Figure C.38